Transport Properties of the Quantum Hall State

by

Dmitri Boris Chklovskii

Submitted to the Department of Physics
in partial fulfillment of the requirements for the degree of

Doctor of Philosophy

at the

MASSACHUSETTS INSTITUTE OF TECHNOLOGY

May 1994

Author .....
Department of Physics
May 11, 1994

Certified by .....
Patrick A. Lee
William and Emma Rogers Professor of Physics
Thesis Supervisor

Accepted by .....
George F. Koster
Chairman of Graduate Committee

Transport Properties of the Quantum Hall State

by

Dmitri Boris Chklovskii

Submitted to the Department of Physics
on May 11, 1994, in partial fulfillment of the
requirements for the degree of
Doctor of Philosophy

Abstract

In this thesis, I analyze the transport properties of the two-dimensional electron gas(2DEG) in the quantum Hall regime. This analysis is based on the model in which the 2DEG breaks into compressible and incompressible regions.[1] I first describe the progress in the study of the quantum Hall effect from its experimental discovery to the point where the role of the compressible liquid became crucial. The key concept here is the existence of the incompressible state.

In Chapter 2 I show through a self–consistent electrostatic calculation that wide compressible strips are present parallel to the edges of a sample.[2] This leads to an explanation of certain data from equilibration experiments.

In Chapter 3 I analyze the effect of compressible strips on the conductance of a narrow wire.[3] The presence of the compressible state leads to narrow plateaus in conductance vs. magnetic field plots. These predictions are yet to be tested.

The model of compressible and incompressible regions is used in Chapter 4 to study transport properties of the 2DEG in the bulk.[4] I show that depending on the level of disorder in a sample one can have either narrow or wide compressible regions. In the first case the conventional network model analysis applies, while in the second case I use the composite fermion approach to obtain transport properties. This provides a way of understanding the nature of the compressible state. The main predictions of this part are on the longitudinal resistivity peak values in the quantum Hall effect in the limit of zero temperature. These predictions are compatible with existing experimental data.

Thesis Supervisor: Patrick A. Lee
Title: William and Emma Rogers Professor of Physics

---

[1] A.L. Efros, Solid State Commun. **67**, 1019 (1988), S. Luryi in *High Magnetic fields in Semiconductor Physics*, edited by Landwehr (Springer, New York, 1987).

[2] D.B. Chklovskii, B.I. Shklovskii, and L.I. Glazman, Phys. Rev. B **46**, 4026 (1992); **46**, 15606(E) (1992).

[3] D.B. Chklovskii, K.A. Matveev, and B.I. Shklovskii Phys. Rev. B **47**, 12605 (1993).

[4] D.B. Chklovskii and P.A. Lee,Phys. Rev. B **48**, 18060 (1993).

Acknowledgments

I wish to express my gratitude to my advisor, Patrick Lee, whose thoughtful advice, encouragement, guidance and support have made this thesis possible. Patrick was always ready to share with me his ideas, many of which have been incorporated in this work. His views on physics and beyond had greatly influenced my perception of the world. It was a great honor for me to work with Patrick and to be treated as equal.

I am grateful to the other members of the condensed matter theory group for many insights into the wonderful world physics. Particulary, I would like to thank Boris Altshuler, Leonid Levitov, Kostya Matveev and Xiao-Gang Wen, who were always happy to share their ideas and to discuss mine. It is impossible to describe how much I learned from them on countless occasions. And every time I was impressed how deep their understanding of physics is. I thank my past and present officemates Richard Berkovitz, Jari Kinaret, Bruce Normand, Menke Ubbens, Hyunwoo Lee for their tolerance and support.

I owe a lot to people at MIT outside of Building 12. I should start with Paul McEuen who introduced me to the concept of edge states and whose ideas were instrumental in the begining of my thesis work. Ethan Foxman was always there to provide an experimentalist's feedback when I needed it. Gennady Shvets was always ready to share his vast knowledge with me. Valya Khoze showed me a high energy attitude to physics and the world. I wish to thank Mikhail Brodsky for his longtime friendship. His love of life was the best encouragement one can get.

This being my first degree, I take an opportunity to thank those who contributed to my becoming a physicist. A mathematician Sergei Rukshin showed to me the beauty of logical thinking and clear presentation. My high school physics teacher Victor Radionov demonstrated to me that these qualities are not limited to math. My first advisor Mikhail D'yakonov showed me how to do beautiful physics. His great patience and originality I will be always trying to match.

It is impossible to express my greatest gratitude to my family. Their love and support were absolutely crucial on my way into physics. I am honored to have my father as my first physics teacher and a colleague. I can only hope to match the depth of his insight and the sharpness of his intuition. My mother's understanding and readiness to help will always be an example of how selfless a person can be. My brother's curiosity constantly reminded me that being young is not an excuse for ignorance.

I wish to thank all my friends who made life at MIT a lot of fun: Paul Volfbein, Anton Andreev, Sergei Seleznev, Mika Efros and many others.

Last but not the least, I wish to thank Stella who gave me her love and support.

Contents

List of Figures

Chapter 1

Introduction

The connection between science and technology is a two-way street. Just as technology can not develop without a sufficient scientific base, science is ultimately dependent on advances in technology.

The creation of one of the major objects of research for today's condensed matter physicists, the two-dimensional electron gas (2DEG), only became possible thanks to tremendous progress in semiconductor technology. Another development, superconducting magnets, allowed us to study the 2DEG in extremely strong magnetic fields, up to 30T. Combination of these two devices lead to a discovery of the quantum Hall effect (QHE) first integer [34] and later fractional[35].

The essence of these effects is in the quantization of Hall conductance and vanishing of longitudinal resistivity.[20] The quantized values are expressed through fundamental constants $R_H = (1/f)h/e^2$. f is integer in the integer quantum Hall effect and $f = p/q$, where p and q are integers, in the fractional quantum Hall effect. This quantization of the Hall resistance does not vary from sample to sample. This is very surprising considering the presence of disorder and its variation between samples. The level of disorder only determines which quantized values are observed and which are not. Moreover the Hall conductance values are not sensitive to the sample geometry. The only requirement is to the topology and quality of the contacts, meaning that their respective order should correspond to a Hall meaurement. These properties have made it possible to use the quantum Hall effect as a resistance standard. But, this is not the only reason to study this effect. The interest in the quantum Hall effect is due to a great variety of challenging problems related to many recent developements in other fields.

It became clear, soon after the discovery, that the quantum Hall effect owes its existence of the presence of the gap in the density of states.[20] The origin of this gap is different for the integer and fractional QHE. In the integer case the gap comes from the Landau quantization of the electron spectrum, thus being equal to the effective electron cyclotron frequency. In the fractional case the gap is due to the formation of a strongly correlated electron state; its exact nature remains an interesting problem. However, there are many similarities between the two effects. Once the existence of the gap is established, the argument for the conductance quantization proceeds along the same lines in both cases. Also, the experimental values of longitudinal resistivity

near a half-filled Landau level and around zero magnetic field look amazingly similar.

The quantum Hall state with an excitation gap is often referred to as an incompressible fluid implying that there is a jump in the chemical potential at certain densities. This state has a uniform electron density determined by having f electrons per magnetic field flux quantum. The properties of this state have been studied intensively, both theoretically and experimentally[20]. Most of the early data could be explained in terms of this state and its resistivity tensor. This was close to the spirit of traditional condensed matter physics which usually considered bulk effects.

The importance of edge effects was first pointed out by Halperin[22]. The idea is as follows: Landau levels are bent at the edge of the sample by the confining potential. Their intersection with the Fermi level is referred to as edge states. In other words edge states are 1D electron states localized at the edge of the 2DEG and propagating in one direction. Classical analogy of these states is in the drift of electron in crossed electric and magnetic fields. These excitations are gapless as opposed to the bulk of the sample allowing to observe them despite their reduced dimensionality. Now there are multiple experimental manifestations of the existance of the edge states; to name a few, nonlocal transport, edge magnetoplasmons, and interference effects. Experimentally, importance of the edge states has been recognized through non-local transport measurements. These are measurements performed by using so-called non-ideal contacts. The outcome of these experiments cannot be explained in terms of a local resistivity tensor. To explain them a new approach has been developed[2] where edge states are considered as one-dimensional chiral channels connecting voltage and current probes. The success of this theory made the concept of edge states widely popular. It is amazing that in most cases one does not have to know the exact structure of edge states.

The detailed structure of edge states is a difficult problem. It is important for understanding tunneling and magnetoplasmon experiments. The original picture in terms of noninteracting electrons (see Fig.2-1), although conceptually useful, did not allow to understand certain experimental facts and make quantitative predictions. The analysis of the structure of edge states led to a realization of the importance of a new quantum Hall state: a compressible liquid. Earlier, it was realized that the compressible state is formed in the bulk of the sample due to disorder[13].

In the next Chapter, I show that the simplest consequence of electron-electron interactions is the formation of wide compressible liquid strips at the edge. This leads to different estimates of the inter-edge-state spacing, which determines equilibration length between edge states. This picture is often used to analyze the results of experiments, but some new techniques would certainly be needed to resolve the structure of edge states in full detail.

Another effect of interaction is in reducing the plateau widths in the conductance of a narrow channel, discussed in Chapter 3. This is related to the quantization of the conductance through a narrow channel, which has been observed in the absence of magnetic field. The similar effect for a bulk sample has been predicted by Efros[13].

In both cases the theory is based on the solution of an electrostatic model in which compressible strips are represented by equipotential conductors, while incompressible ones are insulators with fixed electron density.

The problem with the compressible state is that, if one ignores correlations, electron states are highly degenerate, making it a reasonable starting point only for static cases such as the density distribution. For predictions about the dynamic properties, this is definitely insufficient. The needed theory for the compressible state has been motivated by different kind of experiments.

When the mobility of the 2DEG became sufficiently high, it became possible to observe anomalies in the 2DEG properties at magnetic fields where no incompressible liquid is thought to exist. Although there are no remarkable features in DC transport, other measurement techniques such as the surface acoustic wave propagation and tunneling experiments show a new kind of behavior in those regions. These observations are related to the existance of the compressible state which is essentially the same as the compressible strips in the edge states.

The explanation of these observations has been proposed recently in terms of the Fermi-liquid of composite fermions[42]. The concept of composite fermions is rooted in the anyon theory and in the work of Jain[46], who has emphasized an intimate relation between the integer and fractional quantum Hall effect. The essence of this concept is in considering a correlated electron state as a Fermi-liquid of composite fermions, which are obtained from electrons by the attachment of two magnetic flux quanta. Thus when a Landau level is half-filled composite fermions do not see any effective magnetic field and form a Fermi-liquid.

Recently there have been several experimental discoveries which showed that the composite fermions are at least as real as the Fermi-liquid quasiparticles. I believe that this opens an exciting new field in the study of correlated electron states.

In the final chapter, I use the composite fermion approach to analyze the structure of the compressible liquid in the edge states and in bulk. I first consider an electrostatic model which shows the crossover between narrow and wide edge channels. Then I argue that the difference in edge states structure is manifested in the longitudinal resistivity peaks which can be understood through a network of edge channels. To understand the nature of wide edge channels, I consider the motion of composite fermions in a non-uniform magnetic field which arises from the electron density variations. Some of the predictions of this theory are compared to experimental data. The comparison shows that in some cases there is a good agreement while in the other there is a difference in absolute values. The possible reasons for this are discussed in Chapter 4.

Chapter 2

Electrostatics of edge channels

2.1 Introduction

Magnetotransport along edge states that are formed in high-mobility two-dimensional electron gas (2DEG) attracted significant attention in the recent years (see, e.g., reviews [1]). Such transport allows us to understand a number of experiments on the integer quantum Hall effect (IQHE) regime as well as in the fractional (FQHE). Particularly, it allows to analyze the impact on conductance measurements[2] of current leads, and relaxation processes between electron states quantized by a strong magnetic field. The overlap between electron wave functions belonging to different edge states is exponentially small. This makes the geometry of these states and separation between the adjacent ones crucial in all transport phenomena. This geometry depends strongly on the shape of the potential confining the electrons. The bare potential (formed by an external metallic electrode - gate, or by etching process) is usually smooth on the scale determined by magnetic length $\lambda = (c\hbar/eH)^{1/2}$ and one can use quasiclassical approach in the description of edge states geometry.

A naive one-electron picture is based on the assumption that the bare potential bends Landau levels and the positon of the edge states is given by their intersection with the constant Fermi level, see Fig. 2-1(a-c). This picture has a serious drawback from the experimental point of view. A strong separation between the edge states from the smoothness of the confining potential reduces the relaxation rate between edge states too strongly: it is difficult to obtain equlibration length that does not exceed significantly the sample size of any realistic experimental parameters. From the theoretical point of view, the one–electron picture fails to account for screening and its modification in a strong magnetic field. Magnetic field modulates the electron density of states making the screening highly dependent on the filling factor, changing in the region of interest from its bulk value to zero at the boundary of 2DEG.

The effect of screening in the presence of a magnetic field was included in a qualitative picture of edge states by Beenakker [3] and Chang [4]. They divide the electron gas into alternating strips of incompressible and compressible states, the former originating from the discontinuities of the chemical potential dependence on filling factor, $\mu(\nu)$.

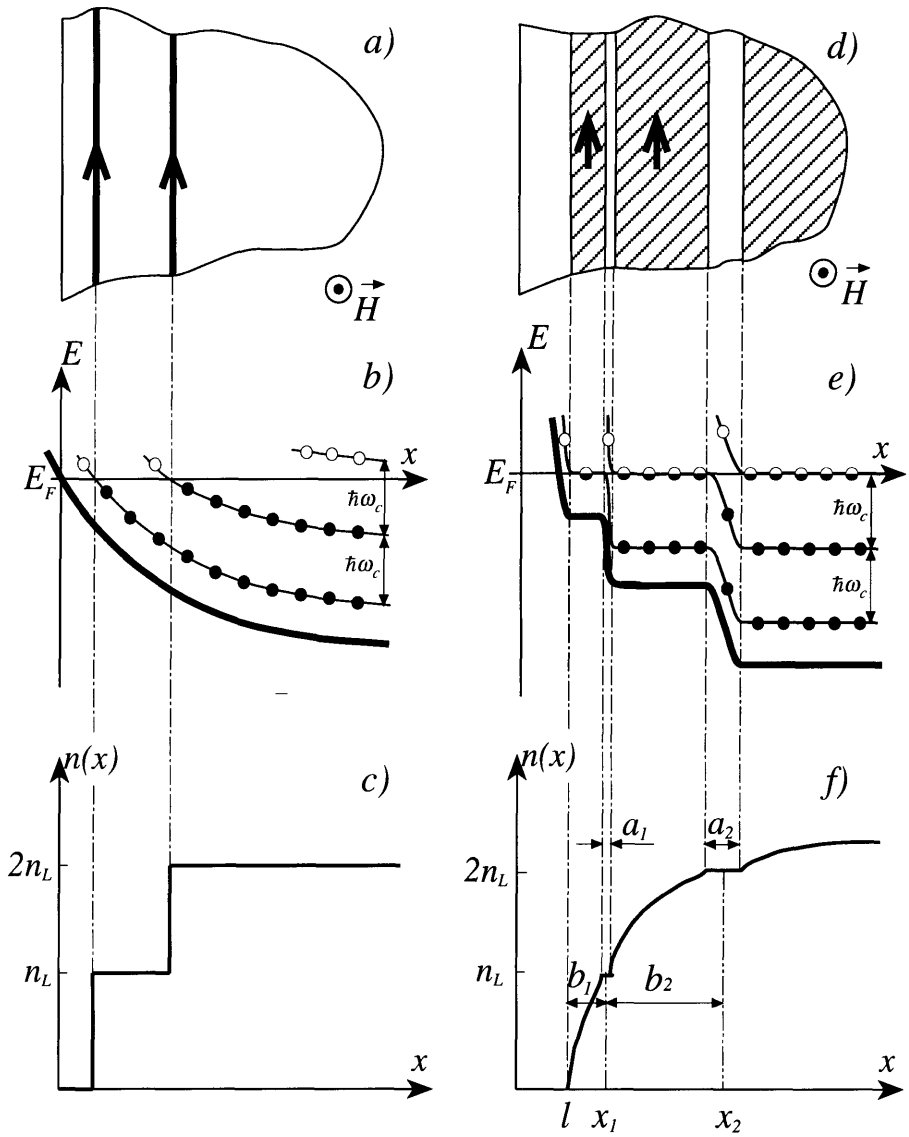

Figure 2-1: Structure of spinless edge states in the IQHE regime. (a–c) One-electron picture of edge states. (a) Top view on the 2DEG plane near the edge. Arrows designate electron flow direction in the two edge channels. (b) Adiabatic bending of Landau levels along the increasing potential energy near the edge. Energy is measured from the Fermi level. Circles represent local filling of the Landau levels: • – occupied and ∘ –empty. (c) Electron density as a function of the distance to the boundary. (d–f) Self–consistent electrostatic picture.(d) Top view of the 2DEG near the edge. Shaded strips represent regions with non-integer filling factor (compressible liquid), unshaded strips represent integer filling factor regions (incompressible liquid). Arrows show the direction of electron flow. (e) Bending of the electrostatic potential energy and the Landau levels. Circles represent local filling of the Landau levels: • – occupied , ∘ –partially occupied, and ∘ –empty. (f) Electron density as a function of distance to the middle of the depletion region.

Existing treatments [3],[4] lack a quantitative approach that could yield the geometric dimensions and positions of those strips. Knowledge of them is necessary for the explanation of transport experiments involving edge states, in particular selective population of the edge states by the point contacts and relaxation between them (see, e.g., [5, 6]).

In this paper we present a quantitative electrostatic treatment of the edge states in the case of gate–induced depletion that is self-consistent and free of unjustified assumptions about the external potential. We obtain the dependence of the widths of compressible and incompressible liquid strips on the filling factor. These widths scale with the width of the depletion layer l that separates the gate and the boundary of the 2DEG as l(compressible) and as $(a_B l)^{1/2}$ for IQHE and as $(\lambda l)^{1/2}$ for FQHE(incompressible). Here a_B is the Bohr radius $a_B = \hbar^2\epsilon/m_{eff}e^2$, for a semiconductor with a dielectric constant ϵ and effective electron mass m_{eff}. Length l is controlled by the gate voltage V_g and is very large usually (several thousand angstroms). Therefore we find the incompressible strips to be parametrically more narrow than the adjacent compressible ones, the innermost being the widest (see Figure 2-1(d-f)). This can serve to explain the high equilibration rate of all the states but the innermost one [5]. Our results provide an explanation of the experimentally observed equilibration length dependences on magnetic field in the IQHE regime. Difference in equilibration rates for 1/3 and 2/3 FQHE edge states [6] is also discussed.

The chapter begins with the formulation and solution of the electrostatics problem at the gate–induced 2DEG edge in the absence of magnetic field. In section 2.3 we study the magnetic field–induced redistribution of charge in the vicinity of the incompressible strip forming so–called dipolar strip. In Section 2.4 we generalize our treatment to the case when several dipolar strips are formed. In Section 2.5 we discuss tunneling through the incompressible strip and the relation of our theory to experiment including influence of disorder. Section 2.6 contains our major conclusions.

2.2 Electrostatics of gate-induced depletion in zero magnetic field

The 2DEG density in GaAs/AlGaAs heterostructures is defined by the concentration of donors located behind a spacer layer. In our model[7] we neglect the donor concentration fluctuations and the discreteness of their charge. This means that far from the boundaries electron density is homogeneous and equal to the one of the positive background (n_0). The boundary of the 2DEG is created by applying a negative voltage $-V_g$ to a metal half-plane serving as a gate. We neglect the distance from the gate to the 2DEG plane and the spacer layer thickness. Thus the positive background, the gate, and the 2DEG all belong to the same plane ($z = 0$)(see Fig.2-2). The validity of this assumption will be discussed below. The half-space $z < 0$ is occupied by the semiconductor with dielectric constant $\epsilon \gg 1$. As the system is invariant in y-direction, the problem becomes effectively two-dimensional.

Let us discuss, first, what happens qualitatively. At zero gate voltage (or some cut off voltage in real devices) the electron density (being zero under the gate) reaches

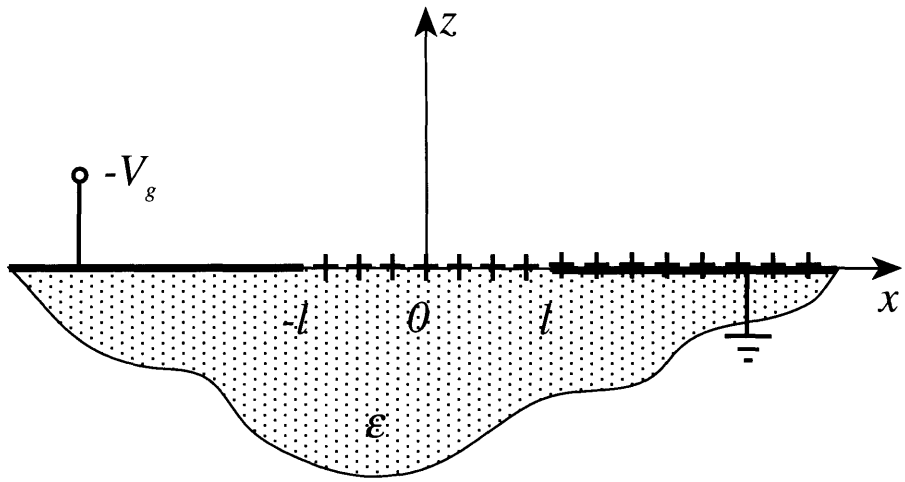

Figure 2-2: Two–dimensional capacitor formed at the 2DEG edge. Thick lines represent two conductors: the gate at potential -V_g on the left and the grounded 2DEG on the right. Pluses represent a uniform positive background due to donors. Dotted area is occupied by a semiconductor with high dielectric constant ϵ.

its bulk value n_0 right at the gate edge. By applying a negative potential to the gate electrons are repelled from it leaving a depleted strip behind. The width of this strip $2l$ is defined by V_g. Also one may expect the density of the 2DEG to grow gradually from 0 at the end of the depletion to n_0 in the bulk where it compensates the positive background. In our treatment we rely on the smallness of the parameter $a_B/l \sim E_F/V_g$ which gives the ratio of the screening length r_s to the characteristic length scale. This means that the x–component of electric field is screened out completely. Hence, the potential is constant in the area occupied by electrons, and the problem is the one of a capacitor with both metal plates in the same plane. In addition, there is a uniformly charged insulator of width $2l$ filling in the slit between the plates. Following Ref.[7], we solve the electrostatic problem for given V_g, l, and n_0, and we find l from the condition that the electron gas boundary should be in mechanical equilibrium. This means that electric field $E_x(x = l)$ should be zero both to the left and to the right of the boundary ($\lim_{x\to l-0} E_x = \lim_{x\to l+0} E_x = 0$).

A high value of dielectric constant in semiconductors ($\epsilon \gg 1$) allows us to solve the Laplace equation in the half-space $z < 0$, using the simplified boundary conditions

$$\phi(x, z = 0) = \begin{cases} -V_g, & x < -l \\ 0, & x > l, \end{cases} \tag{2.1}$$

$$\left.\frac{d\phi(x,z)}{dz}\right|_{z\to -0} = \frac{4\pi e n_0}{\epsilon}, \quad |x| < l. \tag{2.2}$$

The solution can be given as a sum $\phi = \phi_1 + \phi_2$ of harmonic functions ϕ_1 and ϕ_2 that

satisfy separately the conditions

$$\phi_1(x, z=0) = \begin{cases} -V_g, & x < -l \\ 0, & x > l, \end{cases} \tag{2.3}$$

$$\left.\frac{d\phi_1(x,z)}{dz}\right|_{z\to -0} = 0, \quad |x| < l, \tag{2.4}$$

$$\phi_2(x, z=0) = 0, \quad |x| > l \tag{2.5}$$

$$\left.\frac{d\phi_2(x,z)}{dz}\right|_{z\to -0} = \frac{4\pi e n_0}{\epsilon}, \quad |x| < l. \tag{2.6}$$

Both functions can be found using the theory of complex variables. At $z = 0$ the first one is given by[8]

$$\phi_1(x, z=0) = \frac{-V_g}{2} + \frac{V_g}{\pi}\arcsin(x/l), \quad |x| < l. \tag{2.7}$$

The derivation of the second function is reproduced in Appendix A,

$$\phi_2(x, z=0) = \frac{4\pi e n_0}{\epsilon}(l^2 - x^2)^{1/2}, \quad |x| < l. \tag{2.8}$$

Both solutions have square-root singularities in the electric field ($E_x = -d\phi/dx$) at $x = l$ which can be cancelled out only if [7]

$$l = \frac{V_g \epsilon}{4\pi^2 n_0 e}. \tag{2.9}$$

The singularity at $x = -l$ remains, but should not cause any problem as this boundary is fixed and electrons are confined. The density of the 2DEG for l defined in Eq.2.9 is given by(see Fig.2-3)

$$n(x) = \left(\frac{x-l}{x+l}\right)^{1/2} n_0, \quad x > l. \tag{2.10}$$

These results deserve a discussion. It is important to mention that l is the only scale in the electrostatic solution. It defines the electron density variation as well as the width of the depletion strip. l is proportional to the gate voltage. Its numerical value for $V_g = 1$ V, $n_0 = 10^{11} cm^{-2}$ and $\epsilon = 12.5$ is $l = 2200$ Å. We would like to emphasize that this is a very large length. The typical spacer thickness is about 500 Å. The gate to 2DEG distance is usually of the same order, ≈ 800 Å. This justifies bringing all the charges into one plane. Also for a typical value $a_B = 100\text{Å}$ condition $a_B/l \ll 1$ is satisfied. In a real system we do not expect our solution to be accurate on the scale less than a_B. At large distance from the gate $x \gg l$ Eq.2.10 approximately yields

$$n(x) \approx (1 - l/x)n_0. \tag{2.11}$$

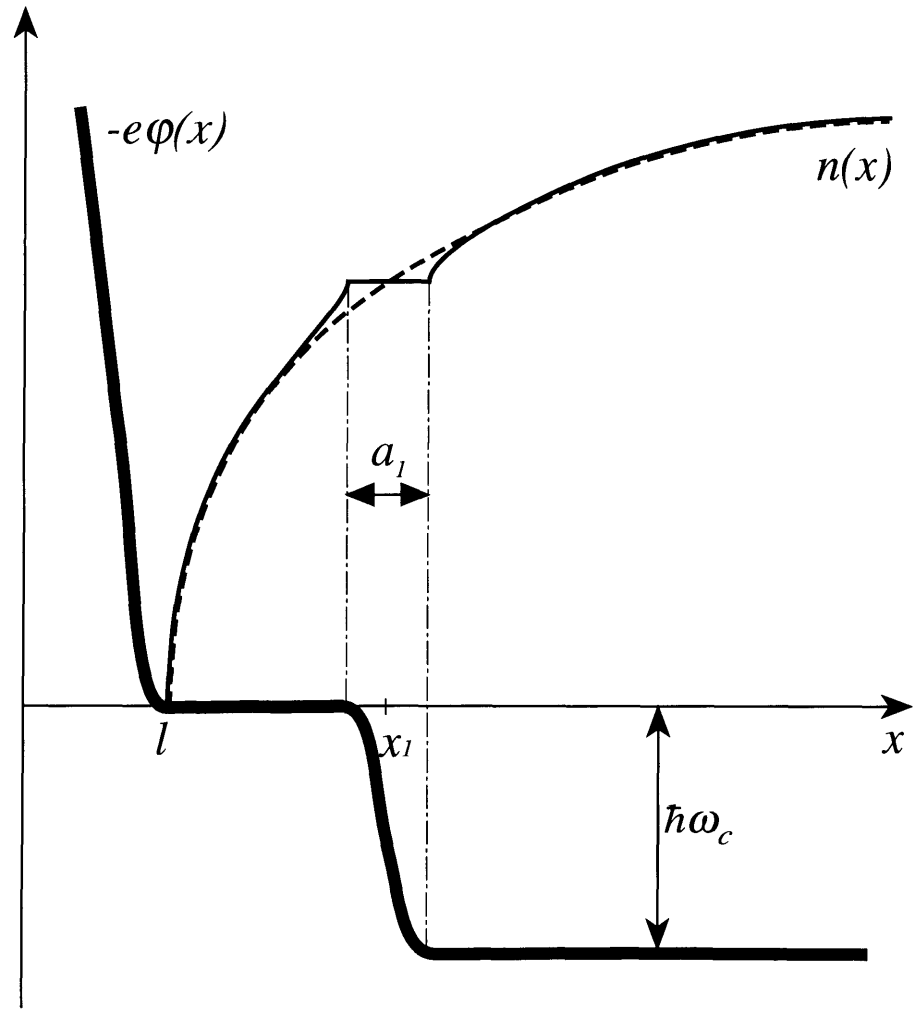

Figure 2-3: 2DEG edge at magnetic field corresponding to the bulk filling factor $\nu_0 = 1.5$. Dashed line is the electron density at zero magnetic field. Full line is the electron density and fat line is the electrostatic energy at $\nu_0 = 1.5$.

Despite the fact that the width of the depletion strip has been found for the gate-confined 2DEG we believe that our result can be also applied to the etched structures. In that case the half-width of the forbidden gap takes the place of the gate voltage due to the pinning of the Fermi level by the surface states. The width of the edge depletion ($2l$ in our notation) has been studied experimentally by Choi, Tsui and Alavi[9]. They obtained the value $5000 \pm 2000\mathring{A}$ for a 2DEG density $n_0 = 1.2\text{x}10^{11} cm^{-2}$, which is in a reasonable agreement with our estimate.

2.3 Dipolar strip formation in high magnetic field

Our next step is to consider the effect of strong magnetic field H in the IQHE regime. Here we ignore the electron spin. Due to the smallness of the parameter $\hbar\omega_c/eV_g$

(where $\omega_c = eH/m_{eff}c$ is a cyclotron frequency) at any reasonable magnetic field we expect that the width of the depletion region given by Eq.2.9 will remain practically unchanged. Also, one might anticipate that the electron density distribution(2.10) obtained from electrostatics will not change significantly. This is because of a huge work needed to be performed against electrostatic forces in order to produce a variation.

The only effect of the magnetic field from the electrostatic point of view is the periodic dependence of 2DEG screening properties on the filling factor ν caused by the oscillations in the density of states . Screening at integer filling factors ($\nu = k, k = 1, 2, 3...$) is absent while at non–integer ν it is very strong. This leads to the formation of the alternating compressible and incompressible liquid regions. The latter ones are characterized by different integer filling factors $\nu = k$ [3],[4]. Near the boundary these regions should take the form of strips parallel to the gate edge. The location of the k-th incompressible liquid strip x_k (measured from the middle of the depletion strip) can be found by substituting $n(x) = k/2\pi\lambda^2$ in Eq.2.10 and solving it for x.

$$x_k = l\frac{n_0^2 + k^2 n_L^2}{n_0^2 - k^2 n_L^2} = l\frac{\nu_0^2 + k^2}{\nu_0^2 - k^2}, \tag{2.12}$$

where we use the notation $n_L = 1/2\pi\lambda^2$ for the electron density corresponding to one completely filled Landau level and $\nu_0 = n_0/n_L$ is the filling factor far away from the boundary.

Let us ignore effects of disorder for a while. Then the density of states is given by a set of δ-functions centered at $(k - 1/2)\hbar\omega_c$ and the screening length r_s as a function of the filling factor takes the following form

$$r_s = \begin{cases} \infty, & \nu = k \\ 0, & \nu \neq k \end{cases} \tag{2.13}$$

This means that the electrostatic potential is constant throughout any one compressible strip just as in metal. Electric field in the incompressible strips is unscreened. Our model is similar to the one proposed in Ref.[10] for a Coulomb island.

For simplicity, we consider initially the 2DEG edge at magnetic fields such that ν_0 satisfies the inequality $1 < \nu_0 < 2$ so that only one incompressible strip is formed. An example of such a situation corresponding to $\nu_0 = 1.5$ is shown in Fig.2-3. The electrostatic solution 2.10 does not now give the minimum energy state, as there is an additional energy cost $\hbar\omega_c$ involved in creating electron density exceeding $\nu = 1$. Clearly we could gain in energy by relocating some of the electrons from the second Landau level to the first one near x_1. This would create a flat region in the density distribution with the density corresponding to $\nu = 1$ (see Fig.2-3). This region is an incompressible strip discussed above. The drop of the potential between its edges should be $\hbar\omega_c/e$, bringing the second Landau level to the Fermi level. On the both sides of the incompressible strip we have a compressible liquid where the electric field is completely screened out. This charge distribution can be thought of as an electrostatic solution (2.10) plus an additional charge causing the voltage drop. We call this additional charge pile up *a dipolar strip* because of its similarity to the

three–dimensional dipole layer.

In order to find the width of the incompressible strip a_1 we need to solve an electrostatic problem similar to the one considered above. We solve the Laplace equation in the half–space $z < 0$ for the given boundary conditions including a_1. Then we find the strip width a_1 from the requirement for electric field to be zero at $x = x_1 \pm a_1/2$. The boundary conditions for this problem are the following

$$\phi'(x, z = 0) = \begin{cases} -V_g, & x < -l \\ 0, & l < x < x_1 - a_1/2 \\ \hbar\omega_c, & x > x_1 + a_1/2, \end{cases} \tag{2.14}$$

$$\left.\frac{d\phi'(x,z)}{dz}\right|_{z\to -0} = \begin{cases} \frac{4\pi e n_0}{\epsilon}, & -l < x < l \\ \frac{4\pi e}{\epsilon}(n_0 - n_L), & |x - x_1| < a_1/2. \end{cases} \tag{2.15}$$

Solution of the Laplace equation can be found as a sum $\phi' = \phi'_1 + \phi'_2 + \phi$ of harmonic functions ϕ'_1, ϕ'_2, and the zero magnetic field solution ϕ. The first two satisfy the conditions

$$\phi'_1(x, z = 0) = \begin{cases} 0, & x < x_1 - a_1/2 \\ \hbar\omega_c, & x > x_1 + a_1/2, \end{cases} \tag{2.16}$$

$$\left.\frac{d\phi'_1(x,z)}{dz}\right|_{z\to -0} = 0, \quad |x - x_1| < a_1/2, \tag{2.17}$$

$$\phi'_2(x, z = 0) = 0, \quad |x - x_1| > a_1/2, \tag{2.18}$$

$$\left.\frac{d\phi'_2(x,z)}{dz}\right|_{z\to -0} = \frac{4\pi e}{\epsilon}(n(x) - n_L) = \frac{4\pi e}{\epsilon}\left.\frac{dn(x)}{dx}\right|_{x=x_1}(x - x_1), \quad |x - x_1| < a_1/2. \tag{2.19}$$

Here we make two approximations based on the smallness of the parameter a_1/x_1 which is confirmed below. First, we extend conditions 2.16,2.18 to include $x < l$. By doing this we neglect the charge distribution tail from the dipolar strip at the distances of order of x_1 away from this strip. Second, we substitute the exact $n(x)$ 2.10 by the first two terms in its Taylor series around x_1 in Eq.2.19. Function ϕ'_1 can be obtained from ϕ_1 by making the following substitutions: $V_g \to \hbar\omega_c$, $l \to a_1/2$,and $x \to x - x_1$. Then ϕ'_2 is obtained in Appendix A. Just as in the case with no magnetic field, both solutions display singularities in electric field E_x at the incompressible strip edges ($x = x_1 \pm a_1/2$). However, due to symmetry of this problem they cancel out on both sides at a same value of a_1 given by

$$a_1^2 = \frac{2\epsilon\hbar\omega_c}{\pi^2 e^2 dn/dx|_{x=x_1}}. \tag{2.20}$$

This equation defines the dipolar strip width. Magnetic field–induced electron density in the dipolar strip is given by (see Fig.2-4)

$$\Delta n = \frac{a_1}{2}\left.\frac{dn}{dx}\right|_{x=x_1} \begin{cases} t, & |t| < 1 \\ t(1 - (1 - t^{-2})^{1/2}), & |t| > 1, \end{cases}$$

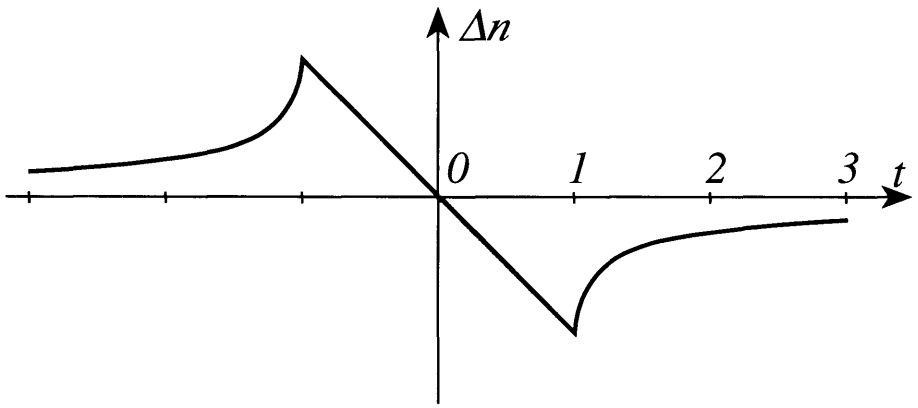

Figure 2-4: Magnetic field–induced additional electron density in the dipolar strip.

in terms of normalized coordinate $t = 2(x - x_1)/a_1$.

Eq.2.20 can be obtained from simple qualitative arguments. On one hand, the drop of electrostatic potential across a dipolar strip is $\hbar\omega_c/e$. On the other hand, it is equal to the characteristic electric field E_x inside the strip $e(dn/dx)|_{x=x_1}a_1/\epsilon$ times its width a_1 thus yielding

$$\frac{e^2 dn/dx|_{x=x_1} a_1^2}{\epsilon} \approx \hbar\omega_c. \tag{2.21}$$

Eq.2.21 gives an estimate for a_1, which coincides with Eq.2.20 up to a numerical factor.

From both the qualitative and quantitative derivations of Eq.2.20 we see that the appearance of the dipolar strip is a property of the 2DEG that is more general than the particular electrostatic problem under study. It arises in any situation when a zero magnetic field 2DEG has small gradient of concentration. This gradient can be caused by the potentials of inhomogeneously distributed ionized donors as well as by gate–induced confinement of 2DEG. The former case was studied by several authors [11, 12, 13]. Efros [14] was the first to propose the qualitative argument leading to Eq. 2.20. His estimate of the width of the regions occupied by incompressible liquid, being expressed in terms of disorder–induced $\bigtriangledown n$, agrees qualitatively with our Eq.2.20.

Let us rewrite Eq.2.20 in terms of filling factor ν_0. From Eq.2.10

$$dn/dx|_{x=x_1} = n_0 \frac{l}{(x_1 + l)(x_1^2 - l^2)^{1/2}}. \tag{2.22}$$

Substituting x_1 from Eq.2.12 in Eq.2.22 and recalling Eq.2.20, we express a_1^2 in terms of ν_0

$$a_1^2 = \frac{8\epsilon\hbar\omega_c l}{\pi^2 e^2 n_L} \frac{\nu_0^2}{(\nu_0^2 - 1)^2} = a_B l f(\nu_0). \tag{2.23}$$

Here, we took into account that $\epsilon\hbar\omega_c/2\pi e^2 n_L$ is the Bohr radius $a_B = \hbar^2\epsilon/m_{eff}e^2$

and $f(\nu_0)$ is a dimensionless function $\frac{16}{\pi}\frac{\nu_0^2}{(\nu_0^2-1)^2}$. Now we are in a position to check the assumption we made about the smallness of a_1. Making use of eq.(12,23) we find

$$\frac{a_1}{x_1} = \frac{4}{\pi^{1/2}}\frac{\nu_0}{\nu_0^2+1}(\frac{a_B}{l})^{1/2}. \tag{2.24}$$

Since $a_B \ll l$ Eq.2.24 justifies the crucial assumption regarding the smallness of the dipolar strip width.

2.4 Alternating strips of compressible and incompressible liquid: quantitative description.

Now we generalize the above consideration to the case when M Landau levels are completely filled far from the edge (M is the integer part of ν_0). Here M dipolar strips form at the edge. Their positions are given by Eq. 2.12. The dipolar strip widths defined by Eq.2.20 are easily generalized for any number $k = 1, ..., M$

$$a_k^2 = \frac{2\hbar\omega_c\epsilon}{\pi^2 e^2 dn/dx|_{x=x_k}}. \tag{2.25}$$

It is helpful to introduce $b_k = x_k - x_{k-1}$, which is essentially the width of the compressible strip to the left from x_k. At $\nu_0 \gg 1$ and $k \gg 1$ it can be found from

$$b_k = \frac{n_L}{dn/dx|_{x=x_k}}. \tag{2.26}$$

Combining equations (25,26) we find

$$a_k^2 = \frac{4}{\pi} b_k a_B, \quad (\nu_0 \gg 1, k \gg 1). \tag{2.27}$$

A key assumption in the derivation of Eq.2.27 is the existence of the concentration gradient dn/dx in the zero magnetic field solution which did not enter the final expression. Hence, the area of applicability of this relation is more general than just the solution for the gate depleted 2DEG boundary. For example, it can be applied to etched structures.

Going back to the original problem we can rewrite Eq.(26,27) using Eq.(10,12) in terms of the filling factor ν_0

$$a_k = \frac{4}{\pi^{1/2}}(a_B l)^{1/2}\frac{\nu_0 k^{1/2}}{\nu_0^2 - k^2}, \tag{2.28}$$

$$\frac{a_k}{b_k} = \frac{1}{(\pi)^{1/2}}\left(\frac{a_B}{l}\right)^{1/2}\frac{\nu_0^2 - k^2}{\nu_0 k^{1/2}}, \quad (\nu_0, k \gg 1). \tag{2.29}$$

We would like to mention here that the boundary conditions (2.19) should be altered for the case where a_k is much smaller than the distance to the surface of the

semiconductor. Then we have

$$\left.\frac{d\phi_2'(x,z)}{dz}\right|_{z\to -0} = \frac{2\pi e}{\epsilon}(n(x)-n_L) = \left.\frac{2\pi e}{\epsilon}\frac{dn(x)}{dx}\right|_{x=x_1}(x-x_1), \quad |x-x_1| < a_1/2 \ (19a)$$

instead of 2.19, leading to the value of a_k larger than in Eq.2.28 by factor $2^{1/2}$. We think that this correction is relevant only for the outer states.

For the inner edge states ($\nu_0 - k \ll \nu_0$) one gets

$$a_k = (\frac{4}{\pi})^{1/2}(a_B l)^{1/2}\frac{\nu_0^{1/2}}{\nu_0 - k}, \tag{2.30}$$

$$\frac{a_k}{b_k} = (\frac{4}{\pi})^{1/2}(\frac{a_B}{l})^{1/2}\frac{\nu_0 - k}{\nu_0^{1/2}}. \tag{2.31}$$

Using $a_B = 100$ Å and $l = 2200$ Å we see that for inner edge states ($\nu_0 - k \approx 1$), although a_k is large, a very strong inequality $a_k/b_k \ll 1$ holds. It means that the approximation of independent and non-interacting dipolar strips used above works well. When we move towards outer edge states, the inequality $a_k/b_k \ll 1$ becomes weaker and eventually fails at small enough k.

Another important condition of validity of our theory is that the compressible liquids on both sides of incompressible strip k should screen well on the scale of a_k, i.e., behave like a good metal. We see two conditions for such behavior: 1)electron(hole) concentration on the $k+1$st(kth) Landau level at the distance a_k from the kth incompressible liquid strip is larger than a_k^{-2},

$$\left(a_k \left.\frac{dn}{dx}\right|_{x=x_k}\right) a_k^2 \gg 1 \tag{2.32}$$

2) The size $\lambda k^{1/2}$ of electron wavefunctions for the kth Landau level satisfies inequality

$$\lambda k^{1/2} \ll a_k \tag{2.33}$$

One can show that at $na_B^2 > 1$ and $k > \nu_0/2$ condition 2.33 is violated earlier than 2.32 with decreasing magnetic field. Using Eq.2.30 we can rewrite 2.33 in the form

$$\lambda \ll \frac{(a_B l)^{1/2}}{\nu_0 - k}, \quad \text{for } \nu_0 - k \ll \nu_0 \tag{2.34}$$

Because of large value of l inequality 2.34 for the inner channels ($\nu_0 - k \approx 1$) does not lead to substantial restrictions. With decreasing k inequality2.34 becomes more critical. We do not think that violation of inequality 2.33 leads to a collapse of the dipolar strip, though our theory is not applicable in this case.

So far we considered the IQHE regime ignoring the spin splitting of Landau levels. The crucial thing in our theory was the presence of a discontinuity in the chemical potential (equal to $\hbar\omega_c$) which led to the formation of incompressible liquid strips.

Thus our theory can be generalized to include electron spin by substituting spin-splitting energy instead of cyclotron energy. In the similar way are formed the edge states in the fractional quantum Hall effect (FQHE) regime. Then the quasiparticle energy gap Δ_f takes place of $\hbar\omega_c$ in our theory[3],[4]. Positions of the incompressible strips (x_f) with filling factors f ($f = p/q = 1/3, 2/3, 1/5, ...$) are given by the slightly modified Eq.2.12

$$x_f = l\frac{\nu_0^2 + f^2}{\nu_0^2 - f^2}. \tag{2.35}$$

Their widths can be found from Eq.2.20, with an extra factor $2^{1/2}$. We use boundary condition (19a) because we anticipate the narrowness of fractional strips;

$$a_f = \left(\frac{4\epsilon q\Delta_f}{\pi^2 e^2 dn/dx|_{x=x_f}}\right)^{1/2} = \frac{4(2qc_f)^{1/2}}{\pi^{1/2}}\frac{\nu_0 f^{1/2}}{\nu_0^2 - f^2}(\lambda l)^{1/2}. \tag{2.36}$$

Here we used expression $\Delta_f = c_f e^2/\lambda\epsilon$ for the fractional energy gap. If Eq. 2.36 yields $a_k < \lambda$, then the incompressible strip does not form.

2.5 Tunneling through the incompressible liquid strip: comparison with experiment

In this section we discuss our theory in relation to two experiments (one in the IQHE regime, the other in the FQHE regime). We start with the IQHE regime. Alphenaar et al.[5] studied equilibration among edge channels using a technique due to van Wees[25]. Current was injected only in the outermost channel, and its redistribution among the remaining channels was measured. It was shown that when filling factor ν_0 decreases in the vicinity of integer occupation ($N-0.3 < \nu_0 < N+0.3$) equilibration length $L_{N-1,N}$ between the $(N-1)$st and Nth channel grows rapidly and becomes too large to be measured at $\nu_0 \approx N - 0.3$. One of the most surprising results was the fact that in spite of a strong dependence of $L_{N-1,N}$ on ν_0 it is a periodic function with the period 1 (for ν_0 varying from 5 to 12). Indeed, functions $L_{N-1,N}(\nu_0)$ for various N collapsed on one curve if presented as functions of $\Delta\nu$. We would like to concentrate on this fact and show that $L_{N-1,N}$ depends on magnetic field only through $\Delta\nu = \nu_0 - N$ for $N \gg 1$.

Tunneling between adjacent edge states is determined by overlap of the corresponding wave functions. Therefore equlibration length $L_{N-1,N}$ depends crucially on the ratio a_{N-1}/λ. Substituting $k = N - 1 \gg 1$ in Eq.2.28 we find

$$a_{N-1}/\lambda = \frac{(8a_B l n_0)^{1/2}}{\Delta\nu + 1} = \left(\frac{eV_g}{\pi^2 E_B}\right)^{1/2}\frac{1}{\Delta\nu + 1}, \tag{2.37}$$

where $E_B = e^2/2a_B\epsilon$ is the Bohr energy of the hydrogen-like impurity in GaAs . This result proves that the equilibration length is a function of $\Delta\nu$ independent of N and explains the striking behavior of $L_{N-1,N}$ vs. ν observed in experiment [5].

Substituting $V_g = 1V$ and $E_B = 6meV$ one gets

$$\frac{a_{N-1}}{\lambda} \approx \frac{4}{\Delta\nu + 1}. \tag{2.38}$$

We see that in the range of interest ($N - 0.3 < \nu_0 < N + 0.3$) ratio a_{N-1}/λ is quite large. It is well-known, that under these conditions even a small amount of disorder increases the tunneling rate [16, 17, 18]. The dependence $\ln L_{N-1,N} \sim (a_{N-1}/\lambda)^2$ that is valid in the "clean case" is altered by disorder and changes the quadratic function in the above estimate to almost linear dependence: $\ln L_{N-1,N} \sim (2a_{N-1}/\lambda)\,[\ln A]^{1/2}$, where $A \gg 1$ at small disorder and decreases with increasing disorder. For the data of Ref.[5] the latter estimate seems to be more appropriate.

It is interesting to mention that the number of completely filled edge states changes by one when $\Delta\nu$ changes sign ($M = N - 1$ for $\Delta\nu < 0$, $M = N$ for $\Delta\nu > 0$) . It means that, in principle, one more equilibration length $L_{N,N+1}$ related to the width a_N may become relevant. But from our point of view under the conditions of Ref.[5] corresponding ratio

$$\frac{a_N}{\lambda} = \left(\frac{eV_g}{\pi^2 E_B}\right)^{1/2} \frac{1}{\Delta\nu} \approx \frac{4}{\Delta\nu} \tag{2.39}$$

for $0 < \Delta\nu < 0.3$ is too large to make equilibration observable and the bulk of the sample is completely decoupled from the Nth channel.

Now we would like to give a more detailed interpretation of the experimental observations made in Ref.[5]. We start with the magnetic field corresponding to ν_0 greater than integer number N ($\nu_0 \approx N + 0.4$). According to our picture there are N incompressible liquid strips dividing 2DEG edge into N edge channels and the bulk region occupied by compressible liquid. Equilibration among N edge channels occurs easily due to small distances between them. However the bulk region is separated from the Nth edge channel by a dipolar strip which is wide enough to prevent their equilibration. At this magnetic field resistance measurement with non–ideal contacts injecting and detecting current in the outermost Landau level only will yield the result $R = h/e^2N$. Now we increase magnetic field thereby decreasing ν_0. This leads to the growth of the widths of dipolar strips. The first dipolar strip to become wide enough to quench equilibration (besides the Nth one which is already very wide) is the $(N-1)$st. This leads to a gradual decoupling of the Nth edge channel. When the value of ν_0 crosses N the Nth dipolar strip becomes infinitely large and disappears creating a new bulk region out of the Nth edge channel to take the place of the old one. However this should not affect the described measurement as the $N + 1$ incompressible region was already uncoupled. As we keep decreasing ν_0, the $(N-1)$st dipolar strip grows wider and wider making the equilibration into Nth channel less likely, making R closer to its value for $N - 1$ channels $R = h/e^2(N - 1)$. Finally, at some value $\nu_0 \approx N - 0.3$, the $(N + 1)$st dipolar strip becomes so wide that no measurable equilibration occurs. Then, we find quantized value of $R = h/e^2(N - 1)$. Further increase of magnetic field does not affect R (forming a plateau on R vs. H plot) until the width of the $(N - 2)$nd dipolar strip becomes large enough to quench equilibration into the $(N-1)$st edge channel. And then the whole cycle repeats itself.

Our theory of edge states provides a satisfactory explanation of experimental observations of the anomalous QHE with so–called non–ideal contacts which probe only some edge channels[5]. In the same experiment[5] the usual "bulk" QHE was observed while using standard probes. There is a significant difference in the physics of "bulk" and anomalous QHE. Quantization of the Hall resistance in the former case is due to the localization of the bulk electron states. Quantization observed with non–ideal probes occurs at different values of magnetic field and is due to the lack of equilibration. This effect is not a macroscopic one (it should vanish in sufficiently long samples) and usually the quantization is not as good as in the "bulk" QHE. While disorder is crucial for the observation of the bulk effect, it may destroy the anomalous QHE. We already discussed disorder–assisted tunneling between the edge states. Now we consider the effect of long–range disorder on the edge states geometry using the approach due to Efros [13, 14, 19].

Spatial scale of the random potential created by the random distribution of donors is of the order of the spacer layer thickness s. Let us use w to designate the amplitude of random potential. If $w < \hbar\omega_c$ and $s < a_k$ then disorder does not change the general structure of alternating compressible and incompressible liquid strips. Changes occur only at the edges of compressible strips where the density of electrons (in almost empty Landau level) or holes (in almost filled Landau level) is less than the charge density needed to compensate the random potential. The strips of localized compressible liquid appear at the edges of compressible strips (see Fig.2-5). Equilibration between delocalized states of compressible liquid involves hopping through localized strips as well as tunneling through the incompressible strip. If temperature is not too low the typical hopping length is of the order of s. It means that even in the presence of disorder with $s < a_k$ equilibration process is dominated by the tunneling on distance a_k. Thus our conclusion about periodical dependence of $L_{N-1,N}$ on ν_0 remains valid when the random potential satisfies conditions $w < \hbar\omega_c$ and $s < a_k$. If disorder is strong ($w > \hbar\omega_c$) then continuous incompressible strips of the width a_k do not exist. Many islands of compressible liquid are formed inside each strip. The only relevant hopping length in this case is s and we can not arrive to the periodical dependence of $L_{N-1,N}$ on ν_0.

Now we turn our attention to the FQHE regime. Let us make an estimate of the positions and widths of the incompressible liquid strips under the conditions of experiment performed by Kouwenhoven et al.[6] This experiment(similar to the one discussed above) was performed at the bulk filling factor $\nu_0 = 1$, and the existence of decoupled fractional edge channel was demonstrated on the lengths exceeding 2μm . According to our theory two dipolar strips are formed at filling factors 1/3 and 2/3. Their positions are (Eq.2.35) $x_{1/3} = \frac{5}{4}l$ and $x_{2/3} = \frac{13}{5}l$. Substituting $V_g = 3$V, $n_0 = 1.8\text{x}10^{11}cm^{-2}$ in Eq.2.9 we get $l = 3600$Å. From Eq.2.36 using $\lambda = 90$Å$(B = 7.8\text{T})$ and $c_{1/3} = c_{2/3} = 0.03$[20] we find

$$a_{1/3} = 350\mathring{A} = 3.8\lambda, \tag{2.40}$$

$$a_{2/3} = 800\mathring{A} = 8.8\lambda. \tag{2.41}$$

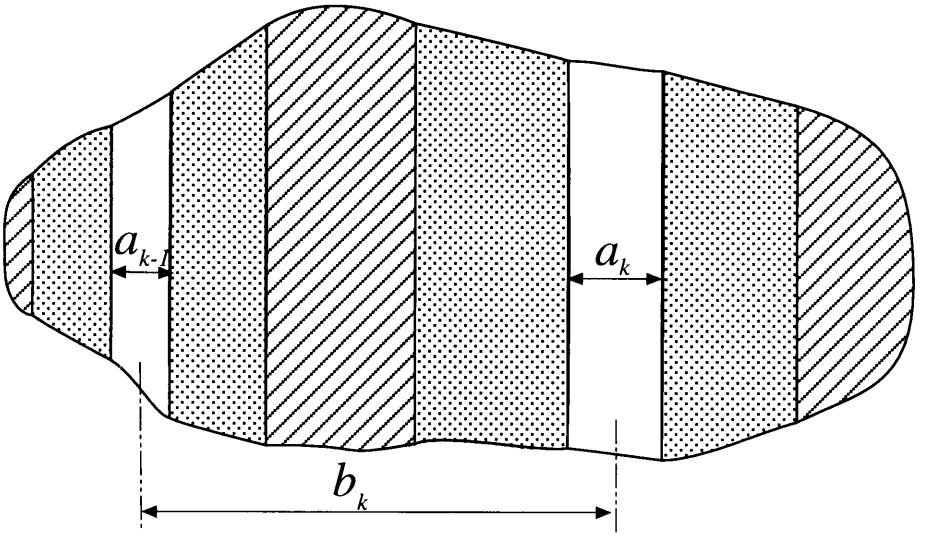

Figure 2-5: Edge channels in the presence of disorder. Shaded areas represent delocalized compressible liquid. Dotted regions are occupied by localized compressible liquid. The rest is incompressible liquid.

This gives the idea why only the innermost channel was decoupled in the experiment[6]. The same measurements were done[6] on another sample with higher electron concentration $n_0 = 2.3\text{x}10^{11} cm^{-2}$ and consequently smaller l at given voltage. At $V_g = 3\text{V}$ no decoupling was observed ($a_{2/3}/\lambda = 5.5$), but at $V_g = 4.5\text{V}$ ($a_{2/3}/\lambda = 6.8$) they saw the decoupling of the innermost channel. These observations are in qualitative agreement with our theory.

2.6 Conclusion

In this chapter we studied the distribution of the electron density in 2DEG near the gate–induced edge. This is an electrostatic problem that can be solved analytically owing to the smallness of the 2DEG screening length in comparison with the depletion width $2l$. In the absence of magnetic field, l is the only relevant length scale for the electron density distribution. Magnetic field does not change this distribution on a rough scale. Exceptions are only narrow strips near the lines where an integer number of Landau levels are fully occupied. A small portion of charge is redistributed forming dipolar strips in the vicinity of those lines. The dipolar strip produces a steep drop in the electrostatic potential which brings the next Landau level to the Fermi level, see Fig.2-1(e). A complete analytical description of dipolar strips is thereby obtained. The width of such a strip of incompressible liquid is much smaller than the width of an adjacent strip of compressible liquid. Moreover, these widths obey the universal relation, Eq.2.27, that does not depend on magnetic field or their distance from the 2DEG boundary. We associate the equilibration between two neighboring edge states with the tunneling through the dividing them dipolar strip. This should give a

better estimate of the equilibration rate than one–electron model, because the dipolar strips are relatively narrow. Formulae for the widths of these strips obtained in this chapter allow us to analyze the dependence of the equilibration length on magnetic field and gate voltage. In particular, we explain the experimentally observed periodic dependence of the rate of equilibration between two innermost edge channels on the filling factor in the IQHE regime. The knowledge of incompressible strips widths was used also to discuss the difference in equilibration rates for 1/3 and 2/3 FQHE edge states.

2.7 Acknowledgements

This work was done in collaboration with B.I. Shklovskii and L.I. Glazman.[45] We are indebted to P.L. McEuen, A.D. Stone, R. G. Wheeler who called our attention to the importance of edge states electrostatics. Authors wish to thank K.A. Matveev for careful reading of the manuscript and making a series of helpful comments. We are grateful to E.B. Foxman, P.A. Lee, P.L. McEuen and I.M. Ruzin for helpful discussions. We would like to thank A.L. Efros and the authors of Ref.[5] for sending us their papers prior to publication. Two of us (L. G. and B. S.) acknowledge their support by the NSF grant no. DMR 91 - 17341. L. G. is also supported by Research Funds of the Graduate School of the University of Minnesota. One of us (D. C.) is supported by the NSF grant no. DMR 89 - 13624.

Chapter 3

Ballistic conductance of interacting electrons in the quantum Hall regime

3.1 Introduction

Magnetotransport of the high–mobility two–dimensional electron gas (2DEG) in narrow channels has attracted significant theoretical and experimental attention in recent years[1]. The quantization of conductance has been observed as a function of magnetic field and channel width [21], and can be explained by employing the concept of edge states that are formed along the lines of constant potential in a high mobility 2DEG[22, 23]. According to the Landauer–Buttiker transmission approach[24, 2], if one ignores backscattering, conductance is given by the number of edge states which pass through a narrow channel.

One-electron picture of a channel is based on the assumption that a smooth parabolic potential bends Landau levels; the positon of the edge states is given by the intersection of Landau levels with the constant Fermi level (see Fig.3-1a–c). According to this picture, as the magnetic field is lowered, narrow edge channels appear in pairs in the middle of the channel. At any given magnetic field there is an even number of edge channels, with half of them going in one direction and the other half in the opposite direction; conductance is strictly quantized in the units of $e^2/2\pi\hbar$. Thus the two–terminal conductance G as a function of magnetic field should vary in a step–like manner, with the plateaus connected by steep rises. This prediction of the one-electron picture does not agree with experiment very well even for short and "clean" channels [25]: rises can have the same extent as the plateaus or be even wider. This disagreement casts doubts on the applicability of the one–electron picture of edge states.

The effect of screening in the presence of a magnetic field was included in a qualitative picture of edge states by Beenakker [3] and Chang [4].

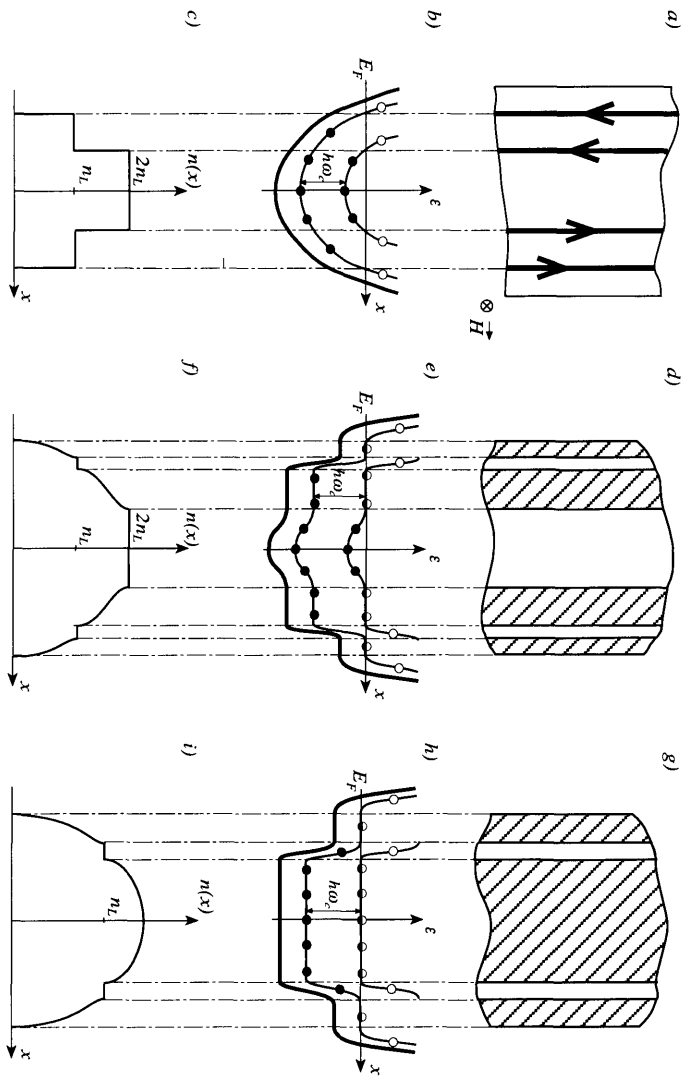

Figure 3-1: Structure of a narrow 2DEG channel in the IQHE regime. (a–c) One-electron picture of edge states. (a) Top view of the narrow 2DEG channel. Arrows designate electron flow direction in the edge states. (b) Adiabatic bending of Landau levels by a smooth external potential. Energy is measured from the Fermi level. Circles represent local filling of the Landau levels: • – occupied and ∘ – empty. (c) Electron density distribution in the channel. (d–i) Self–consistent electrostatic picture. (d–f) Narrow channel of the 2DEG in the I–state. (d) Top view of the 2DEG channel. Shaded strips represent areas with a non–integer filling factor (compressible strips). Unshaded strips represent integer filling factor regions (incompressible liquid). (e) Bending of the electrostatic potential energy and the Landau levels. Circles represent local filling of the Landau levels: • – occupied , ∘ – partially occupied, and ∘ – empty. (f) Electron density distribution in the channel. (g-i) Narrow channel of the 2DEG in the C–state. (g) Top view of the 2DEG channel.(h) Bending of the electrostatic potential energy and the Landau levels. (i) Electron density distribution in the channel.

They divided the electron gas, confined by a slowly varying external potential, into alternating strips of incompressible and compressible liquids, the former originating from the discontinuities of the chemical potential dependence on the filling factor, $\mu(\nu)$. (For the IQHE, incompressible and compressible strips correspond to integer and non–integer numbers of filled Landau levels respectively.) Screening is almost perfect within the compressible strips, which behave like metal strips at constant potential. They are separated by insulator–like incompressible strips where all the potential drops occur. The works of Beenakker[3] and Chang [4] offer only a qualitative picture of edge channels; and left open the question about the widths of compressible and incompressible strips. The quantitative approach was developed recently by Chklovskii *et al.* [45], who showed that the width of a strip of incompressible liquid is much smaller than the width of an adjacent strip of compressible liquid.

Chklovskii *et al.* solved analytically the electrostatics problem for the gate–induced edge of the 2DEG, exploiting the smallness of the screening length in the 2DEG in comparison with the width $2l$ of depletion layer between the gate and the 2DEG. In the absence of magnetic field, l is the only relevant scale for the electron density distribution. Application of magnetic field does not change this distribution on a rough scale. The only exceptions are narrow strips near the lines where an integer number of Landau levels is fully occupied. A small portion of charge is re–distributed forming incompressible *dipolar strips* in the vicinity of those lines. The dipolar strip produces a steep drop in the electrostatic potential which brings the next Landau level to the Fermi level. Chklovskii *et al.* obtained a complete analytical description of the dipolar strip, which agreed with the calculations performed by Kane[27] for a slightly different geometry. Similar results have been obtained by Efros[14] in the theory of screening of a random long–range potential.

In this paper we present a quantitative electrostatic treatment of the narrow channel formed by the gate–induced depletion. In this case electron density has a dome–like shape with characteristic width b which is still much larger than the screening length r_D (equal to the effective Bohr radius a_B in the semiconductor). At the periphery of the channel our results do not differ qualitatively from the description of the edge of the 2DEG occupying a half–plane. New phenomena appear in the center of the channel near the maximum in electron density. Depending on the situation in the center, the channel can be in two different states. In the first state, there is a strip of incompressible liquid in the center of the channel and the total number of compressible strips is even (see Fig.3-1(d–f)). We refer to this situation as an I–state. In the second state the center is occupied by compressible liquid and there is an odd number of compressible strips, Fig.3-1(g–i). We name this a C–state.

Let us start from the C–state at a strong magnetic field and consider a transition to the I–state with decreasing magnetic field. When the magnetic field is lowered, the topmost Landau level becomes completely filled in the middle, which signals the appearance of the new incompressible strip in the center (C–I transition). Electrons that would be in the middle in the absence of magnetic field are now pushed aside due to the gap in the electron spectrum. Charge redistribution creates what we call a *quadrupolar strip*: additional charge density is positive in the center and negative

on the sides. The potential from the quadrupolar strip lowers the first empty Landau level, and with decreasing magnetic field eventually brings it to the Fermi level. This induces the appearance of the new compressible strip in the center (I–C transition) which splits the quadrupolar strip into two dipolar strips of opposite polarity. In this work we present an analytic solution for the quadrupolar strip based on the existence of the small parameter a_B/b, and calculate the values of magnetic field at which all the described C–I and I–C transitions occur. The range of magnetic field at which an I–state exists turns out to be narrower than the range of the adjacent C–state .

The ultimate goal of this paper is to formulate a theory for the magnetoconductance of a narrow channel. The two–probe conductance G in the I–state was considered by Beenakker[3] for the fractional quantum Hall regime. An extension of his approach to the case of interacting electrons in the integer quantum Hall regime gives

$$G = \frac{e^2}{2\pi\hbar}k, \tag{3.1}$$

where $k = 0, 1, 2, 3...$ is the number of Landau levels occupied in the central incompressible strip. This result coincides with the prediction of the one–electron picture of edge states [22],[2], but is valid only for the range of magnetic fields corresponding to the I–state. In the C–state a new question of the conductance of the central compressible strip arises. The contribution of the partially filled Landau level to the two–terminal conductance measurement depends crucially on the presence of disorder. In a long channel with a sufficient degree of disorder, the conductance of the central strip is much smaller than $e^2/2\pi\hbar$ and can be neglected. Here we deal with the opposite case of the short channel and therefore neglect the influence of disorder. In this case the two–terminal conductance is quantized only in the I–state. We calculate the widths of the plateaus and the shape of the rises using a general expression for conductance:

$$G = \frac{e^2}{2\pi\hbar}\nu_H(0). \tag{3.2}$$

In this equation the occupation number $\nu_H(0) = n_H(0)/n_L$, where $n_H(0)$ is the electron concentration in the center of the channel as a function of magnetic field, and n_L is the electron density of one completely filled Landau level. Eq.(3.2) is proven below for one simple case, and we make the hypothesis that it is true in general. In the I-state Eq.(3.2) is reduced to Eq.(3.1).

One can view Eq.(2) as a simple generalization of the Landauer-Buttiker transmission approach to a C-state. One can imagine that the central compressible strip is symmetrically divided into an even number of "substrips" or "subchannels" running along the lines of constant density. Then, like in the coventional transmission approach, subchannels on the right and left sides of the compressible liquid acquire electrochemical potential of the two opposite terminals. The electrochemical potential drop occurs in the center of the strip, where the whole non-equilibrium current is concentrated. This explains why the two-terminal conductance is proportional to the concentration in the center of the channel.

It is natural to present the dependence of G on H using instead of a magnetic field an occupation number $\nu(0) = n(0)/n_L$, where $n(0)$ is the density in the center

of the channel at $H = 0$. The corresponding plot (see Section 3.4) shows plateaus of constant $\nu_H(0)$ when the channel is in the I-state, as well as the deviation of $\nu_H(0)$ from $\nu(0)$ on the rises corresponding to the C-state. Note that plateaus are substantially narrower than the rises. This is the main result presented in the paper.

This seems to differ from the conventional transmission approach which predicts almost vertical rises for a one-dimensional channel. We would like to explain the origin of this descrepancy. Both theories give steep rises as a function of the Fermi level. The difference is that if one takes a parabolic self-consistent potential (this was usually done in the one-electron picture) than steep rises as a function of the Fermi level translate into steep rises as a function of external parameters such as magnetic field H or gate voltage V_g. In our theory the self-consistent potential (or better to say electron energy) is very peculiar: due to the metallic screening it is constant within a compressible strip. This means that steep rises as a function of the Fermi level translate into smooth rises as a function of external parameters H and V_g.

We begin (Section 3.2) with the model for the gate–induced 2DEG channel and the charge distribution at zero magnetic field. In section 3.3 we study the influence of high magnetic field on the distribution of electron density. We consider in detail the redistribution of charge near the center of the channel forming the quadrupolar strip. In Section 3.4 we discuss magnetotransport in a narrow channel under the conditions of a two–terminal measurement. Section 3.5 contains the derivation and discussion of Eq.(3.2). In Section 3.6 we apply our theory to a quantum point contact which is a practical realization of a narrow channel. Section 3.7 contains our major conclusions.

3.2 Electron density distribution at zero magnetic field

We adopt a simplified model of the split–gate device on the GaAs/AlGaAs heterostructure, proposed by Glazman and Larkin[7], and Larkin and Shikin[28]. In this model (see Fig.3-2), ionized donors are represented by a uniform positive background of constant two–dimensional charge density en_0. Far from the gates the 2DEG compensates for the positive background, so the electron concentration in the bulk is equal to n_0. The split gate is represented by two semi–infinite metal planes separated by the gap centered at $x = 0$. The width of this gap is $2d$. Negative voltage V_g is applied to both halves of the gate, depleting the 2DEG underneath them, and confining the electrons to a narrow channel. The whole system is translationally invariant along the y-axis. In the model considered the positive background, the split gate, and the 2DEG are all in the same plane $z = 0$ (Fig.3-2), a simplification we will justify later. The half–space $z < 0$ is occupied by a semiconductor with a high dielectric constant $\epsilon \gg 1$. Since a_B is much less than the characteristic length scale of the density distribution, the screening radius of the 2DEG is taken to be zero. Then the 2DEG in the channel behaves much like a metal strip of width $2b$, differing only in that the edges of the 2DEG can move. Thus we have to include a condition for them to be in mechanical equilibrium: the x-component of electric field should be zero both to the left and to the right of each edge.

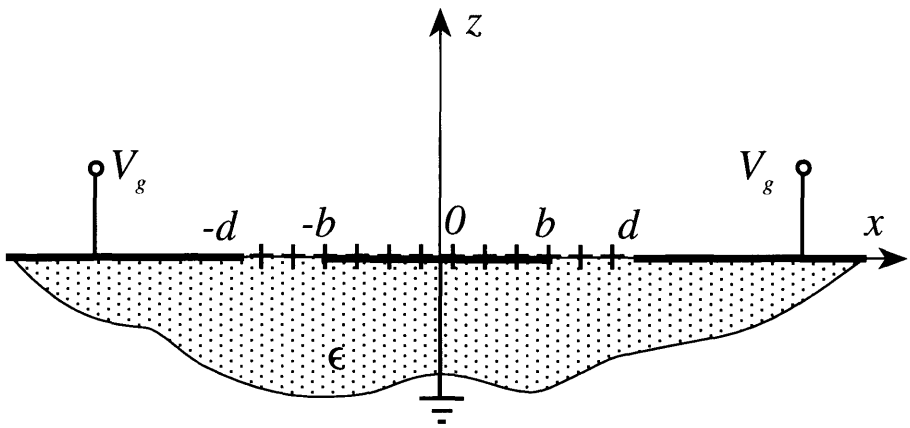

Figure 3-2: Electrostatic system formed in a narrow 2DEG channel. Thick lines represent conductors: split gate at potential V_g with the grounded 2DEG in the middle. Plusses represent a uniform positive background due to ionized donors. Dotted area is occupied by a semiconductor with high dielectric constant ϵ, while the half-space $z > 0$ is vacuum.

The problem is reduced to the solution of the Laplace equation $\Delta\phi = 0$ in the half-space $z < 0$, with mixed boundary conditions:

$$\phi(x, z = 0) = \begin{cases} 0, & |x| < b, \\ V_g, & |x| > d, \end{cases} \tag{3.3}$$

$$\left.\frac{d\phi(x,z)}{dz}\right|_{z\to -0} = -E_z(x,z)|_{z\to -0} = \frac{4\pi e n_0}{\epsilon}, \quad b < |x| < d. \tag{3.4}$$

Positioning of all the charges at the interface of two media with dielectric constants ϵ and 1 leads to a factor $4\pi/(\epsilon + 1) \approx 4\pi/\epsilon$ in Eq.(3.4). In order to ensure mechanical equilibrium of the 2DEG edges at $x = \pm b$, we set

$$E_x(x, z = 0)|_{x\to -b-0} = E_x(x, z = 0)|_{x\to b+0} = 0. \tag{3.5}$$

The solution of the Laplace equation satisfying conditions (3.3),(3.4),(3.5) was given by Larkin and Shikin[28]. They found an electron density distribution

$$n(x) = n_0 \left(\frac{b^2 - x^2}{d^2 - x^2}\right)^{1/2} \tag{3.6}$$

in the 2DEG. The half–width of the 2DEG strip b can be found by solving the equation

$$V_g = -\frac{4\pi e n_0 d}{\epsilon}\left[\mathrm{E}\left(\sqrt{1 - b^2/d^2}\right) - \frac{b^2}{d^2}\mathrm{K}\left(\sqrt{1 - b^2/d^2}\right)\right], \tag{3.7}$$

where E(x), K(x) are complete elliptic integrals. It was also pointed out in Ref.[28] that near the pinch-off, when $b \ll d$, electron density distribution is close to that formed in a parabolic confining potential in the perfect screening approximation,

$$n(x) \approx n_0 \frac{(b^2 - x^2)^{1/2}}{d}. \tag{3.8}$$

In the opposite limit, $2l \equiv d - b \ll d$, the two edges can be treated independently, and each of them is described by the formulas of Ref.[45].

Bringing all the charges into the same plane is justified if $d - b$ and b are much larger than the spacer thickness and the distance between the gate and the 2DEG plane. Let us check this condition for the channel of lithographic width $2d = 5000$Å: for $V_g = -1$V, $n_0 = 4 \cdot 10^{11}\text{cm}^{-2}$ and $\epsilon = 12.5$ we find $2b = 2600$Å. This length, as well as $d - b$, is much larger than the spacer layer thickness and the distance from the 2DEG to the gate. These numbers also confirm the validity of the perfect screening approximation since in GaAs $a_B = 100\text{Å} \ll b$.

Despite the fact that this electron density distribution has been found for the gate-confined 2DEG, we believe that the result can also be applied to etched structures. In that case the half-width of the forbidden gap would take the place of the gate voltage in Eq.(3.3,3.7) due to the pinning of the Fermi level by the surface states.

3.3 Narrow channel in a strong magnetic field: formation of the quadrupolar strip

Let us consider the effect of strong magnetic field H on the 2DEG in a narrow channel, while neglecting electron spin. Due to the smallness of the parameter $\hbar\omega_c/eV$ ($\omega_c = eH/m_{eff}c$ is a cyclotron frequency) at any reasonable magnetic field, we expect that the electron density distribution(3.6) obtained from electrostatics will not be altered significantly. This is because of the huge amount of work which must be performed against electrostatic forces in order to produce any variation.

The only effect of the magnetic field on electron density distribution is due to the periodic dependence of screening properties of the 2DEG on the filling factor ν, caused by the oscillations in the density of states. The density of states is given by a set of δ-functions centered at $(k - 1/2)\hbar\omega_c$. The screening length r_D as a function of the filling factor takes the following form:

$$r_D = \begin{cases} \infty, & \nu = k \\ 0, & \nu \neq k, \end{cases} \tag{3.9}$$

i.e. screening at integer filling factors is absent while at non–integer ν screening is very strong. This leads to formation of the alternating strips of compressible and incompressible liquid[3, 4]. The electrostatic potential remains constant throughout any one compressible strip, whereas it changes by $\hbar\omega_c$ between the inner and outer edges of an incompressible strip . As was shown in Ref.[45], incompressible strips are narrower than compressible ones. Their locations can be found by solving the

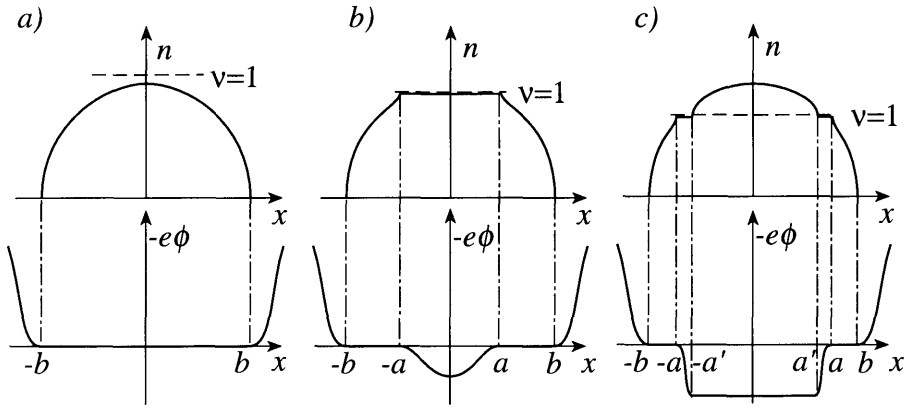

Figure 3-3: Evolution of the potential and 2DEG density distribution with decreasing magnetic field.

equation $n(x) = kn_L$ using $n(x)$ from Eq.(3.6) .

First, we would like to discuss qualitatively what happens as magnetic field is lowered slowly, starting from a value high enough for all electrons in the channel to be on the first Landau level. Our results will be presented in terms of the quantity

$$\nu(0) = \frac{n(0)}{n_L} = \frac{b}{d}\frac{n_0}{n_L}, \tag{3.10}$$

where $n(0) = n(x)|_{x=0}$ stands for the electron concentration in the absence of magnetic field. Initially, when $\nu(0) < 1$ the electron density distribution is well–described by Eq.(3.6), and illustrated in Fig.3-3(a). (Here we ignore the FQHE.) At the moment, when $\nu(0) = \nu_1 = 1$ a flat region, $n(x) = n_L$, starts to develop in density distribution(Fig.3-3(b)), thus indicating the first C-I transition. The new density distribution $n_H(x)$ can be thought of as the solution $n(x)$ obtained without magnetic field (Eq.(3.6)), plus some redistributed density $\Delta n(x)$ (see Fig.refcdn(a)) . The distribution $n(x)$ can be approximated near its maximum as

$$n(x) = n(0) + \frac{1}{2}n''x^2, \tag{3.11}$$

where $n'' = \frac{d^2n}{dx^2}|_{x=0}$. The redistributed electron density has the form

$$\Delta n(x) = n_L - n(x) = n_L - n(0) - \frac{1}{2}n''x^2. \tag{3.12}$$

One can see that $\Delta n(0) < 0$ when $n_L < n(0)$, and that $\Delta n(x)$ changes sign at some x ($n'' < 0$, see Fig.3-4(b)). Eq.(3.12) is valid only within the incompressible strip. One can see from Eq.(3.12) that the magnetic field–induced redistribution of charge has a quadrupolar character: redistributed charge $-e\Delta n(x)$ is positive in the middle and negative on the sides.

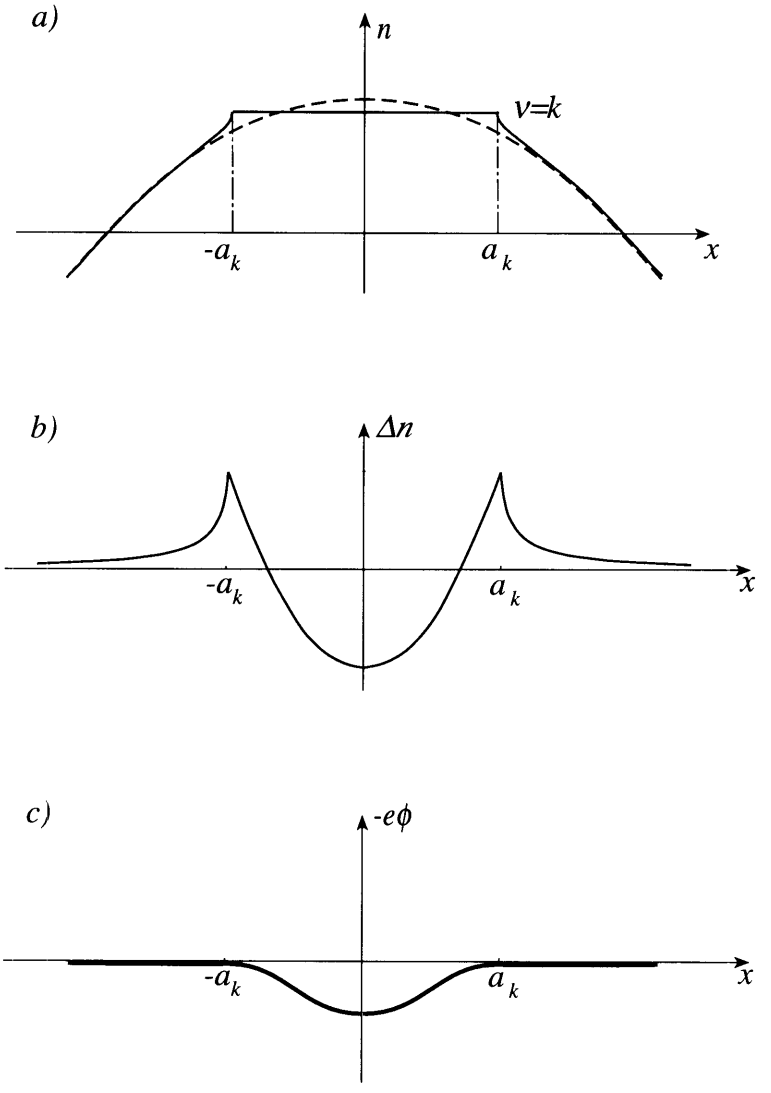

Figure 3-4: The quadrupolar strip.(a) Magnetic field–induced electron density re–distribution near the center of the channel.(b) Magnetic field–induced additional electron density in the quadrupolar strip.(c) Electron potential energy as a function of position.

If one considers the dipolar strip of Ref.[45]-[14] as reminiscent of a $p-n$ junction, then the quadrupolar strip can be said to resemble a $p-n-p$ structure.

The quadrupolar strip creates a minimum of potential energy in its center (see Fig.3-4(a),3-3(b)). As $\nu(0)$ increases further and the depth of this minimum reaches the value of $\hbar\omega_c$, electrons start to fill up the second Landau level ($\nu(0)=\nu_1'$). This leads to the formation of a new compressible strip in the middle of the incompressible one, indicating the first I-C transition. Simultaneously, the quadrupolar strip breaks into two dipolar strips of the opposite polarity.

Let us estimate the width of the incompressible strip at the I-C transition. The depth of the potential well $\Delta\phi$ in the center of the quadrupolar strip is of the order of the characteristic electric field $E \approx e|n''|a^2/\epsilon$ times ea, and the new compressible strip appears at $x=0$ when $\Delta\phi=\hbar\omega_c$ or

$$\frac{e^2|n''|a^3}{\epsilon}=\hbar\omega_c. \tag{3.13}$$

Eq.(3.13) gives

$$a \approx \left(\frac{\epsilon\hbar\omega_c}{e^2|n''|}\right)^{1/3} \approx \frac{(a_B b^2)^{1/3}}{(1-(b/d)^2)^{1/3}}, \tag{3.14}$$

where $a_B=\epsilon\hbar^2/m_{eff}e^2$ is the Bohr radius in the semiconductor and we used expression

$$|n''|=n_0\frac{1}{bd}(1-\frac{b^2}{d^2})=n(0)\frac{1}{b^2}(1-\frac{b^2}{d^2}) \tag{3.15}$$

that follows from Eq.(3.6).

Using Eq.(3.14) we obtain for the interval $\Delta\nu_1$ of the filling factor $\nu(0)$ corresponding to the first I–state

$$\Delta\nu_1=\nu_1'-\nu_1 \approx \frac{|n''|a^2}{n_L} \approx \left(\frac{a_B}{b}\right)^{2/3}(1-\frac{b^2}{d^2})^{1/3}, \tag{3.16}$$

up to a numerical factor which can not be obtained in this estimate. One can see that in the limit of wide channel $\Delta\nu_1$ goes to zero.

We now move from order of magnitude estimates to the exact analytical theory of the kth quadrupolar strip, formed when k Landau levels are filled in the center. This theory yields numerical factors omitted in Eq.(3.14),(3.16). The theory is based on the fact that the half–width of the incompressible strip a is much smaller than the widths of the adjacent compressible strips. (One can see this from Eq.(3.14) keeping in mind that a_B is the smallest length in the problem.) The charge distribution can then be thought of as the one described by Eq.(3.6) plus some additional charge which is localized in the vicinity of $x=0$ due to the magnetic field.

We can now find the additional charge distribution by solving an electrostatics problem, where compressible strips are represented by the grounded plates of a two–dimensional capacitor. These plates are taken to be semi–infinite because they are much wider than the incompressible strip in between. The gap between two plates (of the width $2a$) is filled by a charged insulator. We must solve the Laplace equation

in the half–space $z < 0$ with mixed boundary conditions:

$$\phi(x, z = 0) = 0, \quad |x| > a, \tag{3.17}$$

$$E_z(x, z)|_{z\to -0} = -\frac{2\pi e}{\epsilon}(\frac{n''}{2}x^2 + (\nu(0) - k)n_L), \quad |x| < a. \tag{3.18}$$

Here we use a boundary condition(3.18) which differs from Eq.(3.4) by a factor of 2. This is because we anticipate the width of the quadrupolar strip to be much smaller than the distance from the 2DEG plane to the surface, which implies that the electric field is concentrated within the semiconductor. The approximation of semi–infinite plates can only be justified if we find a solution in which electric field E_z decays at large distances from the gap. Thus we set a condition

$$\lim_{x\to+\infty} E_z(x, 0) = \lim_{x\to-\infty} E_z(x, 0) = 0. \tag{3.19}$$

We also have the condition of mechanical equilibrium at the edges which is similar to Eq.(3.5):

$$E_x(x, z = 0)|_{x\to a-0} = E_x(x, z = 0)|_{x\to -a+0} = 0. \tag{3.20}$$

This problem can be solved by employing the methods of complex analysis. (As an alternative, the less general but very simple method involving Chebyshev polynomials is presented in the Appendix B.) Because ϕ is the solution of the Laplace equation, it can be viewed as the imaginary part of an analytic function $F(\zeta)$, where $\zeta = x + iz$. The electric field is then given by

$$E_x = -\mathrm{Im}\left[\frac{dF}{d\zeta}\right], \tag{3.21}$$

$$E_z = -\mathrm{Re}\left[\frac{dF}{d\zeta}\right]. \tag{3.22}$$

The solution satisfying conditions (3.17,3.18) and having the correct behavior at infinity(3.19) is given by

$$\frac{dF}{d\zeta} = \frac{2\pi e}{\epsilon}\left\{(\nu(0) - k)n_L\left(1 - \frac{\zeta}{\sqrt{\zeta^2 - a^2}}\right) + \frac{n''}{2}\left(\zeta^2 - \frac{\zeta^3 - \zeta a^2/2}{\sqrt{\zeta^2 - a^2}}\right)\right\}. \tag{3.23}$$

In general this solution has singularities in the electric field at $x = \pm a$. Therefore it satisfies the equilibrium condition (3.20) only if

$$(\nu(0) - k)n_L + n''a^2/4 = 0. \tag{3.24}$$

Then

$$\frac{dF}{d\zeta} = -\frac{\pi e n''}{\epsilon}\left\{\frac{a^2}{2} - \zeta^2 + \zeta\sqrt{\zeta^2 - a^2}\right\}. \tag{3.25}$$

By making use of Eq.(3.22), we find the redistributed electron density in the quadrupo-

lar strip (see Fig.3-4(b))

$$\Delta n(x) = \frac{n''}{2} \begin{cases} \frac{a^2}{2} - x^2, & |x| < a \\ \frac{a^2}{2} - x^2 + x\sqrt{x^2 - a^2}, & |x| > a. \end{cases} \tag{3.26}$$

It follows from Eq.(3.25) that the electrostatic potential in the strip is given by

$$\phi(x, z = 0) = -\frac{\pi e n'' a^3}{3\epsilon}(1 - (x/a)^2)^{3/2}, \tag{3.27}$$

which has a maximum at $x = 0$. Electrons start to fill up the $k+1$th Landau level ($\nu(0) = \nu'_k$) when

$$\phi(x = 0, z = 0) = \frac{\pi e |n''| a_k^3}{3\epsilon} = \hbar\omega_c/e. \tag{3.28}$$

Thus

$$a_k = \left(\frac{3\epsilon\hbar\omega_c}{\pi e^2 |n''|}\right)^{1/3}, \tag{3.29}$$

$$\Delta\nu_k = \nu'_k - k = \frac{|n''| a_k^2}{4n_L} = \left(\frac{9|n''|}{16 n_L}\left(\frac{\epsilon\hbar\omega_c}{2\pi e^2 n_L}\right)^2\right)^{1/3}. \tag{3.30}$$

Finally, by noticing that $\epsilon\hbar\omega_c/2\pi e^2 n_L = a_B$, recalling that a_B/b is a small parameter and using Eq.(3.15) we find

$$a_k = \left(\frac{6}{k(1 - b^2/d^2)}\right)^{1/3} (a_B b^2)^{1/3}, \tag{3.31}$$

$$\Delta\nu_k = (\nu'_k - k) = \left(\frac{9}{16} k(1 - b^2/d^2)\right)^{1/3} \left(\frac{a_B}{b}\right)^{2/3}. \tag{3.32}$$

Eqs. (3.31,3.32) give the numerical factors omitted in the qualitative derivation, as well as the dependence on the total number of filled Landau levels in the channel k. Let us estimate $\Delta\nu_k$ and a_k using $b = 1300$Å $\ll d$ and $a_B = 100$Å. In this case we obtain $a_k = 1000/k^{1/3}$Å and $\Delta\nu_k = 0.15k^{1/3}$. One can see that the inequality $a_B \ll a_k$ holds when k is not very large,while at the same time the inequality $a_k \ll b$ is not valid for small k. It is possible to describe the problem with an exact system of equations, valid also when $a_k \approx b$. The numerical solution of this system of equations for $k = 1$ yields a value of $\Delta\nu_1$ which is only 10% greater than the one given by Eq.(3.32).

Let us now verify the validity of an important assumption in our theory, namely that the compressible strips on both sides of the central one screen well on the scale of a_k, i.e., behave like a good metal. We see two conditions of such behavior.

The first condition is related to the discreteness of the electron gas. The 2DEG can not screen well on the distances less than an average distance between electrons. The similar statement can be made about the screening by holes of the almost filled kth Landau level. Therefore the hole concentration on the kth Landau level at a

distance a_k from the central incompressible strip is larger than a_k^{-2}, i.e.

$$n'' a_k^4 \gg 1. \tag{3.33}$$

The second condition is related to a large characteristic length (size) of the wavefunction for electrons on high Landau levels (large k). In the quasiclassical approach valid for $k \gg 1$ this length is given by the cyclotron radius $\lambda\sqrt{k}$, where $\lambda = \sqrt{\hbar c/eH}$ is the magnetic length. Local relationships between the filling factor $\nu(x)$ and the charge density, as well as between electrostatic potential and electron energy, used in our theory are valid only at lengthscales larger than $\lambda\sqrt{k}$. This is why for the applicability of our theory the inequality

$$\lambda\sqrt{k} \ll a_k \tag{3.34}$$

should hold.

One can show that at $n(0)a_B^2 > 1$, condition(3.34) is violated earlier than condition(3.33) when the magnetic field is lowered. Using Eq.(3.31) we can rewrite (3.34) in the form

$$k < k_{c1} \equiv \sqrt{\frac{b}{a_B}}(n(0)a_B^2)^{3/8}. \tag{3.35}$$

This means that for the parameters used above, Eq.(3.32,3.31) are valid for the first several plateaus.

So far we have considered the case of spinless electrons. Our theory was based on the presence of a discontinuity in the chemical potential $\Delta\mu_k$ equal to $\hbar\omega_c$ at any integer occupation number k. In a real situation, however, $\Delta\mu_k$ is not equal to $\hbar\omega_c$, and the existence of electron spin makes $\Delta\mu_k$ explicitly dependent on k. In particular, $\Delta\mu_k$ at odd k is determined by the spin–splitting, therefore we expect it to be smaller than $\Delta\mu_k$ at even k. In order to find a_k and $\Delta\nu_k$ for a given discontinuity in the chemical potential, we substitute $\Delta\mu_k$ in place of $\hbar\omega_c$ in Eq.(3.29,3.30). This gives us the correct values of a_k and $\Delta\nu$:

$$a_k = \left(\frac{3\epsilon\Delta\mu_k}{\pi e^2|n''|}\right)^{1/3}, \tag{3.36}$$

$$\Delta\nu_k = \nu_k' - k = \left(\frac{9|n''|}{16n_L}\left(\frac{\epsilon\Delta\mu_k}{2\pi e^2 n_L}\right)^2\right)^{1/3}. \tag{3.37}$$

At low enough temperatures, formation of the incompressible liquid becomes possible at fractional filling factors $f = p/q$, where q is an odd number and p is an integer number. This is due to the discontinuity in the chemical potential related to the FQHE. The number of the incompressible strips formed is determined by the temperature and the level of disorder. The incompressible liquid is characterized by

the energy gap necessary to create a pair of quasiparticles with the charges $\pm e/q$

$$\Delta_f = c_f \frac{e^2}{\epsilon\lambda}, \tag{3.38}$$

where c_f is a small numerical factor. Thus the discontinuity in the chemical potential for the electrons $\Delta\mu_f$ at $\nu = f$ is

$$\Delta\mu_f = q\Delta_f = qc_f \frac{e^2}{\epsilon\lambda}. \tag{3.39}$$

Substituting Eq.(3.39) in Eqs.(3.36,3.37), we find

$$a_f = \left(\frac{6qc_f}{f(1-b^2/d^2)}\right)^{1/3} (\lambda b^2)^{1/3}, \tag{3.40}$$

$$\Delta\nu_f = \left(\frac{9}{16} f(qc_f)^2(1-b^2/d^2)\right)^{1/3} \left(\frac{\lambda}{b}\right)^{2/3}. \tag{3.41}$$

3.4 Two–terminal magnetoconductance.

We now consider magnetoconductance of a short channel where disorder–caused scattering can be totally neglected. Conductance of such a channel in the I–state was derived by Beenakker for the fractional quantum Hall regime[3]. Applying similar ideas to the integer quantum Hall regime gives quantization of conductance in units of $e^2/2\pi\hbar$, which is the same result as in the one–electron picture of edge states[22],[23]. As shown above, intervals of $\nu(0)$ in which the I–state exists ($\nu_k < \nu(0) < \nu_k'$) are quite narrow (Eq.(3.32)). At other values of $\nu(0)$ the channel is in the C–state, meaning that there is a compressible liquid strip in the center of the channel. We could not find in the literature any discussion of the conductance of such a strip. We calculate its conductance in the next section, accounting for Coulomb interaction in the mean–field framework only, and arrive at a very simple expression (Eq.(3.2)) for G . It gives a very natural and continuous transitions between plateaus. At this point, we are not able to prove Eq.(3.2) rigorously for an electron liquid in which correlations are allowed, but we believe that Eq.(3.2) is generally true. In this section, we will calculate $\nu_H(0)$ and then $G(H)$, using Eq.(3.2) as a plausible hypothesis.

If $\nu(0) < 1$, all the electrons are on the first Landau level and have a very short screening radius. (We neglect the FQHE here.) This means that the charge distribution is given by Eq.(3.6), the same as at zero magnetic field. Therefore $\nu_H(0) = \nu(0)$, and from Eq.(3.2) we find

$$G = \frac{e^2}{2\pi\hbar}\nu(0) \qquad \text{at} \qquad \nu(0) < 1. \tag{3.42}$$

At $\nu(0) > 1$, incompressible strips are present and the calculation of $\nu_H(0)$ in the C–state becomes more complicated. We will perform it in the case when the central

compressible strip is narrower then the two adjacent incompressible strips. Then, following the approach of Section 3.3, we consider an electrostatics problem of two conducting semi–planes representing compressible regions and separated by a gap of width $2a$. However, we now have a conducting strip of the width $2a'$ in the gap between them. Additional charge in the incompressible region $a' < |x| < a$ is described by Eq.(3.12), so we have now to solve the Laplace equation with the following boundary conditions:

$$\phi(x, z = 0) = \begin{cases} 0, & |x| > a \\ \frac{\hbar\omega_c}{e}, & |x| < a', \end{cases} \tag{3.43}$$

$$E_z(x, z)|_{z\to -0} = -\frac{2\pi e}{\epsilon}(\frac{n''}{2}x^2 + (\nu(0) - k)n_L), \quad a' < |x| < a. \tag{3.44}$$

To ensure the mechanical equilibrium of the 2DEG edges at $|x| = a', a$ we set

$$E_x(x, 0)|_{x\to -a+0} = E_x(x, 0)|_{x\to a-0} = E_x(x, 0)|_{x\to -a'-0} = E_x(x, 0)|_{x\to a'+0} = 0. \tag{3.45}$$

The condition of the proper behavior at infinity is given by

$$\lim_{x\to+\infty} E_z(x, 0) = \lim_{x\to-\infty} E_z(x, 0) = 0. \tag{3.46}$$

Once again we use complex variables and find the solution in terms of $dF/d\zeta$, which is related to the electric field as described by Eq.(3.21,3.22).

$$\frac{dF}{d\zeta} = \frac{2\pi e}{\epsilon}\left(\left(\zeta^2 - \sqrt{(a^2 - \zeta^2)(a'^2 - \zeta^2)}\right)\frac{n''}{2} + (\nu(0) - k)n_L\right), \tag{3.47}$$

where a and a' should also satisfy

$$(\nu(0) - k)n_L + n''\frac{a^2 + a'^2}{4} = 0 \tag{3.48}$$

in order to fulfill (3.46). Also

$$\frac{\pi e|n''|}{\epsilon}\int_{a'}^{a} dx\sqrt{(a^2 - x^2)(x^2 - a'^2)} = \frac{\hbar\omega_c}{e}. \tag{3.49}$$

The last equation can be rewritten in terms of elliptic integrals[32]

$$\frac{\pi e|n''|a}{3\epsilon}\left\{(a^2 + a'^2)\mathrm{E}\left(\sqrt{1 - (a'/a)^2}\right) - 2(a')^2\mathrm{K}\left(\sqrt{1 - (a'/a)^2}\right)\right\} = \frac{\hbar\omega_c}{e}. \tag{3.50}$$

From Eq.(3.47) the difference between the electron density at $x = 0$ with and without the magnetic field is

$$\nu(0) - \nu_H(0) = \frac{|n''|(a - a')^2}{4n_L} = \frac{(a - a')^2}{a^2 + a'^2}(\nu(0) - k). \tag{3.51}$$

Equations (3.48,3.50,3.51) represent a complete system from which $\nu_H(0)$ can be

found. In the two limiting cases, it yields equations consistent with the earlier results. Setting $a' = 0$ in Eq.(3.50), one arrives at Eq.(3.28). When $a - a' \ll a$, Eq.(3.50) is reduced to

$$\frac{\pi^2 e|n''|}{4\epsilon}(a-a')^2 a = \frac{\hbar\omega_c}{e}. \tag{3.52}$$

By making use of Eq.(3.51) we find

$$\nu(0) - \nu_H(0) = \frac{\epsilon\hbar\omega_c}{\pi^2 e^2 a n_L} = \frac{2}{\pi}\frac{a_B}{a} = \frac{\sqrt{2}}{\pi}\frac{a_B}{b}\left(\frac{\nu(0)(1-\frac{b^2}{d^2})}{(\nu(0)-k)}\right)^{1/2}. \tag{3.53}$$

In this case, we deal with the two narrow dipolar strips which appeared as a result of the splitting of the quadrupolar strip. Indeed, by substituting $n' = n''a$ one can verify that Eq.(3.52) yields a dipolar strip width $a - a'$ in agreement with Eq.(20) of Ref.[45]. (We remind the reader that in Ref.[45] $\epsilon/2$ was used instead of ϵ.) The change of concentration produced by the dipolar strip in the neighboring compressible strips was also found in Ref.[45]. At distance a which is much larger than the dipolar strip width, the change in concentration is

$$\Delta n = \frac{\epsilon\hbar\omega_c}{2\pi^2 e^2}\frac{1}{a}. \tag{3.54}$$

In our case, *two* dipolar strips of opposite polarities give equal decrements of concentration in the center of the channel. Indeed Eq.(3.53) gives Δn twice of that of Eq.(3.54). As $\nu(0)$ grows, two dipolar strips move farther away from the center and their effect on $\nu_H(0)$ decreases.

In Fig.3-5 we plot $\nu_H(0)$ as a function of $\nu(0)$, as obtained from the numerical solution of the system of equations(3.48,3.50,3.51) separately for each interval $k < \nu(0) < k+1$. We also calculate $\nu_H(0)$ as a function of gate voltage at fixed values of the magnetic field (Fig.3-6).

One may wonder how good the approximation of the nearest dipolar strips is at low magnetic fields (large k). Indeed, distant dipolar strips also contribute to $n_H(0)$, but because of their large number and relatively slow decay of Δn with distance (see Eq.(3.54)), the absolute value of their contribution may be comparable to, or even larger than, that of the nearest strips. However the contribution of distant strips is monotonic in the magnetic field. We will discuss this briefly although it is more difficult to observe than the oscillatory contribution of the nearest ones.

The monotonic contribution of the distant dipolar strips is intimately related to the small difference in the electron distribution between the extreme quantum limit ($\nu(0) < 1$) and the zero magnetic field ($\nu(0) \to \infty$). Up to now, we have not distinguished between these two regimes, describing both in the perfect screening approximation in which the charge distribution is given by Eq.(3.6). Actually, in both cases the screening radius is finite and screening is not perfect. Because of this, the channel is somewhat broader and $n(0)$ is slightly smaller than in the distribution of eq.(3.6). Corrections to $n(0)$ are of the order of r_D/b. At $H = 0$, when $r_D = a_B$, we found that the relative correction to the concentration in the center of the channel

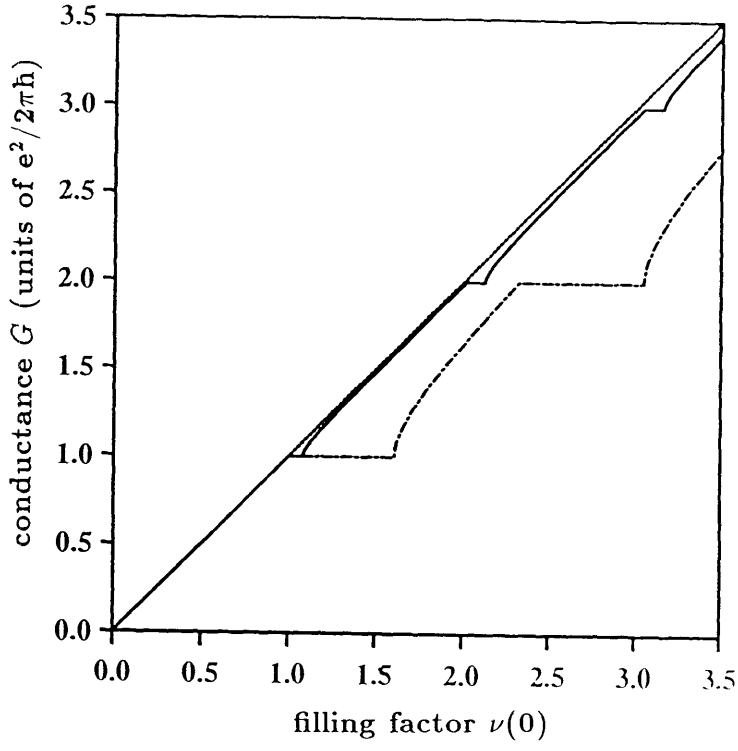

Figure 3-5: Two–terminal conductance of a narrow channel as a function of the filling factor in the center of the channel $\nu(0) = n(0)/n_L$. Dotted line is $\nu_H(0) = \nu(0)$. Solid line corresponds to $a_B/b = 0.05$; dash–dotted line correspomds to $a_B/b = 0.5$.

is $2a_B/\pi b$. For this purpose, we used the Thomas–Fermi approximation, which is valid when $na_B^2 \gg 1$. In the extreme quantum limit ($\nu(0) < 1$), screening is related to electron–electron correlations and the screening radius is of the order of $n^{-1/2}$. If $na_B^2 \gg 1$ then r_D is smaller than a_B. In any case, the charge distribution in the extreme quantum limit is closer to the electrostatic solution given in Eq.(3.6). This means that as the magnetic field is lowered, $n_H(0)$ experiences a small monotonic decrease. This decrease can be understood as a result of the collective action of remote dipolar strips slightly depleting the center of the channel. Practically, this means that plateaus are centered at $\nu = k$ at $k \gg 1$ while at $\nu(0) < 1$ one gets $\nu_H(0) = (1 + \delta_1)\nu(0)$, where δ_1 is of the order of a_B/b.

We remind the reader that our theory works only for $k < k_{c1}$ (see Eq.(3.35)). At $k > k_{c1}$ a finite size of the wavefunction should be included in the theory. It can be shown[29] that $\Delta\nu_k$ grows linearly with k in the range $k_{c1} < k < k_{c2}$ where $k_{c2} = \frac{b}{a_B}(na_B^2)^{1/4}$. At $k \gg k_{c2}$ plateau widths are $\Delta\nu_k = 1$ and the conventional one electron theory of ballistic transport[2] is valid.

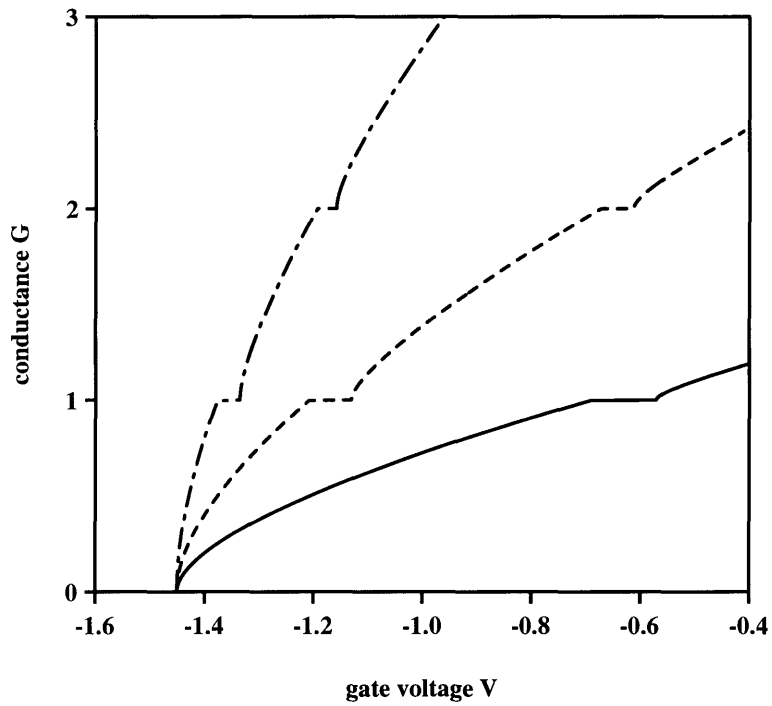

Figure 3-6: Two–terminal conductance of a narrow channel $2d = 5000$Åas a function of gate voltage V_g at different bulk filling factors ν_0 (determined by applied magnetic field). Solid line, $\nu_0 = 1.5$; dashed line, $\nu_0 = 3$; dash–dotted line, $\nu_0 = 6$.

3.5 Relationship between conductance and the filling factor in the center of the channel

In the previous section, we discussed the conductance of a short channel as a function of magnetic field. We used relation (3.2) between the two–terminal conductance and the electron density $n_H(0)$ in the center of the channel. To our knowledge, Eq.(3.2) has not yet been discussed for the most interesting case, of the compressible liquid in the center of the channel. In this section, we substantiate hypothesis (3.2) for the channel in the C–state.

Unfortunately, we are not able to prove Eq.(3.2) for the case of low temperatures $k_BT \ll n^{1/2}e^2/\epsilon$ where taking proper account of electronic correlations is necessary. We have therefore restricted ourselves to the case of high temperatures $k_BT \gg n^{1/2}e^2/\epsilon$. Note that we can still use the electrostatic solution (3.6), because even at $k_BT \gg n^{1/2}e^2/\epsilon$ the screening radius $r_D \sim k_BT\epsilon/ne^2$ may be much less than the widths of compressible and incompressible strips. For the sake of simplicity, we consider the two–terminal conductance at the extreme quantum limit, when the occupation number in the center of the channel $\nu_H(0) = n_H(0)/n_L < 1$. All the electrons occupy the lowest Landau level but their energy ε depends on the coordinate x. One

can find $\varepsilon(x)$ from the condition

$$\left(\exp\left(\frac{\varepsilon(x)-\xi}{k_BT}\right)+1\right)^{-1}=\frac{n(x)}{n_L}, \tag{3.55}$$

where ξ is the electrochemical potential and $n(x)$ is determined by Eq.(3.6). Eq.(3.55) means that the Fermi occupation numbers produce the density of electrons $n(x)$ which coincides with the result of the electrostatic problem Eq.(3.3-3.5). The dependence $\varepsilon(x)$ is shown schematically in Fig.3-7(a). (This dependence may be viewed as the result of a correction to the constant electrostatic potential inside the compressible strip due to the non–vanishing screening radius $r_D \approx k_BT\epsilon/ne^2$.)

The dependence of electron energy on the coordinate means that there is an electric field directed across the channel and consequently a drift of electrons along the channel with velocity

$$v(x)=\frac{\lambda^2}{\hbar}\frac{d\varepsilon}{dx}. \tag{3.56}$$

Apparently, electrons to the left and to the right of the channel center move in opposite directions, and the net current in the equilibrium is zero. Let us consider a non–equilibrium state with a small voltage $V \ll k_BT/e$ applied to the two terminals at the ends of the channel. The dependence $\varepsilon(x)$ is slightly modified as shown in Fig.3-7(b). As electrons to the left and to the right of the center move in opposite directions, they are in equilibrium with different terminals. Thus, if we neglect all scattering processes, the electrochemical potential ξ has a step in the center of the channel:

$$\xi(x)=\begin{cases}\xi_L, & x<0\\ \xi_R=\xi_L+eV, & x>0.\end{cases} \tag{3.57}$$

The current density has the form

$$j(x)=en(x)v(x)=en_L\nu(x)\frac{\lambda^2}{\hbar}\frac{d\varepsilon}{dx}=\frac{e}{2\pi\hbar}f(\varepsilon(x)-\xi(x))\frac{d\varepsilon}{dx}, \tag{3.58}$$

where $\nu(x)=f(\varepsilon(x)-\xi(x))$ is the occupation number for an electron state at point x, $f(\varepsilon)=(e^{\varepsilon/k_BT}+1)^{-1}$. We can now calculate the total current in the channel using Eq.(3.57),(3.58):

$$\begin{aligned} I &= \int j(x)dx=\frac{e}{2\pi\hbar}\left[\int_{\infty}^{\varepsilon(0)}f(\varepsilon-\xi_L)d\varepsilon+\int_{\varepsilon(0)}^{\infty}f(\varepsilon-\xi_R)d\varepsilon\right]= \\ &= \frac{e}{2\pi\hbar}f(\varepsilon(0)-\xi)(\xi_R-\xi_L)=\frac{e^2}{2\pi\hbar}\nu(0)V. \end{aligned} \tag{3.59}$$

Thus, in the absence of disorder and electron–electron scattering, the linear conductance is determined by Eq.(3.2). It is interesting to note that in this approximation the conductivity does not depend on temperature. So far, we have considered the case of high magnetic field when the channel contains only one compressible strip.

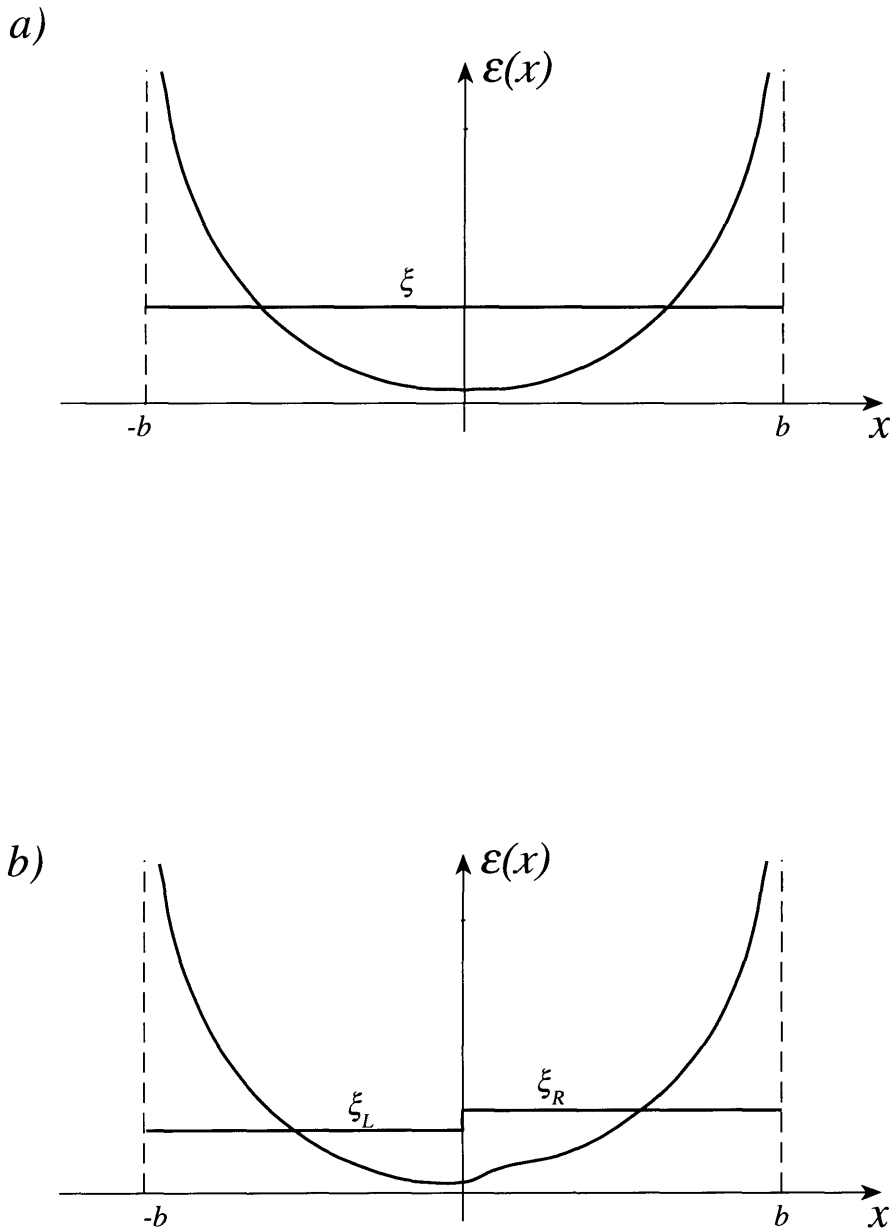

Figure 3-7: Electron energy and electrochemical potential as the functions of the electron position in high–temperature model. (a) Equilibrium state; (b) Current–carrying state.

However, the result (3.2) may be easily generalized for the case of arbitrary $\nu(0)$ by considering several Landau levels.

From the above consideration, it is clear that the conductance is always determined by the occupation number at the point where the drop of electrochemical potential occurs. In other words a nonequilibrium current is usually concentrated near the line of maximum $n(x)$. For example, if the voltages on the confining gates are different and the distribution of electron density across the channel $n(x)$ is asymmetric, $\nu_H(0)$ in Eq.(3.2) must be substituted by the maximum occupation number $(\nu_H)_{max} = \max\{n(x)/n_L\}$.

3.6 Quantum point contacts

So far, we considered a narrow channel which is translationally invariant in the y-direction. In reality, experiments on ballistic transport are carried out with quantum point contacts (see e.g. Ref.[25]), so an electron channel has a finite length and is not necessarily translationally invariant. Usually it has a shape similar to the one shown in Fig.3-8, and our theory can be generalized for this case as well. The electron density $n(x,y)$ at zero magnetic field has a saddle point at $x = y = 0$ and can be described in its vicinity by the expression

$$n(x,y) = n(0,0) - \frac{n_x''}{2}x^2 + \frac{n_y''}{2}y^2 \tag{3.60}$$

Here $n_x'' = |d^2n/dx^2|$, and $n_y'' = |d^2n/dy^2|$. Let us first consider the case of a very strong magnetic field, so that all velectrons belong to the first Landau level. Thus all the channel is occupied by the compressible liquid. The density saddle point is also a saddle point of the energy $\varepsilon(x,y)$. The electrons move along the lines of constant energy, coinciding with the lines of constant density as shown in Fig.3-8.

We can now apply formulas(3.57)–(3.59) to the crossection $y = 0$, and get the result (3.2) with the occupation number taken at the saddle point $x = y = 0$.

In order to understand this result in the framework of the conventional transmission approach one can divide all the compressible liquid into many narrow "subchannels" along the lines of constant density. Then a nonequilibrium current will flow along these channels. It is obvious now that all the channels with $n < n(0,0)$ will pass trough the quantum point contact and all the others will turn back. This explains why $n(0,0)$ plays such an important role.

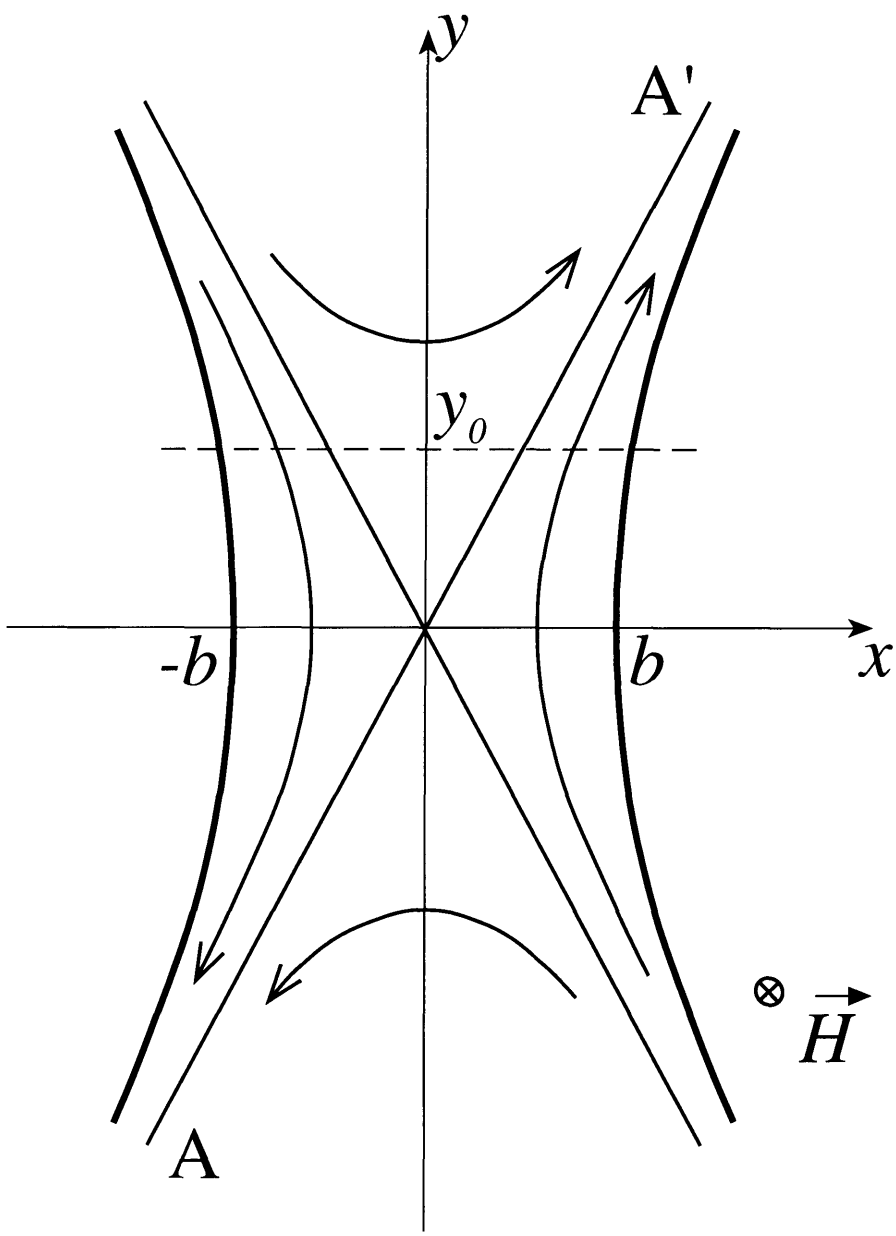

Figure 3-8: Ballistic transport in the quantum point contact. Arrows show the direction of electron drift. Line A-A′ is the equipotential on which the drop of electrochemical potential occurs.

To see that the current in any other crossection ($y = y_0$) has the same value, one should note that according to the directions of arrows in Fig.3-8, the drop of electrochemical potential occurs at the equipotential line A-A′ which passes through the saddle point. It follows from Eq.(3.59) that the electron density at this line (being equal to $n(0,0)$) determines the net current.

To find the widths of the plateaus and the shape of the rises in the function $G(\nu)$ one has to find $n(0,0)$ in a strong magnetic field. Because of the absence of the translational invariance we could not solve this problem analytically as was done for a narrow channel in Section 3.3,3.4.I have solved this problem by a direct numerical minimization of electrostatic energy for different saddle parameters. A detailed account of this work will be published elsewhere[31].

We would like to give here a brief qualitative considerations in the limiting cases. In the limit $n_x'' \gg n_y''$ one reproduces the results derived for a narrow channel provided $n'' = n_x''$. In the opposite limit $n_y'' \gg n_x''$ the widths of the plateaus are obtained by substituting n_y'' in Eq.(3.31). However plateaus are shifted in the direction of small ν so that they end on the line $G = \nu e^2/2\pi\hbar$. Also the square root singularity occurs at the low ν end of the plateaus rather than at the high ν side. In the case $n_x'' = n_y'' = n''$ plateaus are centered on the line $G = \nu e^2/2\pi\hbar$. As shown in Ref.[31] plateaus are slightly wider than given by Eq.(3.31).

Experimental data shows that in some cases plateaus are wider than would follow from our calculation. We attribute this descrepancy to the presence of disorder. Impact of disorder on the formation of compressible strips was discussed in Ref.[45]. Disorder may localize a compressible liquid of small enough density. When a new Landau level starts to fill up with the rising Fermi level the concentration of electrons as well as the width of the new compressible strip grows from zero. Under such conditions there is a range of $\nu(0)$ where all the electrons of the new Landau level are localized. In this range of $\nu(0)$ only totally occupied Landau levels contribute to the conductance, meaning that at zero temperature plateaus should be wider than calculated in this paper. Finite temperature may delocalize a part of electrons on the partially filled Landau level. It means that the plateaus should narrow with temperature. For a very weak disorder a range of temperatures should exist where the localization is destroyed but the temperature is still lower than $\hbar\omega_c$. In this regime our results should be valid quantitatively.

3.7 Conclusion

In this paper, we have studied the distribution of electrons in a narrow channel defined by a split gate. We started with the solution in the absence of magnetic field, which yields a dome–like distribution across the channel. The electron channel width is determined by the gate voltage and is assumed to be larger than the Bohr radius in the semiconductor. Application of a strong magnetic field breaks the channel into alternating strips of compressible and incompressible liquid, thus altering the electron density distribution. We applied knowledge of the charge distribution in strong magnetic field to study ballistic conductance of the quantum point contact

using the following conjecture: *Ballistic conductance of the quantum point contact in strong magnetic field is given by the filling factor at the saddle point of the electron density distribution multiplied by* $e^2/2\pi\hbar$. Hence we identify plateaus in conductance with the situation when there is an incompressible strip in the center of the channel (I–state). This situation is similar to the one–electron picture of edge states.

We presented a complete electrostatic description of the central incompressible strip which we call a quadrupolar strip, finding that it can exist only in narrow ranges of magnetic field or gate voltage. In wider ranges, there is a compressible strip in the center of the channel (C–state), and conductance is not quantized. This situation has no analogy in the one–electron picture of edge states. We solved the electrostatics problem for the density distribution and, using our conjecture, calculated the total conductance curve as a function of magnetic field and gate voltage. Experimental results do not always show narrow plateaus with wide rises. We attribute this discrepancy to the presence of disorder in the channel. For a sufficiently "clean" channel, our theory gives the dependence of conductance on a long list of parameters such as magnetic field, gate voltage, channel width, concentration of ionized donors, and the discontinuities in chemical potential. This allows for a detailed experimental verification of the theory.

3.8 Acknowledgments

This work was done in collaboration with K.A. Matveev and B.I. Shklovskii.[60] We are grateful to A.L. Efros, E.B. Foxman, L.I. Glazman, A.V. Khaetskii, P.A. Lee, B. Normand, I.M. Ruzin, G. Shvetz, F. Stern, D. Tsui for helpful discussions. One of us (D. C.) is supported by the NSF under grant no. DMR 89 - 13624, and the others(B. S. and K. M.) by the NSF grant no. DMR 91 - 17341. The authors acknowledge the hospitality of the Aspen Center for Physics where a part of this work was performed.

Chapter 4

Transport properties between quantum Hall plateaus

4.1 Introduction

The main features of the integer[34] and fractional[35] quantum Hall effect are the quantization of the Hall conductance and the vanishing of the longitudinal resistivity at integer and fractional filling factors correspondingly. The two discoveries have generated enormous amount of activities which resulted in a significant progress in understanding of the properties of the two–dimensional electron gas (2DEG) in a strong magnetic field[20]. From a theoretical point of view the conductance quantization was understood in terms of the Landau quantization for integer filling factors and in terms of the formation of the incompressible liquid[36] for the fractional ones. The exact quantization of the transport coefficients follows from the "gauge argument"[37].

Until recently, much less attention was given to the dissipative regime, which is characterized by an unquantized Hall conductance and a finite longitudinal resistivity. A brief look at experimental data, Fig.4-1, reveals an extraordinary diversity of the observed longitudinal resistivity values, which seem to vary from sample to sample.[1] Recently a significant effort was devoted to providing some theoretical basis for the dissipative regime. The several approaches to this problem include the network model[38, 39], the law of corresponding states[40, 41], and the Fermi–liquid description[42, 43]. However, it is not clear what the relationship between those theories is and whether they can explain the diversity in experimental data.

The purpose of this paper is to incorporate these approaches into a single picture, in which the relationship between various regimes is determined by a single parameter reflecting the level of disorder, and to find the longitudinal resistivity for different values of the parameter. We are able to do this for the case of high–mobility GaAs heterostructures where disorder is known to be of long–range nature: it comes from a non–uniform distribution of donors set back from the 2DEG plane by the spacer thickness d_s. Due to a very good screening by the 2DEG at zero magnetic field the long–range disorder potential is translated into electron density fluctuations. The

[1] We do not consider effects related to the formation of the Wigner crystal in this paper.

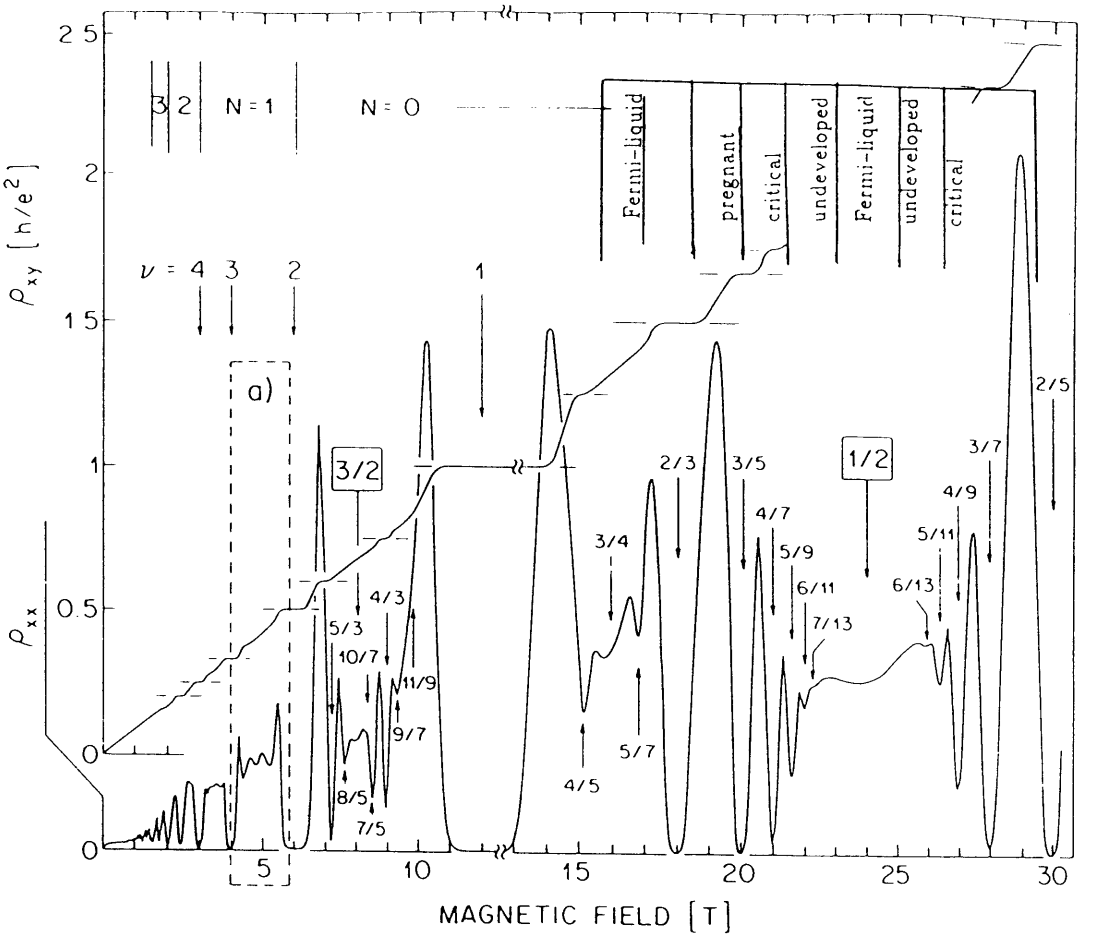

Figure 4-1: ρ_{xx} and ρ_{xy} as a function of the magnetic field in a very high-mobility heterostructure.(Source: Willett et al.[72]) We have added labels to indicate our diagnosis of the principal sequence peaks. Notice that the scale is reduced by the factor 2.5 for magnetic fields higher than 12T.

characteristic lengthscale of these fluctuations is of the order of d_s, while the ratio of the average electron density, n_e, to the typical amplitude of the density fluctuations, δn_e, provides a natural large parameter β, on which our theory is based.

The value of β can be found approximately from the following consideration.[11, 19] In an ungated heterostructure the concentration of ionized donors is equal to the electron concentration n_e. The number of ionized donors in a square with side d_s is equal to $n_e d_s^2$. The typical fluctuation in the number of donors is given by $(n_e d_s^2)^{1/2}$. This leads to the value of the relative density fluctuation

$$\beta = \frac{n_e}{\delta n_e} \sim \sqrt{n_e} d_s. \tag{4.1}$$

A more rigorous calculation of β yielding the numerical factor will be given in Section 4.4.

Our basic picture is that in a strong magnetic field, at a filling factor between the quantum Hall plateaus, the electron system breaks up into the incompressible regions corresponding to the integer or fractional states[11, 13], Fig.4-2. Those regions are separated by edge channels which form a percolating network. Depending on the value of β these edge channels can be either wide or narrow. It turns out that the

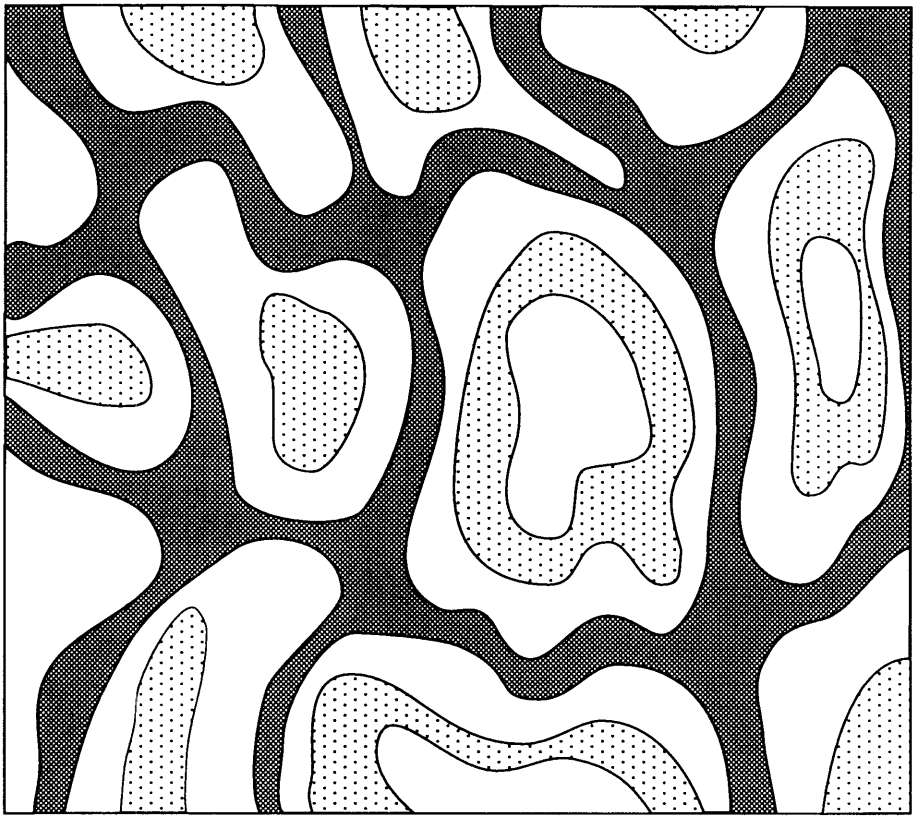

Figure 4-2: Break-up of the electron system into the incompressible and compressible liquid regions. White regions represent incompressible liquid, while shaded regions correspond to compressible liquid: localized edge channels are dotted, extended channels are gray.

transport properties depend crucially on the width of the edge channels.

Although the longitudinal resistivity is measured at a fixed value of β with magnetic field being varied, it is enlightening to consider the evolution of resistivity between the quantum Hall plateaus with the variation of β. In the following we give a summary of the main results of this paper. For the sake of simplicity we consider the case of spinless electrons.

First, let us focus on the resistivity at a half–integer filling factor. In the case of a strong disorder (small β) a peak in longitudinal resistivity between the IQHE plateaus becomes infinitely sharp at low temperature . The related critical phenomena was studied extensively both theoretically and experimentally[44]. Thus we call this peak critical. In this case the edge states in the bulk of the sample (which we refer to as bulk edge states) are very narrow allowing to describe them as one–dimensional channels comprised in a network. The transport properties of such a network have been considered in Refs.[38, 39]. Their result, derived using the Landauer formula as shown in Section 4.3, states that the longitudinal conductivity of a half–filled Landau level is equal to $1/2(e^2/2\pi\hbar)$.

As β is increased the typical gradient of the electron density distribution at zero magnetic field becomes smaller and the bulk edge states acquire a finite width[13, 45, 3, 4], developing into the strips of compressible liquid. This leads to the breakdown of the network model and consequently to the reduction of the peak's height from its critical value. We call this peak "pregnant" because it is about to give birth to the fractional states.

At larger values of β there is no well–defined peak at a half–integer filling factor. Rather one can see a slight depression in the longitudinal resistivity. The edge channel network disappears in this case because the compressible liquid occupies the whole plane. We believe that the proper description in this case is given by the Fermi–liquid of composite fermions[42, 43].

Exactly at a half–integer filling factor the composite fermions do not see any effective magnetic field on average. However, the variation of the filling factor leads to the appearance of the Shubnikov-de Haas oscillations which develop into the quantum Hall effect. Thus the principal sequence of the FQHE is interpreted in terms of the IQHE for the composite fermions.[46] This interpretation allows us to explain the evolution of the longitudinal resistivity peaks between the FQHE plateaus in analogy with the IQHE.

At sufficiently low disorder (large β) a peak in the longitudinal resistivity between the FQHE plateaus developes and becomes critical. The fractional edge channels in the bulk are very narrow. At even larger values of β the fractional peak becomes pregnant because of the finite width of the bulk edge channels. This shows up in the reduction of the peak's height. As β is increased further, the peak starts giving birth to the daughter states of the next generation of fractions. Then a Fermi–liquid state developes at the filling factor at which the center of the peak used to be.

By applying this picture to the successive generations of fractions one can see that in the limit of very low disorder all the even denominator fractional filling factors end up in the Fermi–liquid regime.

To summarize the discussion, the whole lifecycle (β playing the role of time) of a given resistivity peak consists of four periods. The development of the peak is characterized by the growth of the peak's height and the decrease in the resistivity at the adjacent odd denominator fractions. Then the peak becomes critical making it infinitely narrow at zero temperature. In the next stage the peak is pregnant, its height reduced. Then it starts giving birth to the daughter states while staying in the Fermi–liquid regime. At this stage it would be more correct to talk about the even denominator fraction and its vicinity rather than about the peak.

Now we can go back to the experimentally relevant situation where the value of β is fixed for a given sample, Fig.4-1. We will show in this paper that the effective measure of disorder is different from peak to peak or, in other words, the values of β determining transitions between various regimes for a given peak depends on the peak's filling factor. Because of this in Fig.4-1 some peaks are undeveloped, while some are critical and some are pregnant, a few have turned into a Fermi–liquid state.

We consider fractions of the principal sequence of the FQHE defined by the filling factor $\nu = p/(2p+1)$, where p is an integer. The corresponding resistivity peaks between fractions $p/(2p+1)$ and $(p-1)/2p-1)$ fall into one of the following categories

as shown in Fig.4-1:

$$\begin{array}{ll} \text{pregnant peaks,} & \text{for } |p| < p_{c1}, \\ \text{critical peaks,} & \text{for } p_{c1} < |p| < p_{c2}, \\ \text{undeveloped peaks,} & \text{for } |p| > p_{c2}, \end{array} \tag{4.2}$$

In Section 4.4 we find from electrostatic considerations the widths of compressible and incompressible strips as a function of β. This yields the following transition values separating different regimes:

$$p_{c1} \approx \sqrt{\frac{\beta}{2}}, \tag{4.3}$$

$$p_{c2} \approx \left(\frac{\beta}{2}\right)^{4/5}. \tag{4.4}$$

We find the values of the resistivity for the critical peaks in the principal sequence by utilizing the theory of composite fermions. We apply the edge state network model to the fermion system and find the resitivity at the principal sequence peaks between fractions $p/(2p+1)$ and $(p-1)/2p-1)$:

$$\rho_{xx} = \frac{2\pi\hbar}{e^2}\frac{1}{2p^2-2p+1}, \quad \rho_{xy} = -\frac{2\pi\hbar}{e^2}\frac{4p^2-2p+1}{2p^2-2p+1} \tag{4.5}$$

Our values are in agreement with the law of corresponding states[40, 41].

Finally, we address the question of the Fermi–liquid states resistivity. In the composite fermion picture we calculate the resistivity of those states by considering the motion of non–interacting fermions in a fluctuating fictitious magnetic field arising from the density fluctuations. We find that the snake states play an important role in the transport in this regime. Unable to solve exactly the problem for random magnetic field we introduce a model in which the magnetic field varies abruptly between the two values. In this case we can solve the problem by applying the network model to the system of snake states. We find a linear dependence of the resistivity on the magnetic field B:

$$\rho_{xx} = \frac{B}{\beta n_e e c} \tag{4.6}$$

We argue that this result should hold in a realistic case of smooth fluctuations.

The outline of the paper is as follows. Section 4.2 is devoted to the discussion of the transition between narrow and wide edge channels from the electrostatics point of view. In Section 4.3 we review the network model and reproduce the derivation of the conductivity tensor for a half–filled Landau level. In Section 4.4 we consider the long–range disorder and use the results of Section 4.2 to derive the limits of the applicability of the network model. We also derive there the universal values of the resistivity peaks in the FQHE by applying the network model to the fermion system. In Section 4.5 we calculate the resistivity in the Fermi–liquid states at half–integer filling factors. We also formulate a general statement regarding the conductivity of the network model. The generalization to the even–denominator fractions of the

principal sequence is done in Section 4.6. We compare our results with experiment in Section 4.7. Our major conclusions are given in Section 4.8.

4.2 The structure of edge channels in the QHE.

As discussed in the Introduction, long–range disorder in GaAs heterostructures creates electron density fluctuations in the absence of a magnetic field. Upon application of a magnetic field corresponding to a filling factor half–way between quantum Hall plateaus, the electron system breaks up into the incompressible regions with densities given by the quantum Hall states[11, 19, 13], Fig.4-2. Edge channels form along the boundaries of those regions comprising a complicated network. We will address the transport properties of the system by considering this network in detail. In this Section we analyze the general structure of edge channels because of its impact on the transport properties which will be discussed in Section 4.4.

In the conventional one–electron picture it is assumed that the Landau levels are bend adiabatically by the confining potential. The intersection of the Landau levels with the Fermi level determines the location of the edge states. The typical width of an edge state is of the order of the magnetic length, $\lambda = (\hbar c/eB)^{1/2}$. The distance between adjacent edge states is determined by the steepness of the external potential. But in order for the adiabatic approximation to be valid the distance between the edge states should be greater than λ. This implies that in the one–electron picture the distance between the edge states is greater then their width.

The effect of electron–electron interaction on the structure of the edge states has been considered by Beenakker[3] and Chang[4]. They have shown that the formation of the edge states can be viewed as the result of non–linear screening of an external potential by the 2DEG. According to the theory of non–linear screening proposed by Efros[19, 13] the 2DEG breaks up into the alternating strips of compressible and incompressible liquid. The compressible liquid consists of the states lying at the Fermi level which makes it a strongly screening media. On the other hand the incompressible liquid is characterized by the absence of gapless excitations and therefore does not screen.

Chklovskii, Shklovskii, and Glazman[45] gave an analytic solution of the electrostatic problem involving edge states, which agreed with the independent calculation of Kane[27] and an estimate by Efros[14]. It was shown that in a typical external potential compressible strips are wider than the adjacent incompressible ones contrary to the conclusion of the one–electron model. The result of Ref.[45] holds provided the strip dimensions are greater than the semiconductor Bohr radius, which is about 100Å in GaAs.

In this paper we will extend these considerations to include the opposite limit of narrow compressible strips. Although relevance of this limit to the integer edge states in GaAs heterostructures seems doubtfull, it might be important for some other 2DEG confinement schemes. Also we will show that this limit is of major importance in the FQHE regime. Troughout this paper we discuss the transport properties determined by the percolating network of edge channels. As edge channels

follow the lines of constant density we consider the density distribution in the vicinity of a percolating line of constant density. In order to study the structure of edge channels we approximate the zero magnetic field density distribution around this line by a linear expansion. The slope of the density distibution, n' is determined by β. This is equivalent to having in the $z = 0$ plane a background positive charge density constant in the y–direction and varying linearly along the x–axis

$$n(x) = n_0 + n'x. \tag{4.7}$$

Then, in the absence of a magnetic field, the equilibrium electron concentration can be found from the solution with a constant electrochemical potential in the area occupied by electrons. If we neglect the finite screening radius of the 2DEG and look for a solution with a constant electrostatic potential then the electron density distribution is given by Eq.(4.7).

A strong magnetic field creates discontinuities in the chemical potential of the 2DEG at integer filling factors. This leads to the formation of the incompressible liquid strips across which the drop in the electrostatic potential occurs needed to bring the next Landau level to the Fermi level. We adopt a two–gap model in which there are only two identical discontinuities in the chemical potential at the densities $n_0 - \Delta n/2$ and $n_0 + \Delta n/2$:

$$\mu = \begin{cases} -\Delta\mu, & n < n_0 - \Delta n/2, \\ 0, & n_0 - \Delta n/2 < n < n_0 + \Delta n/2, \\ \Delta\mu, & n > n_0 + \Delta n/2, \end{cases} \tag{4.8}$$

In order to find the charge distribution in this case we will treat the compressible regions as metal planes and the incompressible regions as insulators with fixed electron densities, Fig.4-3.

We allow the boundaries between the insulating and conducting regions, given by $\pm x_1, \pm x_2$, to vary. Thus we should solve the Laplace equation with mixed boundary conditions at $z = 0$ plane. Electrostatic potential should be constant throughout each compressible strip

$$\phi(x, z = 0) = \begin{cases} \Delta\mu, & x < -x_2, \\ 0, & |x| < x_1, \\ -\Delta\mu, & x > x_2, \end{cases} \tag{4.9}$$

and the normal component of the electric field is given by the net charge density in each incompressible strip

$$E_z(x, z)|_{z\to -0} = \begin{cases} -\frac{2\pi e}{\epsilon}(n'x - (n_0 - \Delta n/2)), & -x_2 < x < -x_1, \\ -\frac{2\pi e}{\epsilon}(n'x - (n_0 + \Delta n/2)), & x_1 < x < x_2. \end{cases} \tag{4.10}$$

In order to ensure mechanical equilibrium at the boundaries of compressible and incompressible strips we set

$$E_x(x, 0)|_{x\to -x_2+0} = E_x(x, 0)|_{x\to -x_1-0} = E_x(x, 0)|_{x\to x_1+0} = E_x(x, 0)|_{x\to x_2-0} = 0. \tag{4.11}$$

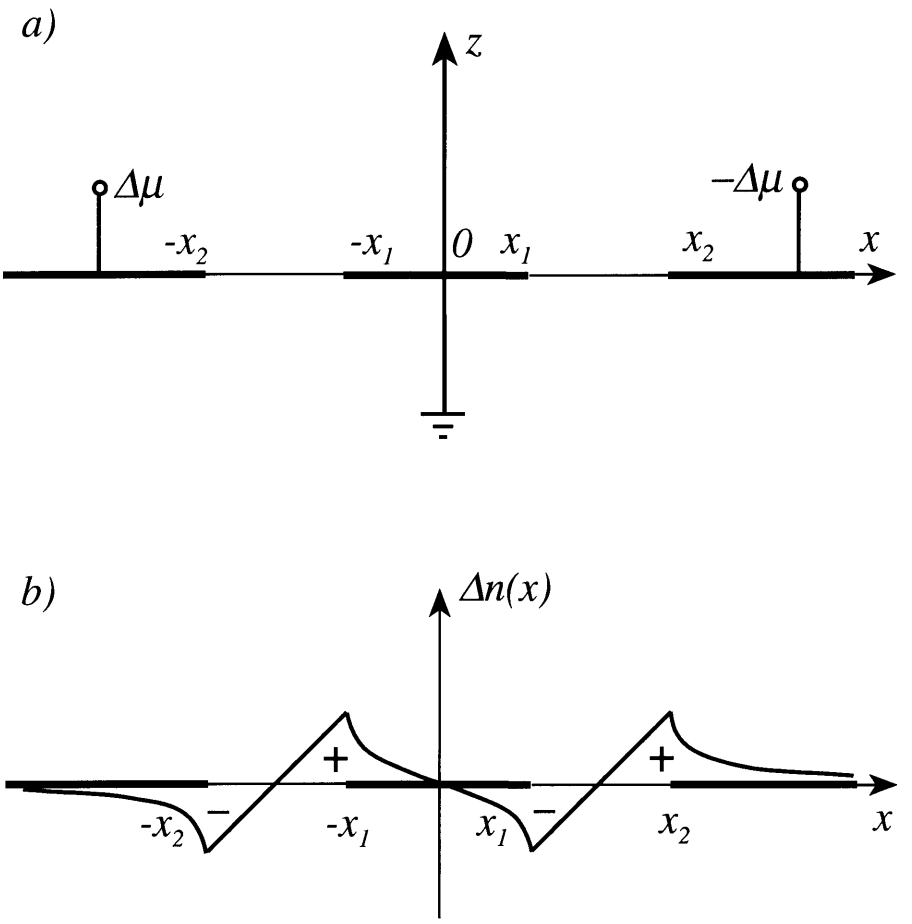

Figure 4-3: (a)The formulation of the electrostatic problem for the two–gap model. Bold lines represent three metal planes. (b)Additional charge density distribution obtained by solving the electrostatics problem.

This problem can be solved as shown in Appendix C by employing the methods of complex analysis. One gets the following system of equations determining the dimensions of the strips:

$$\begin{cases} \int_{x_1}^{x_2} dx \frac{(n'x-\Delta n/2)x^2}{\sqrt{(x_2^2-x^2)(x^2-x_1^2)}} = \frac{\epsilon\Delta\mu}{2\pi e^2} \\ \int_{x_1}^{x_2} dx \frac{n'x-\Delta n/2}{\sqrt{(x_2^2-x^2)(x^2-x_1^2)}} = 0 \end{cases} \tag{4.12}$$

We solved this system of equations numerically. The position of the incompressible strip boundaries as a function of the inverse density gradient is plotted in Fig.(4-4). In the two limiting cases the system allows an approximate solution. If the density gradient is small then the widths of the incompressible strips are much smaller than

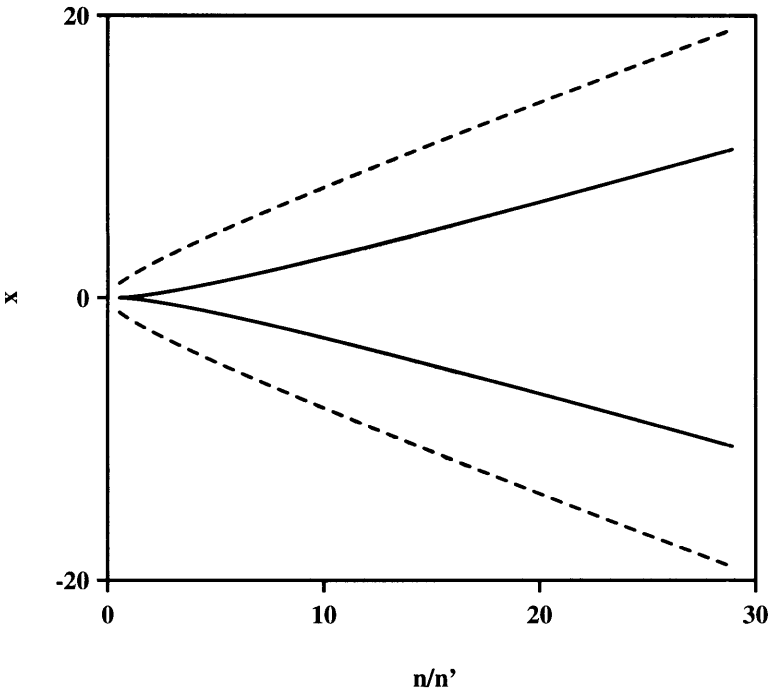

Figure 4-4: The locations of the incompressible strip boundaries $\pm x_1$, $\pm x_2$ as a function of the inverse density gradient. The full lines show the inner boundaries of the incompressible strips and the dashed lines represent the outer boundaries.

the distance between them, Fig.4-5(a). Eqs.(4.12) are reduced to

$$\begin{cases} \int_{x_1}^{x_2} dx \frac{(n'x-\Delta n/2)x}{\sqrt{(x_2-x)(x-x_1)}} = \frac{\epsilon\Delta\mu}{2\pi e^2} \\ n' \frac{x_1+x_2}{2} - \Delta n/2 = 0 \end{cases} \tag{4.13}$$

By solving this system of equations we find

$$(x_2 - x_1)^2 = \frac{4\epsilon\Delta\mu}{\pi^2 e^2 n'} \tag{4.14}$$

$$\frac{x_1 + x_2}{2} = \frac{\Delta n}{2n'} \tag{4.15}$$

These formulas describe two independent dipolar strips of Ref.[45].

When the density gradient is increased the two incompressible strips start to interfere with each other because their widths become comparable to the distance between them. In the extreme limit of a large density gradient the compressible strip is squashed by the incompressible ones, Fig.4-5(b). Then Eqs.(4.12) are reduced to

$$\begin{cases} \int_{x_1}^{x_2} dx \frac{(n'x-\Delta n/2)x}{\sqrt{x_2^2-x^2}} = \frac{\epsilon\Delta\mu}{2\pi e^2} \\ n'\pi = \Delta n \int_{x_1}^{x_2} \frac{dx}{\sqrt{(x_2^2-x^2)(x^2-x_1^2)}} \end{cases} \tag{4.16}$$

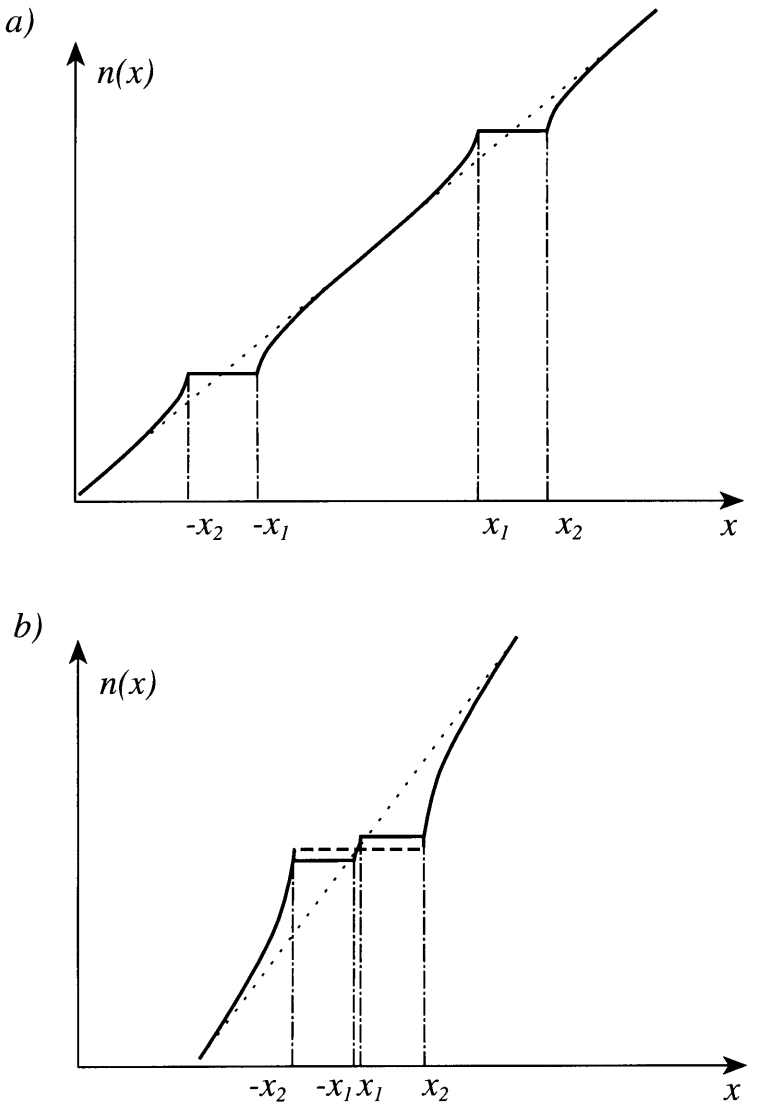

Figure 4-5: The evolution of the electron density distribution with the changing density gradient in the two–gap model. The dotted line shows electron density at zero magnetic field.(a) The $a \ll b$ case, when the two dipolar strips are independent. (b) the $a \gg b$ case when the charge distribution can be thought of as a single dipolar strip (dashed line) plus two slabs with opposite charge.

By solving this equations we find

$$(2x_2)^2 = \frac{4 \cdot 2\epsilon\Delta\mu}{\pi^2 e^2 n'} \tag{4.17}$$

$$x_1 = 4x_2 \exp\left(-\pi \frac{x_2 n'}{\Delta n}\right) \tag{4.18}$$

Eq.(4.17) is just the old expression for the dipolar strip width[45] with the potential drop of $2\Delta\mu$. But Eq.(4.18) is a new result showing that the width of the incompressible strip decreases exponentially fast with increasing density gradient. A similar formula has been derived by Cooper and Chalker[47].

Let us give a qualitative derivation of Eq.(4.18). When the incompressible strips are wide one can ignore the step in electron density between them (dashed line in Fig.4-5(b)) and find x_2 from Eq.(4.17). The appearance of the compressible strip at $x = 0$ can be cosidered as a perturbation which does not affect the value of x_2. Thus we can view the formation of the compressible strip as a charge redistribution that screens out the electric field in the interval $|x| < x_1$ created by the dipolar strip extending from $-x_2$ to $+x_2$.

This redistributed charge density consists of two slabs

$$en(x) = e\Delta n/2, \quad x_1 < x < x_2 \tag{4.19}$$

$$en(x) = -e\Delta n/2, \quad -x_2 < x < -x_1 \tag{4.20}$$

The electric field created by these slabs at $x = 0$ is given by

$$E_x = \int_{x_1}^{x_2} \frac{dx 2\Delta ne}{\epsilon x} = \frac{2\Delta ne}{\epsilon} \ln \frac{x_2}{x_1} \tag{4.21}$$

By setting this field to be equal to the field in the middle of the unperturbed double dipolar strip[45] $E = 2\pi en' x_2/\epsilon$ we find

$$x_1 \approx x_2 \exp\left(-\pi \frac{x_2 n'}{\Delta n}\right) \tag{4.22}$$

in agreement with Eq.(4.18).

In the IQHE regime $\Delta n = n_L = 1/2\pi\lambda^2$ and $\Delta\mu = \hbar\omega_c$. By substituting this in Eq.(4.17,4.18) we find for the incompressible and compressible strips widths $a = x_2 - x_1$ and $b = 2x_1$

$$b = 8a \exp\left(-\frac{2\epsilon\hbar\omega_c}{a\pi e^2 n_L}\right) = 8a \exp\left(-\frac{4a_B}{a}\right), \quad \text{for } b \ll a \ll a_B \tag{4.23}$$

where we have used the Bohr radius in semiconductor $a_B = \hbar^2\epsilon/m_{eff}e^2$. This should

be contrasted with the result of Ref.[45] which can be recovered from Eqs.(4.14,4.15):

$$a^2 = \frac{8}{\pi} a_B b, \quad \text{for } a_B \ll a \ll b \tag{4.24}$$

We would like to point out that the applicability of the Eqs.(4.18,4.23) for the 2DEG in GaAs heterostructures in the IQHE regime is very limited. It only shows that as soon as the gradient becomes high so that $a \approx b$ the compressible liquid strip starts shrinking exponentially fast. Naturally, when b is of the order of the magnetic length, a quantum mechanical consideration is necessary.

Now we extend our treatment to the FQHE regime. We consider first the fractions of the principal sequence with the filling factor of the form $p/2p+1$, where p is either negative or positive integer. In the limit of large $|p|$ the sequence converges towards $1/2$ either from above or below depending on the sign of p.

The most dramatic prediction of the Fermi–liquid theory proposed by Halperin, Lee and Read[42] is for the size of the energy gaps at filling factors $p/2p+1$. They claim that the discontinuities in the chemical potential at these filling factors should be independent of p. This prediction has been recently verified experimentally[48] through a measurement of the activation exponent fo a series of filling factors. As we shall see, this result has important implications on the structure of edge channels in the FQHE regime.

We will use the experimental value for the chemical potential discontinuity found from the activation energy studies at the filling factor $1/3$. According to Ref.[49] it is given by

$$\Delta\mu \approx 0.3 \frac{e^2}{\epsilon\lambda} \tag{4.25}$$

The difference in density between the adjacent filling factors $(p-1)/(2p-1)$ and $p/(2p+1)$ is given by

$$\Delta n = \frac{n_L}{(2p+1)(2p-1)} \tag{4.26}$$

By substituting this in Eq.(4.17,4.18) we find

$$x_1 \approx 4x_2 \exp\left(-\frac{1.2(4p^2-1)\lambda}{x_2}\right) \tag{4.27}$$

or in terms of compressible and incompressible strip widths a and b

$$b \approx 8a \exp\left(-\frac{4p^2\lambda}{a}\right), \quad \text{for } b \ll a \ll p^2\lambda \tag{4.28}$$

in the limit of large p. Similarly from Eqs.(4.14,4.15) we get

$$a^2 \approx 3p^2\lambda b, \quad \text{for } p^2\lambda \ll a \ll b \tag{4.29}$$

The regime described by Eq.(4.28) has a much better chance of being realized in practice for the fractional case as opposed to the integer case. This is because the closeness

of the filling factors between the adjacent fractions of the principal sequence leads to the appearance of the p^2 factor in Eq.(4.28)while the chemical potential discontinuity is independent of p. In Section 4.4 we shall see that the narrow compressible strip limit described by Eq.(4.28) is realized for a certain range of p values.

Next we note that the perfect screening model used in solving the electrostatics model does not take into account the negative screening radius of the compressible liquid[19]. In order to check the validity of our picture in this case we have performed a numerical minimization of the total energy including correlations by looking for a solution with a constant electrochemical potential. We chose the chemical potential to vary linearly as a function of the filling factor, the total drop between two fractions being equal to the chemical potential discontinuity. We find similar behavior as the perfect screening model, except that the compressible strip shrinks even faster then given by the Eq.(4.28). Thus the conclusion is similar to the one in the IQHE regime: the transition from a wide edge channel to a narrow one occures at such value of the density gradient that

$$a \approx b \approx 4p^2\lambda \tag{4.30}$$

The above electrostatic consideration can be generalized to any fractional filling factor, provided the discontinuities in the chemical potential are known.

4.3 Edge states network model.

It is believed that in high–mobility samples dissipation between the quantum Hall plateaus occurs only due to transport in the topmost partially filled (Nth) Landau level. Transport in the other $N-1$ Landau levels is dissipationless because of the absence of gapless bulk excitations. This fact has been confirmed in several experiments on high–mobility GaAs heterostructures[39, 25]. Therefore in order to make predictions on the value of the dissipative conductivity we study a partially–filled Landau level.

We assume that it is possible to describe conductance in the partially filled topmost Landau level with a local resistivity tensor ρ^N. In order to make a connection with experimentally measured quantities such as resistances R_{xx} and R_{xy} it is necessary to take into account the contribution of the lower Landau levels. This is not a trivial problem because these Landau levels, being perturbed by the confining potential, form edge channels at the boundaries of a sample. Hence their contribution may be strongly non-local[5, 50, 51, 52], making it impossible to describe a sample conductivity by a local resistivity tensor.

Szafer et al[39] have considered the interplay of the non–local and local transport effects in detail. They have shown that only in the extreme case of strong equilibration between the edge channels and the bulk can one introduce a conductivity tensor σ, related to the conductivity of the Nth Landau level by

$$\sigma_{xx} = \sigma^N_{xx}, \quad \sigma_{xy} = \sigma^N_{xy} + (N-1)\frac{e^2}{2\pi\hbar}. \tag{4.31}$$

We will continue our discussion in terms of σ^N and σ assuming that Eq.(4.31) holds.

Our results for σ^N should be valid also in the regime when there is a significant non–local contribution to conductance. However in order to interpret experimental measurements in this case one has to analyze the experimental geometry in the spirit of Ref.[39]. An example of such analysis can be found in a recent work by Komiyama and Nii[53].

Throughout this paper we study the contribution to the resitivity from the long–range external potential arising from a non–uniform donor distribution in heterostructures. We ignore the short–range potential fluctuations and keep in mind the zero–temperature limit.

Shapiro[54] has studied the dissipative transport between the quantum Hall plateaus by considering one–electron trajectories in a random external potential in the bulk. He has calculated the scattering rate between different extended states, which leads to the longitudinal resistivity. Shapiro has shown that the conductance of the half–filled Landau level is of the order of $e^2/2\pi\hbar$ and is independent of the Landau level number. Unfortunately, the picture presented in Ref.[54] does not include electron–electron interaction.

In the presence of interactions the 2DEG breaks up into compressible and incompressible regions[11, 19, 13] as shown in Fig.4-2. Compressible strips are nothing else but edge channels, whose conductance in units of $e^2/2\pi\hbar$ is given by the difference in filling factors of the incompressible liquids on both sides of the channels. This result holds even in the presence of interactions as pointed out by Beenakker[3] in the FQHE regime. Therefore we include electron–electron interaction in consideration by applying the concept of the bulk edge states. We give this seemingly absurd name to the states formed at the intersection of the Fermi level with the topmost Landau level which is perturbed by the random potential in the bulk. These edge states follow the equipotential lines forming a random network.

The description of the conductance in a partially filled Landau level with the help of the edge states network has been proposed by Kucera and Streda[38]. In principle the bulk edge channels should form a complicated percolation network. The topology of the network is simplified in the Kucera–Streda model to a square array of current-carrying loops. These loops are linked by scattering barriers transmitting fraction t of the incident current and reflecting the rest $r = 1 - t$ back in the loop. In the mean–field spirit all the trasmission coefficients t are taken to be identical. By applying Landauer formula to this model Kucera and Streda have found a conductivity tensor in terms of r and t, which in turn depend on the average filling factor.

The Kucera–Streda model does not include the effects of quantum interference which should become important away from the point $r = t = 1/2$ and lead to Anderson localisation. Chalker and Coddington[55] have introduced and studied numerically a network model similar to the one of Ref.[38]. They included interference effects and found the divergence of the localization length in this model only at $r = t = 1/2$. However the physical nature of this transition still remains unclear.

We adopt the Kucera–Streda network model for the Landau level exactly at filling factor $1/2$, in which case $r = t = 1/2$. Because of its conceptual importance we give a derivation of the conductivity in this model following the prescription of Ref.[39].

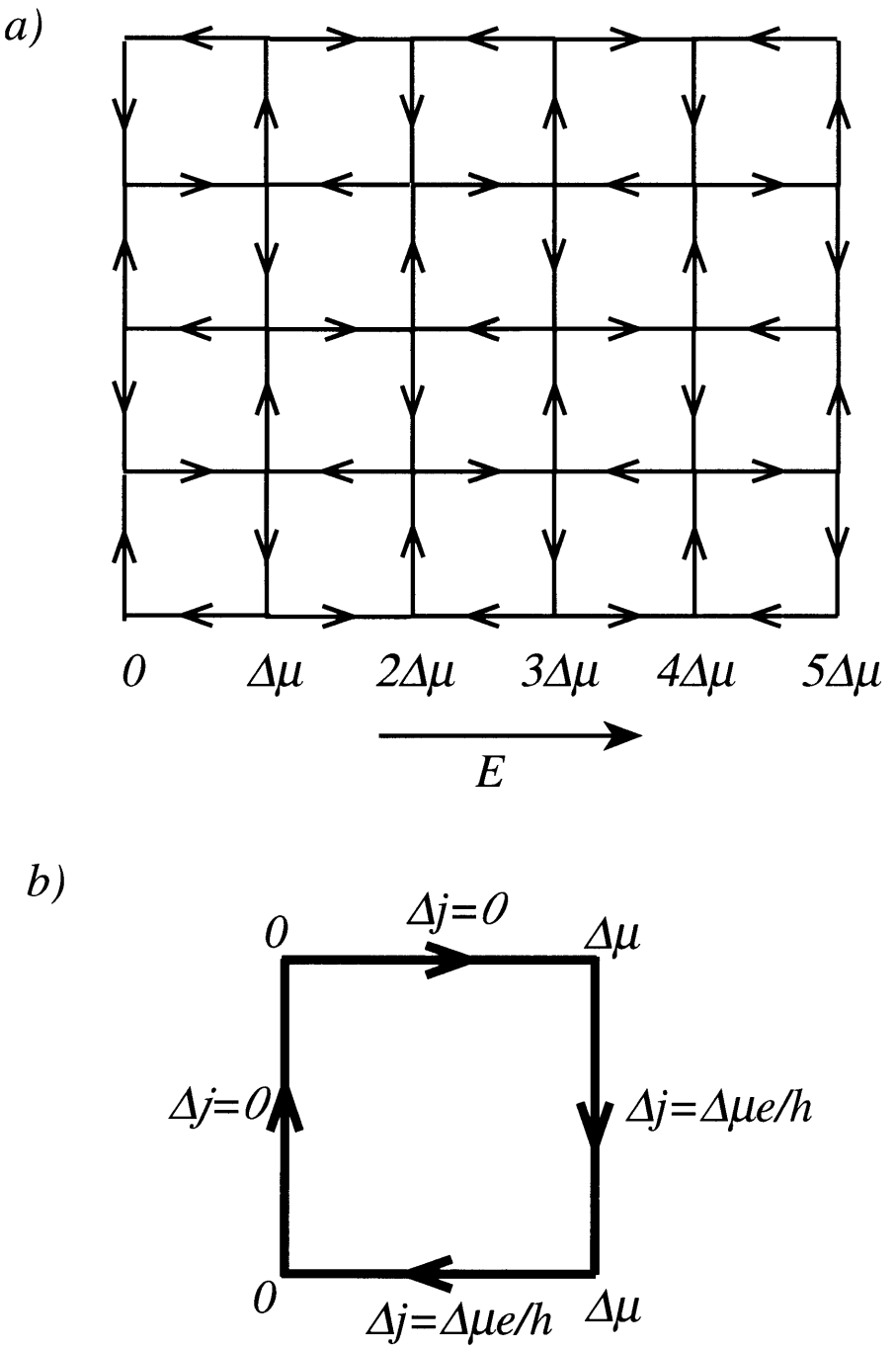

Figure 4-6: (a)The simplified edge states network. Arrows show the directions of propagation along each link.(b)Current carried along the sides of a single square according to Landauer formula.

Let us assume that it is possible to create a uniform electric field E_x in the 2DEG plane. This is equivalent to having a constant gradient of the Fermi level $\nabla\mu = eE_x$ as shown in Fig.4-6(a). Local non-equilibrium currents can be found by considering a single square, Fig.4-6(b).

Because the system is spatially uniform the current density is given by:

$$j_x = \frac{1}{2}\frac{e}{2\pi\hbar}\nabla\mu, \quad j_y = \frac{1}{2}\frac{e}{2\pi\hbar}\nabla\mu. \tag{4.32}$$

Thus the conductivity tensor has the form

$$\sigma_{xx}^N = \frac{1}{2}\frac{e^2}{2\pi\hbar}, \sigma_{xy}^N = \frac{1}{2}\frac{e^2}{2\pi\hbar}, \tag{4.33}$$

which is a special case of the formulas given in Ref.[38].

By adding the contribution of the $N-1$ filled Landau levels according to Eq .(4.31) one gets the following conductivity tensor:

$$\sigma_{xx} = \frac{1}{2}\frac{e^2}{2\pi\hbar}, \sigma_{xy} = (N-\frac{1}{2})\frac{e^2}{2\pi\hbar}. \tag{4.34}$$

This implies that the value of σ_{xx} at the peak should be independent of the Landau level number or, in other words, $\rho_{xx}(N+1/2) \sim B^2$.

The same conductivity tensor has been found by Huo, Hetzel, and Bhatt[56], who have performed a computer simulation of a system of non–interacting electrons on the first Landau level. Their results have been obtained for the case of the short–range disorder suggesting that the result of Eq.(4.34) can be more general than would follow from the above derivation.

It is a formidable task to extract the value of σ_{xx} from the experiments with Hall bars because of non-local transport through edge states[39, 5, 50, 51, 52], non-uniform current distribution[57], and the spin-splitting of the Landau levels, taking place at small N. However there is some evidence[58] that σ_{xx} is independent of N. The absolute value of the conductivity in Ref.[58] was in agreement with Eq.(4.34) although the observation was made for the spin–unresolved peaks. We believe that the use of Corbino geometry or non-contact measurements may help to verify the correctness of Eq.(4.33).

An important assumption in the derivation of Eq.(4.34) was in describing scattering in the nodes of the network by a single scattering probability: only then can one assign a single value of the chemical potential to a node. The validity of this assumption depends crucially on the detailed structure of the bulk edge channels. In particular if the edge channels are wide the scattering of an electron may depend on its position across the channel. This situation will be discussed in terms of composite fermions in Sec.4.6. The limit of extremely wide channels will be treated in the Fermi–liquid framework in Section 4.5.

4.4 Evolution of the QHE in samples with long–range disorder

In the network model reviewed in Section 4.3 the conductivity of a half–filled Landau level is given by the universal value, Eq.(4.33). However the experimental data exhibit a much richer behavior. Not only the absolute values of the resistivity may fluctuate, but also the peaks may not be infinitely sharp in the limit of zero temperature. In this Section we discuss the limits of applicability of the network model relying on the results obtained in Section 4.2.

We start by considering the IQHE regime although the quantitative results obtained for this case are likely to be incorrect because of the importance of the quantum effects. Then we treat the FQHE regime in the same spirit using the concept of composite fermions. We believe that our theory is actually more reliable than in the IQHE case, even though we find a certain disagreement with available data.

In high mobility GaAs heterostructures, widely used to study transport properties of the 2DEG, the major contribution to disorder comes from the long-range potential due to the random distribution of ionized donors behind the spacer layer. For the sake of simplicity we consider the case of a non–correlated donor distribution and assume that the average densities of ionized donors and electrons are identical. Then, following Refs.[59] we have for the deviation δn_i from the average ionized donor density n_i

$$\langle \delta n_i(\mathbf{r}) \rangle = 0, \tag{4.35}$$

$$\langle \delta n_i(\mathbf{r_1}) \delta n_i(\mathbf{r_2}) \rangle = n_i \delta(\mathbf{r_1} - \mathbf{r_2}), \tag{4.36}$$

where $\langle ... \rangle$ denotes a statistical average. By making Fourier transformation of Eq.(4.36) we find

$$\langle \delta n_i(\mathbf{q_1}) \delta n_i(\mathbf{q_2}) \rangle = (2\pi)^2 n_i \delta(\mathbf{q_1} + \mathbf{q_2}). \tag{4.37}$$

As discussed in Ref.[59] because of screening by the 2DEG the deviation δn_e from the average electron density $n_e = n_i$ can be related to δn_i by

$$\delta n_e(\mathbf{q}) = \delta n_i(\mathbf{q}) \exp(-q d_s). \tag{4.38}$$

Then the mean square deviation in the electron density

$$\delta n_e = \frac{\sqrt{n_e/8\pi}}{d_s}. \tag{4.39}$$

Rewriting this in terms of the Fermi wavevector $k_F = \sqrt{4\pi n_e}$ we have

$$\delta n_e = \frac{n_e}{\sqrt{2} k_F d_s} = \frac{n_e}{\beta}. \tag{4.40}$$

Eq.(4.40) defines the value of β in the case of non–correlated donor distribution. In typical high–mobility GaAs heterostructures $\beta \approx 10 - 40$ which makes it a natural large parameter.

It is quite possible that the distribution of ionized donors in heterostructures is correlated. In this case we can still introduce β as a typical relative electron density deviation. However Eq.(4.39) will not hold.

The typical density gradient can be found approximately from Eq.(4.40)

$$n' = \frac{\delta n_e}{d_s} = \frac{n_e}{\beta d_s}. \tag{4.41}$$

Now we can estimate the widths of compressible strips in the percolating network. As was done in Section 4.2 we approximate the density distribution by the linear expansion. Let us first consider the case of the IQHE. As discussed in Section 4.2 the small–gradient regime compressible strips are much wider than the incompressible ones. The typical width of the compressible strips in a strong magnetic field can be found from the condition

$$b = \frac{n_L}{n'}, \tag{4.42}$$

where $n_L = (2\pi\lambda^2)^{-1}$ is the density in each Landau level. By expressing n_L in terms of the Landau level filling factor $N - 1/2$ and subsituting n' from Eq.(4.41) we find

$$b = \frac{\beta d_s}{N - 1/2} \tag{4.43}$$

This formula is only valid when it yields b less than d_s, otherwise it indicates that all the 2DEG is in the compressible state. By equating b with the Bohr radius (as follows from Eqs.(4.23,4.24)) we can find N at which in a given sample the transition to the large–gradient regime takes place:

$$N_c \approx \frac{\beta d_s}{a_B} \tag{4.44}$$

For the filling factor $N > N_c$ the sample should be in the large–gradient regime: the compressible strips are narrow and the incompressible ones are wide. Then the conduction in the topmost Landau level can be described by the network model, yielding conductivity at half–integer filling factors independent of the number of filled Landau levels. In this case the resistivity peaks should scale as B^2.

At $N < N_c$ the description of the conduction in the topmost Landau level with the network model becomes inadequate. This is because the compressible liquid strips are wide and cannot be described as a single channel at the intersections. An essential assumption of the network model that there is an equal chance for an electron at each intersection to scatter left or right breaks down. It is natural to assume that for a wide edge channel one can introduce a quantum number characterizing the location of an electron across the channel. Then the transmission matrix at an intersection will depend on this quantum number. In other words, electrons which are closer to the right–hand side of the channel are more likely to go right at an intersection, while the ones closer to the left side are more likely to go left. We will see in Sec.4.6 that this argument can be made more specific by considering composite fermions.

It has been argued by several authors[13, 60, 47] that the compressible regions are

wide in the IQHE regime, making risers between the quantum Hall plateaus rather wide. Experimentally, it seems that the risers are narrower than expected. This descrepancy has been attributed in Ref.[60] to the localization of the compressible liquid, still an unresolved question. In this paper we take the point of view that localization occurs only for narrow channels on the scales of several network cells.

Our derivation of Eq.(4.44) relied on the fact that the total energy of the electron system can be written in terms of the density distribution. In this sense it is a classical theory, with quantum mechanics entering only with the cyclotron gap. Thus the theory is only valid when all the dimensions of the strips are larger than the typical extent of the electron wavefunctions, which is given by the cyclotron radius $R_c^N = \sqrt{N}\lambda$ on the Nth Landau level. One can see that for the typical values of parameters, N_c obtained from Eq.(4.44) is already outside of the validity region. Moreover, the cyclotron radius in this case is larger than d_s. A detailed quantum mechanical consideration is needed, a problem which remains unsolved.

Now we switch our attention to the FQHE regime, in which the above limitations turn out to be weaker and the described transition may actually be observed.

We focus on the series of fractions with the filling factor given by $p/(2p+1)$, where p is either negative or positive integer. By using Eq.(4.41) we find the width of the compressible strip between filling factors $(p-1)/(2p-1)$ and $p/(2p+1)$ under the assumption $p \gg 1$

$$b = \frac{n_L}{(2p+1)(2p-1)n'} \approx \frac{\beta d_s}{2p^2} \tag{4.45}$$

In order to find the critical value p_{c1} at which there is a transition to the narrow edge channels we combine Eqs.(4.30,4.45)

$$p_{c1} \approx \sqrt{\frac{\beta}{2}} \tag{4.46}$$

One can see that at this value of p the width of the compressible strips b as given by Eq.(4.45) is of the order of d_s. Therefore we think that the numerical factor in Eq.(4.46) is unreliable.

Eq.(4.46) yields the critical fraction $(p_{c1}-1)/(2p_{c1}-1)$ at which the edge channels become narrow and one can apply the network model for $|p| > p_{c1}$. However in the FQHE regime we cannot directly apply Eq.(4.34) because the Landauer formula used in its derivation was obtained for non–interacting electrons. We overcome this problem by transforming the 2DEG to the system of composite fermions. The fractional filling factor $p/(2p+1)$ corresponds to integer effective filling factor p for composite fermions. Consequently the fractional electron edge states correspond to the integer fermion edge states. Thus we can legitimately apply Eq.(4.34) to the fermion system.

We consider the 2DEG at a critical filling factor, when the edge channels between regions with filling factors $(p-1)/(2p-1)$ and $p/(2p+1)$ form a percolating network. The critical filling factor is given by the mean of the two fractions only in a special case when there are no regions with other filling factors in the system. In the general case, however, there may be regions with filling factors less than $(p-1)/(2p-1)$ and greater than $p/(2p+1)$, see Fig.4-2. Thus we believe that the exact position of the

peaks is not universal and may vary from sample to sample. This conclusion does not contradict the results of Ref.[61], where the position of the peaks was found to be described by $(2p-1)/(4p)$ rather than by the mean of $(p-1)/(2p-1)$ and $p/(2p+1)$. The 2DEG with uniform density at filling factor $(2p-1)/(4p)$ corresponds to the fermion system at filling factor $p-1/2$. For convenience in the rest of the paper we will refer to the peaks by fractions of the kind $(2p-1)/(4p)$, although the exact peak position may be slightly different.

Straightforward application of the Eq.(4.34) gives the following conductivity tensor for the system of fermions

$$\sigma_{xx}^{f} = \frac{1}{2}\frac{e^2}{2\pi\hbar}, \quad \sigma_{xy}^{f} = (p-\frac{1}{2})\frac{e^2}{2\pi\hbar}. \tag{4.47}$$

In order to obtain the physical transport coefficients we follow the procedure outlined in Ref.[42]. The first step is to invert the conductivity tensor in order to obtain the resistivity tensor. Then one should add the contribution coming from the Chern–Simons gauge field:

$$\rho_{xx}^{CS} = 0 \quad , \rho_{xy}^{CS} = -2\frac{2\pi\hbar}{e^2} \tag{4.48}$$

This originates from the phase factor in the fermion–electron transformation. A nice qualitative motivation for the summation of the resistivity tensors is described by Zhang[62]. Eventually, we find the following resistivity values for the filling factor $(2p-1)/(4p)$:

$$\rho_{xx} = \frac{2\pi\hbar}{e^2}\frac{1}{2p^2-2p+1}, \quad \rho_{xy} = -\frac{2\pi\hbar}{e^2}\frac{4p^2-2p+1}{2p^2-2p+1}. \tag{4.49}$$

For example, by substituting $p=2$ we find that at filling factor $3/8$ the resistivity tensor is

$$\rho_{xx} = \frac{2\pi\hbar}{e^2}\frac{1}{5}, \quad \rho_{xy} = -\frac{2\pi\hbar}{e^2}\frac{13}{5}, \tag{4.50}$$

or for $p=-3$ (filling factor $7/12$):

$$\rho_{xx} = \frac{2\pi\hbar}{e^2}\frac{1}{25}, \quad \rho_{xy} = -\frac{2\pi\hbar}{e^2}\frac{31}{25}. \tag{4.51}$$

By inverting the resistivity tensor we find that conductivity is given by:

$$\sigma_{xx} = \frac{e^2}{2\pi\hbar}\frac{1}{2(4p^2+1)}, \quad \sigma_{xy} = \frac{e^2}{2\pi\hbar}\frac{4p^2-2p+1}{2(4p^2+1)} \tag{4.52}$$

These transport coefficients are identical to that previously obtained by Kivelson, Lee, and Zhang[41] who mapped the fractional filling factor system onto the dirty boson model and took the boson conductivity such that it yields the universal value(4.34) for the IQHE. Thus our results are in agreement with the law of corresponding states[40, 41].

An advantage of our approach is that having a definite model in mind which

yields Eqs.(4.49,4.52) enables us to give the limits for the validity of these results. We believe that Eqs.(4.49,4.52) are valid under the condition $|p| > p_{c1}$ and describe the critical peaks, i.e. the ones whose width goes to zero in the zero temperature limit.

As was mentioned previously the network model breaks down when the compressible strips become wide which should happen at $p = p_{c1}$. We will explain the nature of this transition from the composite fermion point of view in Sec. 4.6. The values of the resistivity are reduced in this case and the peaks may exhibit some additional structure. We call these peaks "pregnant" because they are about (as disorder is reduced further) to give birth to the daughter fractions. These fractions appear when the compressible strips are wide enough for the incompressible strips of the higher order fractions to form along them.

Having narrow compressible strips is a necessary but not a sufficient condition for the validity of the network model. Another condition is imposed by the requirement that there is no equilibration between the transport edge channels (forming the percolating network) and localized edge channels (forming closed loops) as shown in Fig.4-2. The suppression of the equilibration takes place because of the exponential decay of the wave functions of the edge states inside the incompressible strips. Therefore the equilibration rate is very sensitive to the width of the incompressible strips. This phenomenon has been studied experimentally for the fractional edge states by Kouwenhoven et al[6], Wang and Goldman[63], and Chang and Cunningham[64]. Electrostatics based theoretical interpretation[45] seems to be in a reasonable agreement with the data of Ref.[6].

In the IQHE the characteristic length of the exponential decay of the edge state wavefunction is the magnetic lenth, λ. We think that in the FQHE regime the effective magnetic length for the composite fermions, λ^f, plays a similar role. Therefore the critical width of the compressible strips at which the transport edge channels are practically destroyed is equal to λ^f. In the state with the filling factor $p/(2p+1)$ and electron magnetic length λ the fermion magnetic length is given by

$$\lambda^f = \lambda\sqrt{2p+1} \tag{4.53}$$

Hence the breakdown of the network model takes place when the typical incompressible strip width

$$a = \lambda^f = \lambda\sqrt{2p+1} \tag{4.54}$$

It seems plausible that the same condition should determine the disappearance of the fractionally quantized Hall plateaus and zero longitudinal resistivity values. This is because plateau formation should be due to the existence of the percolating incompressible strip network[11, 19, 13].

It is likely that Eq.(4.54) determines the narrowest possible incompressible strip meaning that there could be no fractional gap for the strips of smaller widths.

The transition to the Fermi–liquid state can be determined from the following considerations. The typical width of the incompressible liquid strips in the state with the average filling factor $(2p-1)/4p$ ($|p| > p_{c1}$) can be found by recalling that the

compressible strips are much more narrow than the incompressible ones. Then the width of the incompressible strips is given by

$$a = \frac{n_L}{(2p-1)(2p+1)n'} \approx \frac{\beta d_s}{2p^2}, \tag{4.55}$$

where we assumed that $p_{c2} \gg 1$. By using the minimum width of the incompressible strip as given by Eq.(4.54) and recalling Eq.(4.40) we find the transition value p_{c2},

$$p_{c2} \approx \left(\frac{\beta}{2}\right)^{4/5} \tag{4.56}$$

Therefore the network model should be applicable in the interval $p_{c1} < |p| < p_{c2}$, where p_{c1} and p_{c2} are given by Eqs.(4.46,4.56). We caution the reader that the numerical factors in Eqs.(4.46,4.56) should not be taken seriously.

We believe that a proper description of the case $|p| > p_{c2}$ should be given in the framework of the Fermi–liquid theory developed in Ref.[42]. We consider this regime in Section4.5.

So far we discussed only the principal sequence of the filling fractions $p/(2p+1)$. Our results can be easily extended to the sequence of fractions converging to any half–integer filling factor. The universal resistivity values (4.49) correspond in this case only to the topmost Landau level. In other words Eq.(4.52) gives the values of σ_{xx}^N and σ_{xy}^N which are related to the experimentally observed transport coefficients as discussed in Section 4.3.

4.5 Transport in the Fermi–liquid regime.

In a recent paper[42] Halperin, Lee and Read have suggested that a 2D system of strongly interacting electrons with Landau level filling factor 1/2 can be transformed to an equivalent system of fermions interacting with a Chern-Simons gauge field, such that the average effective magnetic field seen by fermions is zero. They have argued that even though the gauge field fluctuations lead to divergent corrections to the quasiparticle propagator the Fermi-liquid description of the fermion system is valid. valid. The gauge transformation can also be performed[42] for the system of electrons with the filling factor $N - 1/2$ by attaching two flux quanta only to the electrons on the topmost Landau level. In order to calculate the conductivity of such a system one needs to take disorder into account. As was done in Section 4.4 we consider the case of the long–range disorder caused by a random distribution of ionized donors in GaAs heterostructures. At zero magnetic field the small angle scattering on this potential accounts for the zero temperature resistivity.

One can look at this mechanism from a different point of view. Due to a very strong screening by the 2DEG (screening radius equal to a_B) the long-range potential created by donors is transformed into the electron density fluctuations. Electrons are scattered by the density non-uniformities in a way similar to the propagation of light in a media with the varying index of refraction. The same mechanism exists

for the system of fermions because fluctuations in the local densities of fermions and electrons are identical.

However it was argued in Refs.[42, 43] that another scattering mechanism is important in a strong magnetic field. Due to the density fluctuations of the electron system fermions see an effective fluctuating in space magnetic field. Scattering on this magnetic field accounts for a high resistivity at filling factors $N-1/2$. The amplitude of the effective magnetic field fluctuations is proportional to the density fluctuations of the electron system; and the lengthscale of the fluctuations is equal to the spacer layer thickness d_s.

Halperin, Lee and Read[42] have calculated the conductivity of the fermion system using Born approximation which is valid in the regime when $R_c^f \gg d_s$ (where R_c^f is the fermion cyclotron radius in the effective magnetic field) so that small-angle scattering by the magnetic field fluctuations is dominant. They found that the longitudinal resistance of the electron system is determined by the large parmeter $k_F d_s$ and scales as the square root of the magnetic field. However, it seems that, experimentally, resistance at half–integer filling factors in the Fermi–liquid regime scales linearly[65, 66] with the magnetic field. Halperin et al.[42] argued that the discrepancy is due to the fact that except for $N=1$, the opposite limit $R_c^f \ll d_s$ is more appropriate so that Born approximation is not valid. In this section we calculate the conductivity in this limit.

Let us give an estimate of the effective magnetic field seen by the fermions following Ref.[42]. The typical magnetic field can be found from the typical density fluctuation given by Eq.(4.40), recalling that each fermion carries two flux quanta:

$$\Delta B \approx 2\frac{2\pi\hbar c}{e}\delta n_e \approx 2\frac{2\pi\hbar c}{e}\frac{n_e}{\beta} \tag{4.57}$$

The fermion cyclotron radius in the typical magnetic field ΔB can be found by expressing it in terms of the Fermi velocity v_F and the cyclotron frequency ω_c

$$R_c^f \approx \frac{v_F}{\omega_c} \approx \frac{\hbar k_F}{e\Delta B/c} \tag{4.58}$$

Substituting expression for ΔB and rewriting k_F in terms of the fermion concentration n_f one gets

$$R_c^f = d_s\sqrt{2\frac{n_f}{n_e}} \tag{4.59}$$

The density of fermions coincides with the electron density only at filling factor $1/2$. At filling factor $N-1/2$ the fermion density

$$n_f = \frac{n_e}{2N-1} \tag{4.60}$$

because only sitting on the topmost Landau level electrons are transformed into

fermions. Substituting this in Eq.(4.59) one finds

$$R_c^f = d_s/\sqrt{N-1/2} \tag{4.61}$$

Thus we find that the fermion cyclotron radius in the typical effective magnetic field is smaller than the lengthscale of the magnetic field fluctuations for large N.

It is clear that the conductance in this situation is determined mainly by the fermions that live near the lines of zero effective magnetic field because their cyclotron radius is large. Fermions that live in the areas of strong magnetic field drift slowly along the closed orbits and do not contribute much to the conductance of the system.

We will adopt a simplified model of the effective magnetic field fluctuations. Instead of considering a slowly varying magnetic field we will consider the case when the magnetic field takes only two values ΔB. Thus the whole plane is divided into areas of the typical size d_s where magnetic field has the same magnitude but randomly varying sign.

To calculate the conductance of such a system let us first solve a simpler problem. Let us consider the case when the magnetic field is translationally invariant along the x-axis and is given by:

$$B_z = \Delta B \mathrm{sgn}(y) \tag{4.62}$$

The one–particle Hamiltonian in Landau gauge with the magnetic field described by Eq.(4.62) is given by

$$H = \frac{1}{2m}(p_y^2 + (p_x - \frac{e\Delta B}{c}|y|)^2), \tag{4.63}$$

where p_x and p_y are the components of the momentum. The eigenfunctions of this Hamiltonian can be written in the form

$$\psi = \phi(p_x, y)\exp(i\frac{p_x}{\hbar}x), \tag{4.64}$$

where $\phi(p_x, y)$ is found by solving the equation

$$\frac{d^2\phi}{dy^2} + \frac{2m}{\hbar^2}(E - U_{eff})\phi = 0 \tag{4.65}$$

with the effective potenial, see Fig.4-7:

$$U_{eff} = \frac{1}{2m}(p_x - \frac{e\Delta B}{2c}|y|)^2 \tag{4.66}$$

Eq.(4.65) can be solved quasiclassically. The spectrum is shown in Fig.4-8. One can see that at large positive p_x the eigenvalues are doubly degenerate. They correspond to the eigenstates in a uniform magnetic field centered at $y = \pm p_x$. The total number of states is equal $2N_f$, where N_f is the number of filled Landau levels for fermions in the magnetic field ΔB:

$$N_f = \frac{2\pi\hbar c n_f}{e\Delta B} \tag{4.67}$$

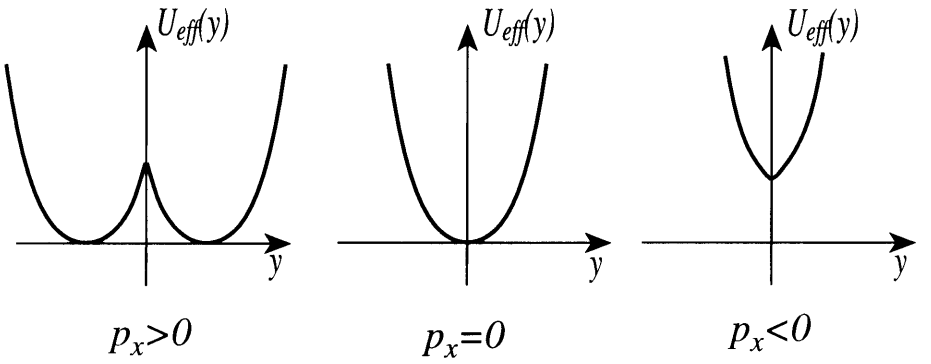

Figure 4-7: Effective potential at different values of p_x.

At smaller p_x the degeneracy is lifted and the states acquire velocity in the y-direction. In order to discuss transport properties we focus on the states at the Fermi level. They are localized near the line $y = 0$ and have a velocity in the x-direction. These states are called the snake states due to the characteristic shape of the classical analogue trajectories. As at $p_x \to -\infty$ all the eigenstates are above the Fermi level the total number of the snake states is $2N_f$. The snake states are reminiscent of the edge states in that they have a single velocity direction. The snake states, however, are all centered at $y = 0$ and are not spatially separated like the edge states.

The conductance of the fermion system along the line $y = 0$ can be found by using the Landauer formula[24].

$$g = 2N_f \frac{e^2}{2\pi\hbar}. \tag{4.68}$$

Going back to the original problem with the magnetic field of varying sign we immediately notice that the snake states form a network very similar to the one considered for the edge states in Section 4.3 and shown in Fig.4-6. This allows us to calculate the conductivity of the fermion system using the line of argument that led to Eq.(4.33):

$$\sigma^f_{xx} = g/2 = N_f \frac{e^2}{2\pi\hbar}, \quad \sigma^f_{xy} = 0 \tag{4.69}$$

Of course an important assumption made in the derivation of Eq.(4.69) was that the cyclotron radius for the topmost Landau level is smaller than the scale of the network.

We would like to formulate now a general statement, of which Eqs.(4.33,4.69) are the special cases. Suppose, one has a system of non–interacting fermions confined in a plane and subject to a perpendicular non–uniform magnetic field and some external potential. Suppose that the distribution of the magnetic field and external potential is such that the plane is broken up into the alternating regions with two filling factors

$$N_1 = \frac{2\pi\hbar c n_1}{eB_1}, \quad N_2 = \frac{2\pi\hbar c n_2}{eB_2} \tag{4.70}$$

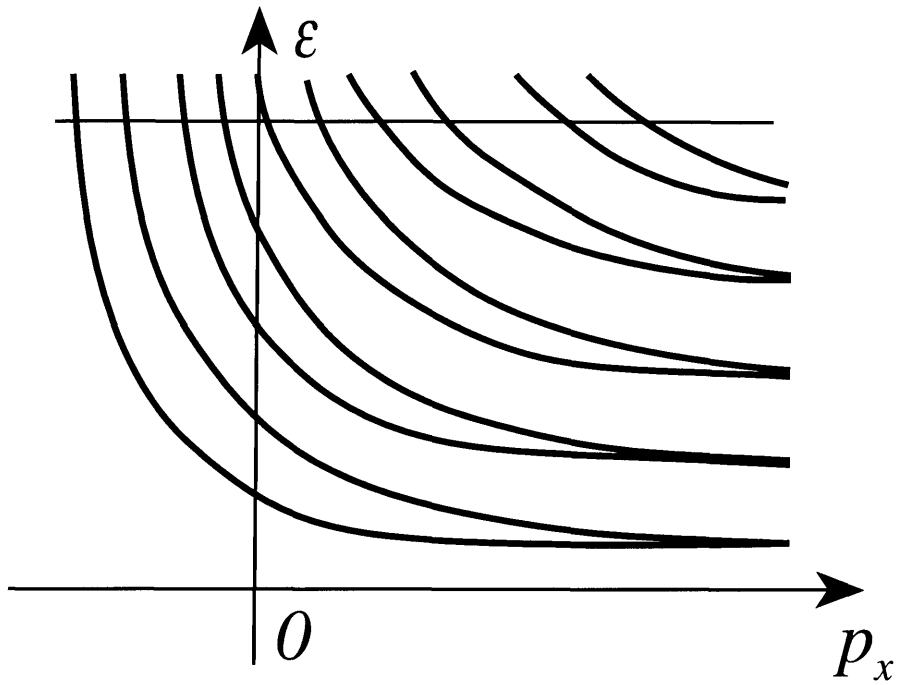

Figure 4-8: Spectrum of the free–particle Hamiltonian with the step–like magnetic field. The double degeneracy at $p_x \to \infty$ represents Landau states to the right and to the left from $y = 0$.

where n_1,n_2 are densities and B_1,B_2 the magnetic fields. We assume that the Fermi level lies in the cyclotron gap inside the regions, henceforth N_1 and N_2 can be positive or negative integers . Then the system can be represented by a network of edge or snake channels. By using the Landauer approach we find the conductivity tensor to be

$$\sigma_{xx} = \frac{|N_1 - N_2|}{2} \frac{e^2}{2\pi\hbar}, \quad \sigma_{xy} = \frac{N_1 + N_2}{2} \frac{e^2}{2\pi\hbar}. \tag{4.71}$$

One can see that when $N_1 = N$, $N_2 = N - 1$ Eq.(4.71) is reduced to Eq.(4.34), and when $N_1 = -N_2 = N_f$ Eq.(4.71) is reduced to Eq.(4.69).

The general result, Eq.(4.71), allows for an accurate calculation of the resistivity at filling factor $N - 1/2$ (in the sharp–step model). The typical magnetic field seen by fermions is given by Eq.(4.57), and the densities of the fermion system are represented by

$$n_1 = \frac{n_e}{2N-1} - \frac{n_e}{\beta}, \quad n_2 = \frac{n_e}{2N-1} + \frac{n_e}{\beta} \tag{4.72}$$

By utilizing Eq.(4.70) we find

$$N_1 = \frac{\beta}{2(2N-1)} - \frac{1}{2}, \quad N_2 = -\frac{\beta}{2(2N-1)} - \frac{1}{2} \tag{4.73}$$

and substituting this in Eq.(4.71) we derive a more accurate then in Eq.(4.69) fermion conductivity tensor

$$\sigma_{xx}^{f} = \frac{\beta}{2(2N-1)}\frac{e^2}{2\pi\hbar}, \quad \sigma_{xy}^{f} = -\frac{1}{2}\frac{e^2}{2\pi\hbar} \tag{4.74}$$

By following the procedure outlined in Ref.[42] we find the conductivity of the Nth electron Landau level to be

$$\sigma_{xx}^{N} = \frac{N-1/2}{\beta}\frac{e^2}{2\pi\hbar}, \quad \sigma_{xy}^{N} = \frac{1}{2}\frac{e^2}{2\pi\hbar} \tag{4.75}$$

By using Eq.(4.31) we find the conductivity tensor

$$\sigma_{xx} = \frac{N-1/2}{\beta}\frac{e^2}{2\pi\hbar}, \quad \sigma_{xy} = (N-1/2)\frac{e^2}{2\pi\hbar} \tag{4.76}$$

Thus we see that σ_{xx} scales as the inverse of the magnetic field. Because $\beta \gg 1$ ρ_{xx} at half–integer filling factors scales linearly with the magnetic field.

In the case when $N_1 = 0$ and $N_2 = -1$ in Eq.(4.73) we have a network consisting of a single fermion edge channel. By going through a standard procedure we find the exact conductivity tensor to be

$$\sigma_{xx}^{N} = \frac{1}{2}\frac{e^2}{2\pi\hbar}, \quad \sigma_{xy}^{N} = \frac{1}{2}\frac{e^2}{2\pi\hbar} \tag{4.77}$$

in agreement with Eq.(4.33) which was obtained without considering fermions.

Our derivation was based on a somewhat artificial model in which the effective magnetic field seen by fermions is assumed to vary in a step-like manner assuming only two values ΔB. This could be realized if the incompressible strips on the sides of the compressible transport strip were wide enough.

A more realistic model may be the linear-step model. In this case the magnetic field is assumed to vary linearly between the regions with opposite magnetic field sign. To study this case let us go back to a single channel problem with magnetic field now given by

$$B = \begin{cases} -\Delta B, & y < -d, \\ \Delta B\frac{y}{d}, & |y| < d, \\ \Delta B, & y > d, \end{cases} \tag{4.78}$$

A similar problem has been considered by Müller[67]. By following the same procedure as for the step–model we arrive to the spectrum of the free–particle Hamiltonian with the magnetic field described by Eq.(4.78) shown in Fig.4-9. The new feature is the existence of the edge states at $p_x > 0$. These are the states which cross the Fermi energy in Fig.4-9 with $\partial e/\partial p_x > 0$. They come in pairs, corresponding to the two possibilities to be to the left and to the right of $y = 0$. One can see that these states have velocity in the direction opposite to the one of the snake states. Because of this it is necessary to consider backscattering from snake to edge states. Of course,

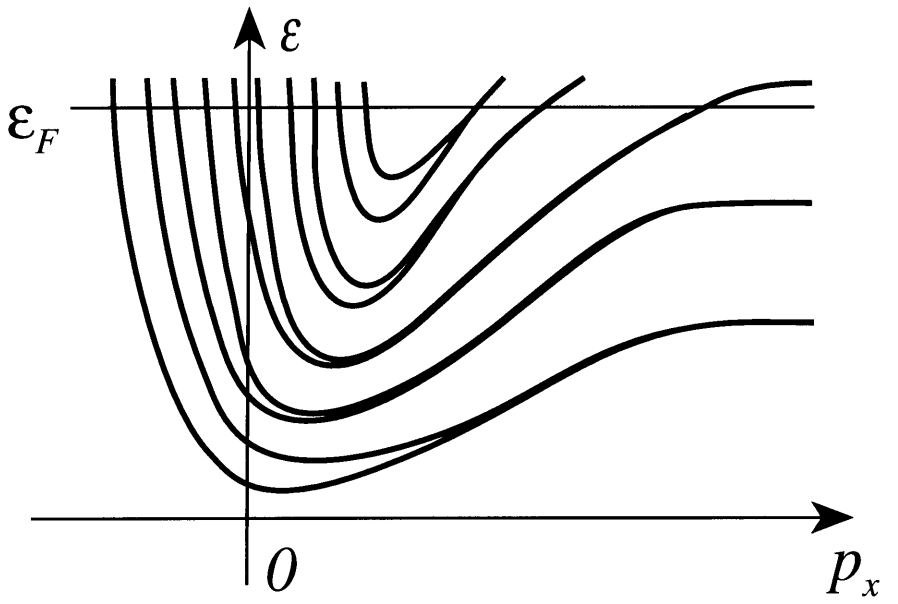

Figure 4-9: Spectrum of the free–particle Hamiltonian with the linear–step magnetic field.

in a translationally invariant magnetic field all the snake and edge states are exact eigenstates, orthogonality of which implies the absence of scattering. We will assume that there exists a small number of short–range scatterers that generate hopping matrix elements.

It seems reasonable to assume that because all the snake states are centered at $y = 0$ they are all coupled to each other. Edge states, on the contrary, are spatially separated and the rate of equilibration may be different between different states. To get an idea of what the real situation might be let us consider the case when all the edge states except the ones corresponding to the lower k Landau levels are coupled to the snake states. Suppose there are N_s channels of snake states i.e. those with $\partial\epsilon/\partial p_x < 0$ in Fig.4-9 (there $N_s = 10$). Then the number of edge channels with $\partial\epsilon/\partial p_x > 0$ which couple to the snake states is $N_s - 2k$ (the factor two comes in because of the degeneracy). If the channel is long enough then all but $2k$ channels should backscatter, meaning that the conductance is given by

$$g = 2k\frac{e^2}{2\pi\hbar} \tag{4.79}$$

The same result has been obtained by Barnes, Johnson, and Kirczenow[68], who considered a general case of directed channels.

One can see from Eq.(4.79) that only if we assume that all the edge channels are coupled to the snake channels Eq.(4.68) is recovered. In reality, the lines of zero magnetic field are not straight: they meander in the random potential. This should

lead to the scattering between edge channels even in the absence of the short–range disorder. Also, in both models, considered so far we had to assume the existence of the insulating regions, where all the states are localized. But in the presence of the scattering, extended states admix to the localized ones. Thus in the limit of strong scattering the network model loses its validity. A more appropriate picture may be that fermion orbits sweep the whole plane, making the concept of channels obsolete. In the following we give a quasiclassical argument which shows that even in this case when all the fermions participate in transport, the result of Eq.(4.69) holds.

In this case a typical electron drifts perpendicular to the magnetic field gradient with the velocity[69]:

$$v_d \approx v_F R_c \frac{\nabla B}{B} \approx v_F \frac{R_c}{d_s} \tag{4.80}$$

A typical fermion changes its direction on a length scale d_s, which we take to be the mean free path. The diffusion constant in this case is given by

$$D \approx d_s v_d \approx v_F R_c. \tag{4.81}$$

By making use of the Einstein relation we find the conductivity to be

$$\sigma_{xx}^f \approx k_F R_c \frac{e^2}{2\pi\hbar} \tag{4.82}$$

in agreement with Eq.(4.69). Of course we can not obtain a numerical coefficient in this estimate and it is not clear whether it should be the same as in Eq.(4.69).

4.6 Composite fermions of higher generations

In Section 4.4 we have described how the peaks of the longitudinal conductance evolve with varying disorder. It was shown that when the fractional peaks first develop they are in the critical state, meaning that their width should go to zero in the low–temperature limit. Then their magnitude is given by Eqs.(4.49,4.52). As disorder is reduced the peaks become pregnant, their height is reduced from the critial values given in Eqs.(4.49,4.52). As disorder is reduced further, fractional daughter states develop on the place of each peak in accordance with the phase diagram proposed in Ref.[42]. These daughter states are in the same relation to the mother state as the fractions of the main sequence to the integer states.

These states should also be characterized by the universal resistivity values, which may be obtained in the spirit of the Eq.(4.49) derivation. According to the proposed in Ref.[42] global phase diagram exactly at the location of the center of the mother peak there is a Fermi–liquid state. We will calculate the conductivity of this state in analogy with what was done for half–integer filling factors in the previous Section.

Let us recall that the idea behind the resistivity calculation for the half–integer filling factors was to attach two flux quanta to the fermions of the topmost Landau level[42]. Then the average effective magnetic field, which acts on the composite fermions is zero. Naturally, the attachment of the flux quanta does not affect the

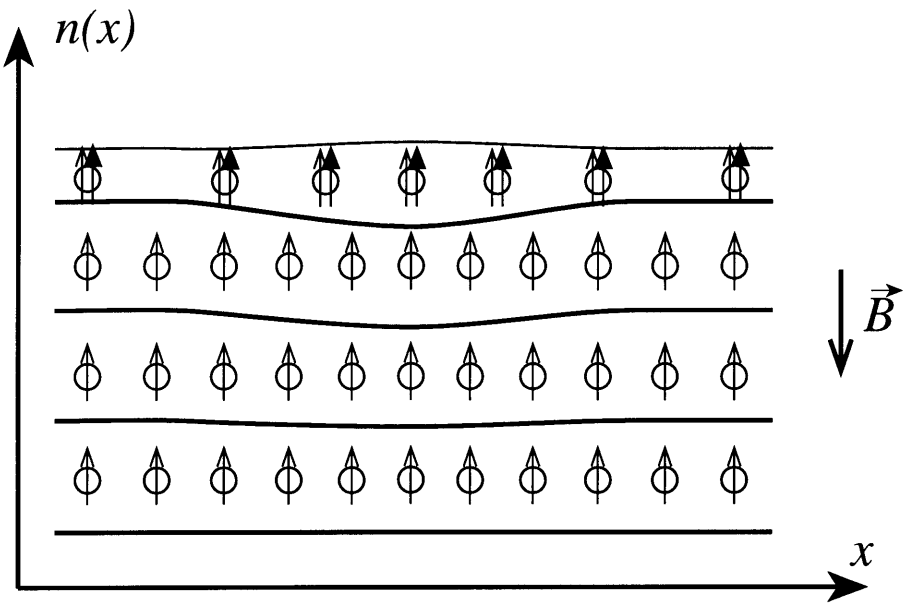

Figure 4-10: The composite fermions picture at the electron filling factor 7/16 ($p = 4$). Each arrow represents two flux quanta. Filled–in arrows represent the flux quanta of the field acting only on the fermions belonging to the topmost Landau level. (They will have opposite direction for the electron filling factor greater than 1/2 ($p < 0$).) The electron density variation results in the decrease in the density on each fermion Landau level except the topmost one.

electrons on the lower Landau level. Thus they see only the external magnetic field.

In a Fermi–liquid state with electron filling factor $(2p-1)/(4p)$ the composite fermions are at filling factor $p - 1/2$. The longitudinal resistivity of the fermion system arises from the transport of the composite fermions on the topmost p Landau level. In order to calculate this contribution we add two flux quanta of another Chern–Simons gauge field to each of those fermions, see Fig.4-10. This field does not act on the composite fermions on the lower Landau levels.

The typical density deviation δn_e is given by Eq.(4.40). However it would be incorrect to identify δn_e with the typical density deviation, δn_p, on the p fermion Landau level. The reason being that these additional fermions also carry flux quanta which produce additional effective magnetic field acting on the fermions of the lower $p-1$ Landau levels, Fig.4-10. In order to find δn_p we write this effective magnetic field in terms of the additional density

$$\Delta B = -\delta n_e \frac{2ch}{e} \tag{4.83}$$

Then the total density deviation due to the fermions on the first $p-1$ Landau levels is

$$\delta n_e - \delta n_p = (p-1)\frac{e\Delta B}{hc} = -2(p-1)\delta n_e \tag{4.84}$$

From this we find the density deviation on the p Landau level

$$\delta n_p = (2p-1)\delta n_e \tag{4.85}$$

The typical magnetic field acting on the fermions of the topmost Landau level and created by the flux attached to the additional fermions consists of the contributions from two gauge fields and is given by

$$\Delta B' = -\delta n_e \frac{2ch}{e} - (2p-1)\delta n_e \frac{2ch}{e} = -4p\delta n_e \frac{ch}{e} \tag{4.86}$$

To calculate the resistivity of the topmost Landau level we can use Eq.(4.71) which involves the filling factors in the regions of the high and low density N_1, N_2. The two filling factors can be found from Eqs.(4.85,4.86) to be

$$N_1 = \frac{\frac{n_e}{2p-1} + (2p-1)\delta n_e}{-4p\delta n_e} = -\frac{\beta}{4p(2p-1)} - \frac{2p-1}{4p} \tag{4.87}$$

$$N_2 = \frac{\beta}{4p(2p-1)} - \frac{2p-1}{4p} \tag{4.88}$$

If N_1 and N_2 become less than one it means that the fermion filling factor is not limited to the interval $[p-1, p]$. In this case the compressible liquid occupies only narrow strips and we should use the edge channel network model. This condition is close to the one in Eq.(4.46).

According to Eq.(4.71) conductivity for the fermions of the second generation is given by

$$\sigma_{xx}^{f'} = \frac{e^2}{2\pi\hbar}\frac{\beta}{4p(2p-1)}, \quad \sigma_{xy}^{f'} = \frac{e^2}{2\pi\hbar}\frac{1}{2} \tag{4.89}$$

By going through the sequence of transformations outlined in Ref.[42] twice we can obtain an expression for the physical resistivity from Eq.(4.89). In the course of transformation we assume that β is the largest parameter in the calculations.

$$\rho_{xx}^{f'} = \frac{2\pi\hbar}{e^2}\frac{4p(2p-1)}{\beta}, \quad \rho_{xy}^{f'} = \frac{2\pi\hbar}{e^2}\frac{(4p(2p-1))^2}{2(\beta)^2} \tag{4.90}$$

By adding the contribution from the Chern–Simons field and inverting the matrix we find

$$\sigma_{xx}^{f} = \frac{e^2}{2\pi\hbar}\frac{4p(2p-1)}{4\beta}, \quad \sigma_{xy}^{f} = \frac{e^2}{2\pi\hbar}(p-\frac{1}{2}) \tag{4.91}$$

By making a transformation to the resistivity tensor and adding the Chern–Simons contribution we get

$$\rho_{xx} = \frac{2\pi\hbar}{e^2}\frac{4p}{\beta(2p-1)}, \quad \rho_{xy} = \frac{2\pi\hbar}{e^2}\frac{-4p}{2p-1} \tag{4.92}$$

The same procedure applied to the filling factors larger than 1/2 leads to the conclu-

sion that the longitudinal resistivity is inversely proportional to the filling factor ν for the even–denominator states of the principal sequence

$$\rho_{xx} = \frac{1}{\nu\beta}\frac{2\pi\hbar}{e^2}. \tag{4.93}$$

At this point we would like to address the question of localization. Although the nature of delocalized states in a strong magnetic field remains unclear, by making the transformation to the composite fermions we can apply the results for localization at zero magnetic field. Strictly speaking, in two dimensions all the states should be localized. However the localization length may be exponentially large, making the effects of localization unobservable. One can see though from Eq.(4.89) that at sufficiently large p the fermion conductivity is close to $e^2/2\pi\hbar$, making localization length small. The localization should manifest itself in the temperature dependence of the resistivities at even–denominator filling factors. The higher is the value of p the easier the fermion system can be localized. At low enough temperatures Eq.(4.93) should only hold for the half–integer filling factors.

It seems possible that pregnant peaks correspond to the situation when all the 2DEG plane is occupied by the compressible liquid. Then the high values of the resistivity are due to the localization of the fermion system.

Now we would like to go back and clarify the meaning of the transition from narrow to wide edge channels which yielded the value of p_{c1}. From the consideration of the last two Sections one can see that the number of the composite fermion channels depends on the magnetic field gradient which is determined by the electron density distribution.

First, let us consider an integer edge channel. When the channel is extremely narrow the effective magnetic field acting on fermions varies in a step–like manner. Then there is just one fermion Landau level crossing the Fermi–level, thus creating a single fermion channel. If the background charge density gradient is reduced the edge channel becomes wider as discussed in Sec. 4.2. The magnetic field gradient becomes smaller, higher Landau levels descend and cross the Fermi–level, leading to the appearance of the pairs of snake and edge channels of composite fermions. The total conductance of the integer channel remains the same because of the opposite velocities of the snake and edge channels. However, we run into difficulties with the network model. It was assumed in Sec. 4.3 that at the intersection each electron can go right or left with probability 1/2. It is clear now that in the wide edge channels different fermion channels would have different scattering probabilities and the network model is oversimplified.

The same argument for the fractional edge channels of the principal sequence can be carried out by considering the channels of the second generation fermions. This elucidates the significance of p_{c1} found in Section 4.4.

4.7 Comparison with experiment

In this Section we compare our results with a series of available experimental observations made on extremely high–mobility GaAs heterostructures.

In Section 4.4 we predict that the conductivity of the critical fractional peaks is universal, Eq.(4.52): it only depends on the peak's filling factor. However the comparison with experiment is complicated by the fact that for any given sample only some peaks are critical and it is hard to determine unambiguously which ones. A peak may look critical but, in reality, be on the early stages of pregnancy, thus having a lower than expected conductivity.

When interpreting the experimental results it is usefull to realize that according to Eqs.(4.49,4.52) the particle–hole symmetry is present for the conductivities of the critical peaks, but not for their resistivities. On the other hand, peaks of the principal sequence at filling factors with the same numerators have the same resistivities.

Extremely helpful for the purpose of verifying the universal values would be an experiment in which the level of disorder is changed continuously. Then the maximum conductivity value achieved by a given peak should approach the universal value. We are aware of only one experiment in which a variation of disorder was attempted. Sajoto et al[65] have studied the FQHE in the GaAs heterostructures, varying the electron density by applying voltage to a back–gate. Because of the dependence of screening on the concentration of carriers this results in varying the level of disorder.

We focus on the observations on sample M73 presented in Fig.3 of Ref.[65]. Let us follow the behavior of the 3/8 ($p = 2$) peak between the 1/3 and 2/5 states. This peak is still undeveloped at the density $n_e = 1.7 \cdot 10^{10}\text{cm}^{-2}$, it looks close to critical at $n_e = 2.2 \cdot 10^{10}\text{cm}^{-2}$ and it is pregnant at $n_e = 5.0 \cdot 10^{10}\text{cm}^{-2}$. (A detailed study of the temperature dependence of the peak's shape could probably verify the diagnosis.) Thus the resistivity for this peak is 4 arb. units. The 7/12 ($p = -3$) peak between the 3/5 and 4/7 states is undeveloped at $n_e = 2.2 \cdot 10^{10}\text{cm}^{-2}$ and it is close to critical at $n_e = 5.0 \cdot 10^{10}\text{cm}^{-2}$. Its resistivity is 1.1 arb. units. The ratio of the resistivities of the two peaks is approximately 3.6. On the other hand, by using Eqs.(4.50,4.51) this ratio should be 5. This disagreement is probably due to the fact that at $n_e = 2.2 \cdot 10^{10}\text{cm}^{-2}$ the 3/8 peak is already pregnant.

The limits of the critical regime are given in Eqs.(4.46,4.56) in terms of β. However we do not think one can use Eq.(4.40) in these criteria because of the possible correlations in the distribution of ionized donors. It seems likely that such correlations exist because of the lower than expected values of the resistivity of the Fermi–liquid states, which we discuss next.

Störmer et al[66], following an earlier conjecture of Chang and Tsui[70] have shown that at relatively high temperature (0.3K) the longitudinal resistivity is amazingly linear with the exception of dips at the integer and odd–denominator filling factors. They introduced parameter β as a ratio of the classical Hall resistivity to the linear approximation of ρ_{xx}. Explanation of the linear behavior was given in Sections 4.5,4.6 in the framework of the composite fermions. We defined β as a microscopic parameter and showed that it enters the expression for ρ_{xx}, Eq.(4.6) the same way as the phenomenological β of Ref.[66]. Therefore we assume our β to be identical to the

one introduced by Störmer et al.

The value of β was found in Ref.[66] to be almost independent of temperature and to to be equal to 23 and 36 for two different samples, while the estimate according to Eq.(4.40) gives 21 and 9.6 correspondingly. Such a big descrepancy for the higher mobility sample probably implies the importance of correlations in the ionized donor distribution. At lower temperatures[48] resistivity at half–integer are mostly unchanged while at other even–denominator fractions it grows significantly.

The linear dependence of the resistivity at half–integer filling factors can also be seen in the data of Refs.[65, 72] at very low temperatures. Again at other even denominator fractions such as 3/8, 1/4, 3/4 the resistivity seems to grow as temperature is lowered.

As discussed in Section 4.6 the Fermi–liquid at filling factors with large p can be easily localized. This could serve to explain the deviation of the resistivity from the values given by Eq.(4.93) at temperatures so low that the inelastic scattering length is larger than the localization length.

The linear dependence of the Fermi–liquid states' resistivity on the magnetic field as described by Eq.(4.93) makes it possible to extract the value of β from experiment without relying on the assumption of an uncorrelated donor distribution.

Below we give the comparison of our predictions of the universal resistivity values, Eq.(4.49) with the results of several experimental groups. We would like to emphasize that the presence of the non–local transport[63] might have severly affected the measurements.

By analyzing the data of Clark presented in Fig.2(a) of Ref.[71] we determine that the peaks at filling factors 7/16, 9/20 and 9/16 are critical, while the peak at 7/12 is probably slightly pregnant. We find that the resistivities of those peaks agree with Eq.(4.49) within the accuracy of 15%.

In a recent paper[48] Du et al have reported the observation of the main sequence fractions up to 9/17 and 9/19. From Eq.(4.93) we find that β is approximately 35. Then according to Eqs.(4.46,4.56) we have $p_{c1} \approx 4$ and $p_{c2} \approx 8$. It seems that in the data of Ref.[48] peaks at filling factors 9/20, 11/24, 13/28 ($p = 5, 6, 7$) and 9/16, 11/20, 13/24 ($p = -4, -5, -6$) are indeed critical. One can see that the resistivity of those peaks does indeed scale in agreement with Eq.(4.49). However the absolute values given by Eq.(4.49) are approximately 6 times smaller then the experimental ones.

By analyzing the data of Willett et al[72], Fig.4-1 we determine that the peaks at filling factors 5/12, 7/16, 9/20 and 7/12, 9/16 are critical. Their resistivities scale in agreement with Eq.(4.49), although the experimental values seem to be 1.5 times larger. We do not have at present any reasonable explanation for the descrepancies in the absolute values.

4.8 Conclusions

In this paper we presented a unified picture of the dissipative transport between the quantum Hall plateaus for the case of the long–range disorder potential. The basic

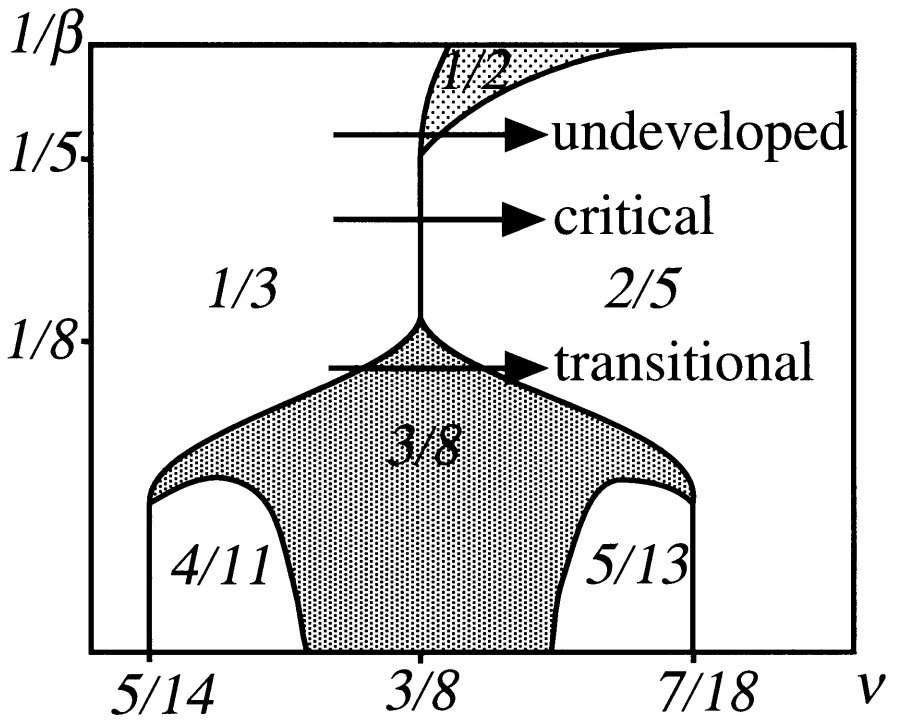

Figure 4-11: The fragment of the global phase diagram of the quantum Hall effect. Arrows show trajectories in the $\beta - \nu$ space corresponding to the existing measurements (sweeping magnetic field at constant disorder). The corresponding peak type is indicated.

assumption is the break–up of the electron system into the incompressible regions with integer or fractional filling factors, separated by the network of edge channels. We have considered the structure of edge channels and applied it to the analysis of the transport in the network.

A diverse experimental data on the longitudinal resistivity can be understood by considering the evolution of a single resistivity peak with the variation of disorder, which we describe by a single parameter β. We have shown that each peak goes through four stages in its life: underdevelopment, criticality, pregnancy, and the Fermi–liquid stage. By considering the electrostatics of edge channels, we have found the values of β which determine the beginning and the the end of the critical regime.

The evolution of the peak can be understood by considering the global phase diagram of the quantum Hall effect proposed in Ref.[42]. We represent disorder by a single parameter β and show the fragment of the phase diagram in Fig.4-11. The different kinds of peaks correspond to sweeping magnetic field at different values of β as shown in Fig.4-11.

Resistivities of the peaks in the critical regime are given by the universal values, which are in agreement with the law of corresponding states. We have obtained these values by making the transformation to the composite fermions and applying the

result for the universal conductivity of the half–filled Landau level to be $1/2(e^2/2\pi\hbar)$. We find that experimentally the relative heights of the critical peaks are in agreement with our prediction, while the absolute values vary from one experimental group to another and are in the worst case several times different. We speculate that this is due to the non–local transport contribution. A detailed experimental study of the absolute values possibly using the Corbino geometry or non–contact measurements is clearly desirable.

When the electron density fluctuations are small, compressible liquid occupies the whole plane. In this regime a proper description is given by the Fermi–liquid theory of the composite fermions. Resistivity in this case arises from the fictitious magnetic field fluctuations ralated to the fluctuations in electron density. We have solved this problem in the case of a step–like variation of the magnetic field by invoking the concept of the snake states. We have found a great similarity between the edge state and the snake state networks and give a general formula for the conductivity tensor of the network.

We have found that the resisistivity of the half–integer Fermi–liquid states and of the principal sequence even denominator fractions is linear in the magnetic field and inversely proportional to β. This conclusion is in agreement with the recent experimental results, although the analysis of the slope shows that a model of non–correlated donor distribution is oversimplified. We attribute the experimentally observed low–temperature growth of the resistivity at even–denominator principal fractions to the localization of the fermion system.

4.9 Acknowledgments

This work was done in collaboration with P.A. Lee.[73] We would like to thank B.I. Halperin for many helpful suggestions throughout the course of this work. We also acknowledge useful discussions with B.L. Altshuler, L. Levitov, K.A. Matveev, P.L. McEuen, I.M. Ruzin, B.I. Shklovskii, X.G. Wen. We are grateful to the authors of Refs.[47, 48, 5, 57, 59, 66] for sending us their papers prior to publication. This research was supported by the NSF under grant no. DMR 89 - 13624.

Appendix A

We have to solve the Laplace equation $\Delta\phi(\vec{r}) = 0$ in the half-space $z < 0$ with the following boundary conditions

$$\begin{cases} \frac{d\phi(x,z)}{dz}|_{z\to-0} = \tau(x), & |x| < l \\ \phi(x, z = 0) = 0 & |x| > l, \end{cases} \tag{A.1}$$

As boundary conditions are independent of y the problem becomes two-dimensional. Following Ref.[7] we solve by means of the analytic functions theory. Let us represent $\phi(x, z)$ as an imaginary part of the analytic function $F(\zeta)$ where $\zeta = x + iz$. $F(\zeta)$ should satisfy boundary conditions:

$$\begin{cases} Re\left(\frac{dF}{d\zeta}\right) = \tau(x), & |x| < l \\ Im\left(\frac{dF}{d\zeta}\right) = 0, & |x| > l, \end{cases} \tag{A.2}$$

Now we introduce analytic function

$$f(\zeta) = i\frac{dF}{d\zeta}(l^2 - \zeta^2)^{1/2} \tag{A.3}$$

for which we know the imaginary part everywhere on the real axis:

$$\begin{cases} Im(f(x)) = \tau(x)(l^2 - x^2)^{1/2}, & |x| < l \\ Im(f(x)) = 0, & |x| > l \end{cases} \tag{A.4}$$

With this information we regenerate $f(\zeta)$ in the lower half-plane using Schwartz integral

$$f(\zeta) = \frac{1}{\pi i}\int_{-\infty}^{+\infty} \frac{Im(f(x))}{x - \zeta}dx + c = \frac{1}{\pi i}\int_{-l}^{l} \frac{Im(f(x))}{x - \zeta}dx + c \tag{A.5}$$

where c is a constant of integration. We set $c = 0$. For $\tau(x) = \frac{4\pi e n_0}{\epsilon}$ we obtain

$$\phi(x, z) = \frac{4\pi e n_0}{\epsilon} Im[\zeta + i(l^2 - \zeta^2)^{1/2}] \tag{A.6}$$

For $\tau(x) = \frac{4\pi e x dn/dx|_{x=x_k}}{\epsilon}$ Eq.(46) yields

$$\phi(x,z) = \frac{4\pi e dn/dx|_{x=x_k}}{\epsilon} Im[\frac{1}{2}\zeta(\zeta + i(l^2 - \zeta^2)^{1/2})] \tag{A.7}$$

Appendix B

We present here a general method for solving a certain kind of electrostatics problem in two dimensions which involves Chebyshev polynomials.[1] Consider two metal semi-planes lying in the xy-plane and separated by the insulating strip of width $2a$ and centered at $x = 0$. It carries some charge, characterized by a two–dimensional charge density $\rho(x)$ invariant in the y-direction. All the charges are confined to the $z = 0$ plane. There is also some voltage difference applied to the metal semi-planes. We therefore come to a two–dimensional problem in the xz-plane with the boundary conditions specified at $z = 0$. In principle, this problem can be resolved by solving the Laplace equation in each semi-plane. However, this method is complicated. It was pointed out previously[33] that in this kind of problem, one can utilize the properties of Chebyshev polynomials[32].

The Coulomb law in the two–dimensional system, when all the charges are confined to $z = 0$, yields electric field $E(x) = E_x(x, z = 0)$

$$E(x) = \int_{-\infty}^{+\infty} dx' \frac{2\rho(x')}{x - x'}. \tag{B.1}$$

This integral should be understood in terms of the principal value. Because E_x and E_z can be understood as an imaginary and a real part of an analytic function one can invert Eq.(B.1) using the same line of argument as in the derivation of the Kramers-Kronig relations. This leads to the following relationship:

$$\rho(x) = -\frac{1}{2\pi^2} \int_{-\infty}^{+\infty} dx' \frac{E(x')}{x - x'}. \tag{B.2}$$

In our problem, the electric field is zero in the metal semi-planes (for $|x| > a$), so we rewrite Eq.(B.1) as

$$\rho(x) = -\frac{1}{2\pi^2} \int_{-a}^{a} dx' \frac{E(x')}{x - x'}. \tag{B.3}$$

We now expand the electric field and charge density in orthogonal Chebyshev polynomials

$$\rho(x) = \Sigma C_i U_i(x/a), \tag{B.4}$$

[1] I am grateful to M.I. D'yakonov who showed this method to me.

$$E(x) = \frac{2\pi}{\sqrt{1-(x/a)^2}} \Sigma D_i T_i(x/a), \tag{B.5}$$

and use the following relationship between T_i and U_{i-1} [32]

$$\int_{-a}^{a} dx' \frac{T_i(x'/a)}{(x'-x)\sqrt{1-(x'/a)^2}} = \pi U_{i-1}(x/a). \tag{B.6}$$

Combining Eqs.(B.3–B.6) we find

$$D_i = C_{i-1}. \tag{B.7}$$

This equation provides the following algorithm for solving the given class of electrostatics problems. One should expand the charge density on the strip $\rho(x)$ in Chebyshev polynomials U_i, and the expansion coefficients of the electric field in Eq.(B.5) are then given by Eq.(B.7). The coefficient D_0 should be taken to satisfy the condition on the voltage drop between the plates. Indeed, $T_0/\sqrt{a^2-x'^2}$ gives the electrostatic solution for $\rho(x) = 0$ and a finite voltage drop.

We apply this algorithm to solve the problem which appeared for the quadrupolar strip. The charge density is given by

$$\rho(x) = e(\nu(0)-k)n_L + en''\frac{x^2}{2} = e(\nu(0)-k)n_L U_0(\frac{x}{a}) + en''\frac{a^2}{2}(\frac{1}{4}U_2(\frac{x}{a}) + \frac{1}{4}U_0(\frac{x}{a})). \tag{B.8}$$

This yields an electric field (taking into account the dielectric constant of the media ϵ)

$$\begin{aligned} E_x(x) &= \frac{2\pi e}{\epsilon}\left\{(\nu(0)-k)n_L\frac{T_1(\frac{x}{a})}{\sqrt{1-(\frac{x}{a})^2}} + \frac{n''a^2}{2}\frac{T_3(\frac{x}{a})+T_1(\frac{x}{a})}{4\sqrt{1-(\frac{x}{a})^2}}\right\} = \\ &= \frac{2\pi e}{\epsilon}\left\{(\nu(0)-k)n_L\frac{x}{\sqrt{a^2-x^2}} + \frac{n''}{2}\frac{x^3-xa^2/2}{\sqrt{a^2-x^2}}\right\} \end{aligned}$$

and finally electrostatic potential

$$\phi(x) = \frac{2\pi e}{\epsilon}\left\{(\nu(0)-k)n_L(a^2-x^2)^{1/2} + \frac{n''a^2}{4}(a^2-x^2)^{1/2} - \frac{n''}{6}(a^2-x^2)^{3/2}\right\}. \tag{B.9}$$

Appendix C

We have to solve the Laplace equation in the xz–plane with the mixed boundary conditions given on the x–axis in terms of the electric field:

$$\begin{array}{ll} E_x(x,0) = 0, & \text{for } |x| > x_2, \\ E_x(x,0) = 0, & \text{for } |x| < x_1, \\ E_z(x,0) = 2\pi e(n'x - \frac{n_L}{2}), & \text{for } x_1 < x < x_2, \\ E_z(x,0) = 2\pi e(n'x + \frac{n_L}{2}), & \text{for } -x_2 < x < -x_1, \end{array} \tag{C.1}$$

Instead we will look for an analytic function $F(\zeta)$ ($\zeta = x + iz$), such that

$$\mathrm{Im}F = E_x \tag{C.2}$$

$$\mathrm{Re}F = E_z \tag{C.3}$$

From Eq.(C.1) we know the real and imaginary parts of F on different intervals. However, we have to know the imaginary part of the function on the whole axis in order to determine it in the complex plane. Thus we use another analytic function

$$f = \frac{F}{\sqrt{(\zeta^2 - x_2^2)(\zeta^2 - x_1^2)}} \tag{C.4}$$

By rewriting Eq.(C.1) in terms of this function we have

$$\begin{array}{ll} \mathrm{Im}f(x,0) = 0, & \text{for } |x| > x_2, \\ \mathrm{Im}f(x,0) = 0, & \text{for } |x| < x_1, \\ \mathrm{Im}f(x,0) = -2\pi e(n'x - \frac{n_L}{2})\frac{1}{\sqrt{(x_2^2 - x^2)(x^2 - x_1^2)}}, & \text{for } x_1 < x < x_2, \\ \mathrm{Im}f(x,0) = 2\pi e(n'x + \frac{n_L}{2})\frac{1}{\sqrt{(x_2^2 - x^2)(x^2 - x_1^2)}}, & \text{for } -x_2 < x < -x_1, \end{array} \tag{C.5}$$

The value of f in the complex plane is given by

$$f(\zeta) = \frac{1}{\pi}\int \frac{\mathrm{Im}f(x)dx}{x - \zeta} \tag{C.6}$$

By substituting Eq.(C.5) in Eq.(C.6) and going back to the electric field we find

$$E_z(x,0) = 4ex\sqrt{(1-\frac{x_2^2}{x^2})(1-\frac{x_1^2}{x^2})}\int_{x_1}^{x_2}\frac{dt(n't-\frac{n_L}{2})}{\sqrt{(x_2^2-t^2)(t^2-x_1^2)(1-\frac{t^2}{x^2})}} \tag{C.7}$$

From the condition that the charge density should be zero at $x \to \infty$ it follows that

$$\int_{x_1}^{x_2}\frac{dx(n'x-\frac{n_L}{2})}{\sqrt{(x_2^2-x^2)(x^2-x_1^2)}} = 0 \tag{C.8}$$

The second equation follows from the condition that the potential drop between the metal plates is $\Delta\mu/e$:

$$\frac{2\pi e}{\epsilon}\int_{x_1}^{x_2}\frac{dx(n'x-\frac{n_L}{2})}{\sqrt{(x_2^2-x^2)(x^2-x_1^2)}}x^2 = \frac{\Delta\mu}{e} \tag{C.9}$$

Bibliography

[1] C.W.J. Beenakker and H. van Houten , in *Solid State Physics*, edited by H. Ehrenreich and D. Turnbull (Academic, New-York, 1991) vol.44, M. Büttiker, in *Semiconductors and Semimetals.* , edited by M.Reed vol.35, (Academic, New-York, 1992)

[2] M. Büttiker, Phys. Rev. B **38**, 9375 (1988).

[3] C. W. J. Beenakker, Phys. Rev. Lett. **64**, 216 (1990).

[4] A. M. Chang, Solid State Commun. **74**, 871 (1990).

[5] B. W. Alphenaar, P. L. McEuen , R. G. Wheeler, R. N. Sacks, Phys. Rev. Lett. **64**, 677 (1990), B. W. Alphenaar, Ph.D. Thesis, *Yale University* 1991, B. W. Alphenaar, P. L. McEuen , R. G. Wheeler, R. N. Sacks, to be published in Phys. Rev. B.

[6] L.P. Kouwenhoven, B.J. van Wees, N.C. van der Vaart, C.J.P.M. Harmans, C.E. Timmering, C.T. Foxon, Phys. Rev. Lett. **64**, 685 (1990).

[7] L. I. Glazman, I. A. Larkin, Semicond. Sci. Technol. **6**, 32 (1991).

[8] J. C. Maxwell, *A Treatise on Electricity and Magnetism*, (Clarendon Press, Oxford, 1892).

[9] K.K. Choi, D.C. Tsui, K. Alavi, Appl. Phys. Lett. **50**, 110 (1987).

[10] P.L. McEuen, E.B. Foxman, J. Kinaret, U. Meirav, M.A. Kastner, N.S. Wingreen, S.J. Wind, Phys. Rev. B **45** , 11419 (1992).

[11] S. Luryi, in *High Mgnetic Fields in Semiconductor Physics*, edited by G. Landwehr, (Springer,New-York, 1987).

[12] U. Wulf, V. Gudmundson, and R.R. Gerhardts, Phys. Rev. B **38**, 4218 (1988).

[13] A. L. Efros, Solid State Commun. **67**, 1019 (1988).

[14] A. L. Efros, Phys. Rev. B **45** , 11354 (1992).

[15] B.J. van Wees, E.M.M. Willems, C.J.P.M. Harmans, C.W.J. Beenakker, H. van Houten, J.G. Williamson, C.T. Foxon, and J.J. Harris, Phys. Rev. Lett. **62**, 1181 (1989).

[16] B.I.Shklovskii, Pis'ma Zh. Eksp. and Teor. Fiz. **36**, 43 (1982), [Sov. Phys. - JETP Lett. **36**, 53], B.I.Shklovskii, A.L. Efros, Zh. Eksp. and Teor. Fiz. **84**, 811 (1983), [Sov. Phys. - JETP **57**, 470].

[17] D.G. Polyakov, M.E. Raikh, Solid State Commun. **74**, 1209 (1990).

[18] T. Martin and S. Feng, Phys. Rev. B **44**, 9084 (1991).

[19] A. L. Efros, Solid State Commun. **65**, 1281 (1988).

[20] *The Quantum Hall Effect*, edited by R.E. Prange and S.M. Girvin (Springer-Verlag, New-York, 1987).

[21] G. Timp, A. M. Chang, P. Mankiewich, R. Behringer, J. E. Cunningham, T. Y. Chang, and R. E. Howard, Phys. Rev. Lett. **59**, 732 (1987); M. L. Roukes, A. Scherer, S. J. Allen, Jr., H. G. Craighead, R. M. Ruthen, E. D. Beebe, and J. P. Harbison, Phys. Lett. **59**, 3011 (1987); For quantization in split–gate device see B. J. van Wees, H. van Houten, C. W. J. Beenakker, J. G. Williamson, L. P. Kouwenhoven, D. van der Marel, and C. T. Foxon, Phys. Rev. Lett. **60**, 848 (1988).

[22] B. I. Halperin, Phys. Rev. B **25**,2185 (1982).

[23] P. Streda, J. Kucera, and A. H. MacDonald, Phys. Rev. Lett. **59**, 1973 (1987); J. K. Jain and S. A. Kivelson, *ibid.* **60**, 1542 (1988).

[24] R. Landauer, IBM J. Res. Dev. **1**, 223 (1957).

[25] B. J. van Wees, L. P. Kouwenhoven, E. M. M. Willems, C. J. P. M. Harmans, J. E. Mooij, H. van Houten, C. W. J. Beenakker, J. G. Williamson, and C. T. Foxon, Phys. Rev. B **43**, 12431 (1991).

[26] D. B. Chklovskii, B.I. Shklovskii, and L. I. Glazman, Phys. Rev. B **46**, 4026 (1992); **46**, 15606(E) (1992).

[27] B. E. Kane, Ph.D. thesis, Princeton University, 1988.

[28] I. A. Larkin, V. B. Shikin, Phys. Lett. A **151**, 335 (1990).

[29] B. I. Shklovskii, in preparation.

[30] M. Büttiker, Phys. Rev. B **41**, 7906 (1990).

[31] D. B. Chklovskii, in preparation.

[32] I.S. Gradshteyn, and I.M. Ryzhik, Table of Integrals, Series, and Products (Academic Press, 1980).

[33] V.B. Shikin, T. Demel', and D. Heitman, Zh. Eksp. Teor. Fiz. **96** , 1406 (1989)[Sov. Phys.–JETP **69** , 797 (1990)].

[34] K. von Klitzing, G. Dorda, and M. Pepper, Phys. Rev. Lett. **45**, 494 (1980).

[35] D.C. Tsui, H.L. Störmer, and A.C. Gossard, Phys. Rev. Lett. **48**, 1559 (1982).

[36] R.B. Laughlin, Phys. Rev. Lett. **50**, 1395 (1983).

[37] R.B. Laughlin, Phys. Rev. B **23**, 5632 (1981); B.I. Halperin, Phys. Rev. B **25**, 2185 (1982).

[38] J. Kucera and P. Streda, J. Phys. C **21**, 4357 (1988).

[39] A. Szafer, A.D. Stone, P.L. McEuen, and B.W. Alphenaar, Proceedings NATO ASI on Granular Electronics, Il Ciocco, 1990.

[40] J.K. Jain, S.A. Kivelson, N. Trivedi, Phys. Rev. Lett. **64**, 1297 (1990); **64**, 1993(E) (1990).

[41] S. Kivelson, D.-H. Lee, S.-C. Zhang, Phys. Rev. B **46**, 2223 (1992); D.-H. Lee, S.A. Kivelson, S.-C. Zhang, Phys. Rev. Lett. **68**, 2386 (1992).

[42] B.I. Halperin, P.A. Lee, and N. Read, Phys. Rev. B **47**, 7312 (1993).

[43] V. Kalmeyer and S.-C. Zhang, Phys. Rev. B **46**, 9889 (1992).

[44] see e.g. H.P. Wei, S.Y. Lin, D.C. Tsui, and A.M.M. Pruisken, Phys. Rev. B **45**, 3926 (1992) and references therein.

[45] D.B. Chklovskii, B.I. Shklovskii, and L.I. Glazman, Phys. Rev. B **46**, 4026 (1992); **46**, 15606(E) (1992).

[46] J.K. Jain, Phys. Rev. Lett. **63**, 199 (1989).

[47] N.R. Cooper and J.T. Chalker, to be published in Phys. Rev. B.

[48] R.R. Du, H.L. Störmer, D.C. Tsui, L.N. Pfeiffer, and K.W. West, Phys. Rev. Lett. **70**, 2944 (1993).

[49] T. Chakraborty and P. Pietilainen, *The Fractional Quantum Hall Effect*, (Springer-Verlag, New-York 1988).

[50] B.J. van Wees, E.M.M. Willems, L.P. Kouwenhoven, C.J.P.M. Harmans, J.G. Williamson, C.T. Foxon, and J.J. Harris, Phys. Rev. B **39**, 8066 (1989).

[51] S. Komiyama, H. Hirai, S. Sasa, and S. Hiyamizu, Phys. Rev. B **40**, 12566 (1989).

[52] G. Müller, D. Weiss, S. Koch, K. von Klitzing, H. Nickel, W. Schlapp, ans R. Lösch, Phys. Rev. B **42**, 7633 (1990).

[53] S. Komiyama, H. Nii, Physica B **184**, 7 (1993).

[54] B. Shapiro, Phys. Rev. B **33**, 8447 (1986).

[55] J.T. Chalker, and P.D. Coddington, J. Phys. C **21**, 2665 (1988).

[56] Y. Huo, R.E. Hetzel, and R.N. Bhatt, Phys. Rev. Lett. **70**, 481 (1993).

[57] I.M. Ruzin, to be published in Phys. Rev. B.

[58] J.K. Luo, H. Ohno, K. Matsuzaki, T. Umeda, J. Nakahara, and H. Hasegawa, Phys. Rev. B **40**, 3461 (1989).

[59] F.G. Pikus, and A.L. Efros to be published in Phys. Rev. B.

[60] D.B. Chklovskii, K.A. Matveev, and B.I. Shklovskii Phys. Rev. B **47**, 12605 (1993).

[61] V.J. Goldman, J.K. Jain, and M. Shayegan, Phys. Rev. Lett. **65**, 907 (1990).

[62] S.-C. Zhang, Int. J. Mod. Phys. B **6**, 25 (1992).

[63] J. K. Wang and V. J. Goldman, Phys. Rev. Lett. **67**, 749 (1991), J. K. Wang and V. J. Goldman, Phys. Rev. B **45**, 13479 (1992).

[64] A. M. Chang, J.E. Cunningham, Phys. Rev. Lett. **69**, 2114 (1992).

[65] T. Sajoto, Y. W. Suen, L. W. Engel, M. B. Santos, and M. Shayegan, Phys. Rev. B **41**, 8449 (1990).

[66] H.L. Störmer, K.W. Baldwin, L.N. Pfeiffer, and K.W. West, Solid State Commun. **84**, 95 (1992).

[67] J.E. Müller, Phys. Rev. Lett. **68**, 385 (1992).

[68] C. Barnes, B.L. Johnson, and G. Kirczenow, Phys. Rev. Lett. **70**, 1159 (1993).

[69] *Classical Electrodynamics*, p. 585, by J.D. Jackson. (John Wiley & Sons, New–York)

[70] A.M. Chang and D.C. Tsui, Solid State Commun. **56**, 153 (1985).

[71] R.G. Clark, Physica Scripta, **T39**, 45 (1991).

[72] R. Willett, J.P. Eisenstein, H.L. Störmer, D.C. Tsui, A.C. Gossard, and J.H. English, Phys. Rev. Lett. **59**, 1776 (1987).

[73] D.B. Chklovskii and P.A. Lee, Phys. Rev. B **48**,18060 (1993).

3636-2